ASEAN
Journal of Scientific and Technological Reports
Online ISSN:2773-8752

Vol. 26 No. 4, October - December 2023

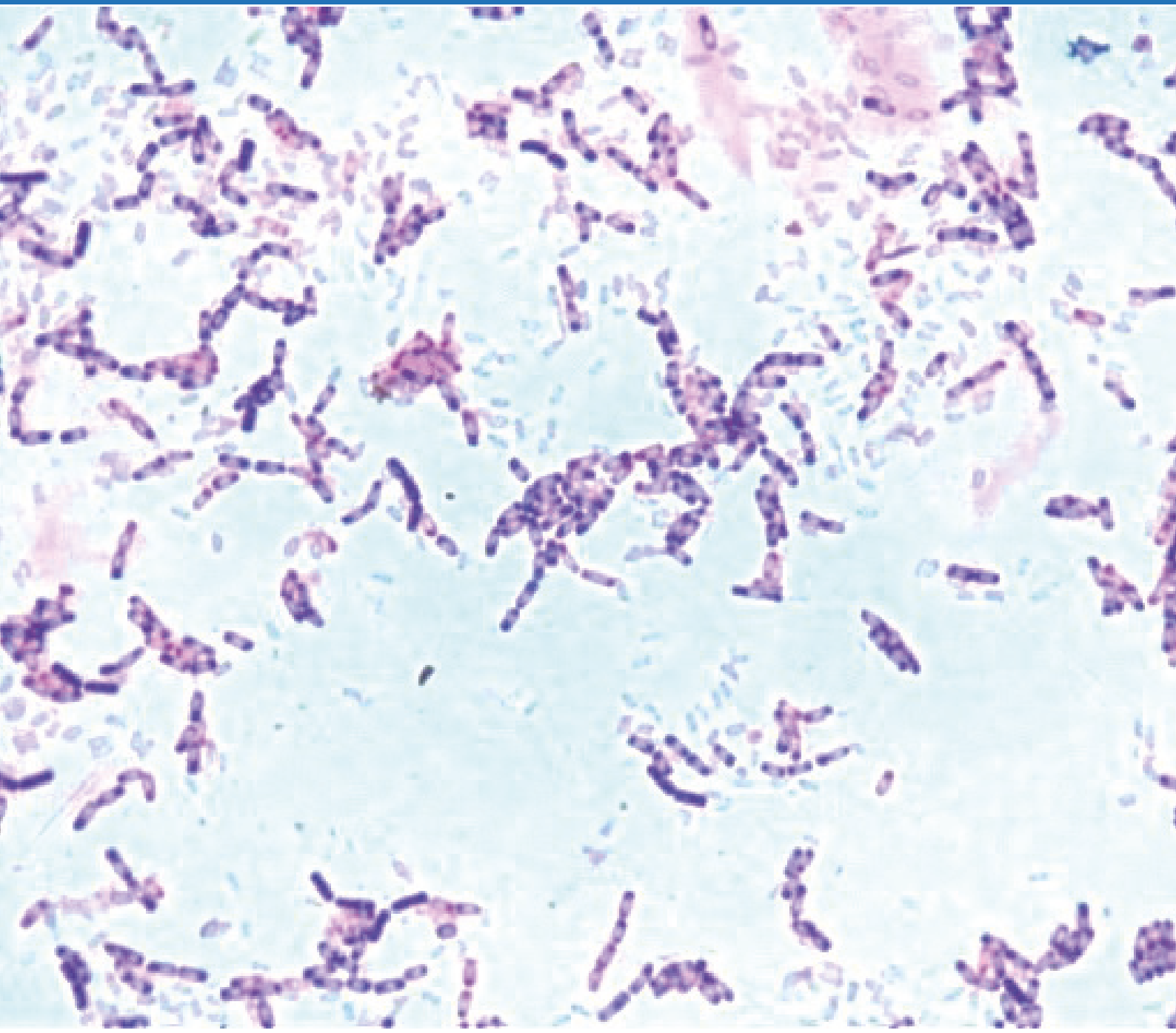

ISSN 2773-8752 (online)
https://ph02.tci-thaijo.org/index.php/tsujournal/issue/view/16952

ASEAN Journal of Scientific and Technological Reports (AJSTR)

Contact Us Institute of Research and Innovation, Thaksin University
222 M. 2 Ban-Prao sub-district, Pa-Pra-Yom district, Phatthalung province, Thailand
Tel. 0 7460 9600 # 7242 , E-mail: aseanjstr@tsu.ac.th

List of Contents

Contents Page

Phytochemicals, antioxidant, and antibacterial activities of fresh and dried Chinese chive (*Allium tuberosum Rottler*) leaf extracts **1**

Benyapa Kalasee, and Pimonsri Mittraparp-arthorn

Utilization from Residues Trunk and Frond of oil palm with Pretreated Two-Stage Steam Explosion for Bioethanol and Biogas processing in Biofuel Refinery **11**

Tussanee Srimachai, Chaiyoot Meengam, Prawit Kongjan, and Kiattisak Rattanadilok Na Phuket

Period Change Analysis of a W Uma-type Binary: V417 Aquilae **21**

Supanee Maichandee, Torik Hengpiya, and Wiraporn Maithong

The off-cardinal alignment of Chiang Mai's City Plan in Relation to the Orion's Belt **29**

Chayapon Iemsonthi, Seksit Lorwilai, Panuwit Sankaokam, Orapin Riyaprao, and Cherdsak Saelee

Comparison of different extraction methods for the extraction of major bioactive compounds from Kao-Kum Doi-Saket (Oryza sativa L.) **38**

Sureewan Rajchasom, Pornsawan Sombatnan, Janyawat Tancharoenrat Vuthijumnonk, and Phanida Suphiratwanich

Changing of chlorophyll contents in Caulerpa lentillifera after five-days harvest **47**

Bongkot Wichachucherd, Kattinat Sagulsawasdipan, and Eknarin Rodcharoen

Effects of Ultrasonic Stimulation and Light Intensity on the Growth Rate and Biomass Productivity of Chlorella ellipsoidea in a Closed-Batch Cultivation System **54**

Sudarat Theerapisit, Somrak Rodjaroen, and Siriluk Sintupachee

Effects of Ultrasonic Stimulation and Light Intensity on the Growth Rate and Biomass Productivity of Chlorella ellipsoidea in a Closed-Batch Cultivation System **67**

Sudarat Theerapisit, Somrak Rodjaroen, and Siriluk Sintupachee

ASEAN
Journal of Scientific and Technological Reports
Online ISSN:2773-8752

ASEAN
Journal of Scientific and Technological Reports
Online ISSN:2773-8752

Research article

Phytochemicals, Antioxidant, and Antibacterial Activities of Fresh and Dried Chinese Chive (*Allium tuberosum* Rottler) Leaf Extracts

Benyapa Kalasee[1], and Pimonsri Mittraparp-arthorn[2*]

[1] Faculty of Science, Prince of Songkla University, Songkhla, 90110, Thailand; Yok.benyapa@gmail.com
[2] Faculty of Science, Prince of Songkla University, Songkhla, 90110, Thailand; pimonsri.m@psu.ac.th
* Correspondence: pimonsri.m@psu.ac.th

Citation:
Kalasee, B. and Mittraparp-author, P. Phytochemicals, antioxidant, and antibacterial activities of fresh and dried Chinese chive (*Allium tuberosum* Rottler) leaf extracts. *ASEAN J. Sci. Tech. Report*. **2023**, *26*(4), 1-10. https://doi.org/10.55164/ajstr.v26i4.249336

Article history:
Received: April 30, 2023
Revised: July 22, 2023
Accepted: August 8, 2023
Available online: September 30, 2023

Abstract: Chinese chive (*Allium tuberosum* Rottler) is a nutrient-rich vegetable widely cultivated in Southeast Asia, including Thailand. The objectives of this study were to assess the phytochemical compounds present in fresh and dried Chinese chives obtained through aqueous extraction and to investigate their biological activities, particularly their antioxidant and antibacterial properties. In this study, fresh and dried Chinese chive leaves were extracted using water to obtain fresh Chinese chive extract (FCCE) and dried chive extract (DCCE). The extracts were characterized for their phytochemical compounds and evaluated for their bioactive properties. Based on GC-MS analyses, 5 major bioactive compounds found in both FCCE and DCCE were 2-methoxy-4-vinyl phenol, dimethyl sulfone, n-hexadecanoic acid, 2-hydroxy-gamma-butyrolactone, and furaneol. The FCCE and DCCE extracts exhibited antioxidant properties with the IC50 values of 7.25 ± 0.14/8.62 ± 0.02 mg/ml and 4.91 ± 0.29/6.66 ± 0.03 mg/ml for FCCE and DCCE determined by DPPH/ABTS assays, respectively. Antibacterial activities of FCCE and DCCE against food pathogenic bacteria demonstrated that both extracts could inhibit *Bacillus cereus*, *Staphylococcus aureus*, *Salmonella* sp., *Listeria monocytogenes*, *Escherichia coli*, *Vibrio cholerae*, and *V. parahaemolyticus* with the same MIC value (8 mg/ml). Therefore, this study provided a basic knowledge of Chinese chive as a potentially promising source of natural bioactive ingredients for various applications in food technology.

Keywords: Antibacterial activity; antioxidants; Chinese chives; food pathogens

1. Introduction

Chinese chives, also known as garlic chives, belong to the Liliaceae family and the *Allium* genus, which includes garlic, leek, and onion. Chinese chives are popular in Southeast Asia, South Asia, and some Middle Eastern countries [1]. In Thailand, the province with the largest cultivation area is Ratchaburi. There are also reports that Klong U-Tapao Sub-district, Hat Yai District, Songkhla Province, popularly cultivated large quantities of Chinese chives with a total plantation area of about 96,000 square meters, and most are exported to Malaysia [2]. Thai people usually consume fresh Chinese chives with Thai stir-fried rice noodles (Pad Thai) or cooked as dumplings (Gui Chai). In other countries, some of the most popular dishes from the Chinese chives are Korean chive salad (Kimchi) and Japanese pan-fried dumplings (Gyoza).

and dietary fiber content [3]. Additionally, Chinese chives have health advantages and have been utilized as herbal medicine to treat asthma and conditions including diarrhea, hematemesis, and snakebite [4]. The crushed leaves contained volatile sulfur-containing substances, which could reduce the risk of cardiovascular and inflammatory disorders [5].

Chinese chives are rich in various phytochemicals that offer potential health benefits. Notably, Sulphur compounds, including diallyl disulfide and diallyl trisulfide, are responsible for the distinct aroma and taste of Chinese chives and have been studied for their possible anticancer and anti-inflammatory properties [6]. The presence of phenolic compounds like ferulic acid and caffeic acid provides antioxidant and anti-inflammatory benefits, helping to combat oxidative stress and promote overall health [7]. Additionally, Chinese chives contain flavonoids, a group of polyphenolic compounds known for their strong antioxidant properties. These can counteract harmful free radicals and potentially reduce the risk of chronic diseases, supporting overall well-being [8].

The majority of people around the world are struggling with the problems of foodborne illnesses caused by foodborne pathogens. The food market has identified the pathogenic bacteria, mainly *Bacillus cereus, Listeria* spp., *Staphylococcus aureus*, *Escherichia coli*, *Salmonella* spp., and *Vibrio* spp. [9]. To reduce cases, antimicrobial substances from edible sources have been studied. Various assays have previously screened the antimicrobial activities of Chinese chives extracted by different methods. For example, antibacterial activities of 25, 50, and 75 mg/ml of Chinese chive crude extracts have been reported by the modified agar well diffusion method and the highest antibacterial activity was obtained from 75 mg/ml of the steam distillation extract against *B. cereus* and *L. monocytogenes* [10]. In addition, the antibacterial activity of a water extract of Chinese chive against 21 *Helicobacter pylori* was shown by the disk diffusion method and the minimum inhibitory concentration (MIC) value obtained by the agar dilution method was 2.45 mg DW/ml [11]. Hence, there is a great interest in examining the possibility of using Chinese chive as natural ingredients in food or food products. Therefore, this study aimed to evaluate the phytochemical compounds of fresh and dried Chinese chives obtained by the aqueous extraction method and determine their biological activity, including antioxidant and antibacterial properties.

2. Materials and Methods

2.1 Bacterial Strains

Food pathogenic bacteria used in this study were *B. cereus* PSU3874, *L. monocytogenes* PSU6205, *S. aureus* ATCC25923, *E. coli* ATCC25922, *Salmonella* sp. PSU411, *V. cholerae* PSU6072, and *V. parahaemolyticus* ATCC17802. All isolates were obtained from the microbial culture collection at the Division of Biological Science, Prince of Songkla University, Thailand, and were stored in 20% glycerol at -80 °C.

2.2 Preparation of fresh and dried Chinese chives

Chinese chives were purchased from a local grower at Khlong-u Tapao in Songkhla province of southern Thailand. Fresh Chinese chives were chopped into small pieces and rinsed under running water. Fresh leaves were dried in a hot air oven at 40 °C for 2 days or until dried for dried Chinese chives. All samples were blended into a fine powder [12].

2.3 Extraction of Chinese chives extract

Chinese chive powders obtained from fresh and dried leaves were extracted with hot water following the method previously described by Hernandez *et al*., 2017 with some modifications [12]. In a heating oven, 100 g of fresh and dried Chinese chives powders were soaked in 500 ml hot distilled water at 60 °C for 30 minutes. After filtration through double layers of muslin, the solutions were concentrated by freeze dryer (Martin Christ, Osterode am Harz, Germany) by freezing at -80 °C for 24 hours before taking to freeze drier at -45 °C for 3 days. The freeze-dried extracts were kept in dark storage at 4 °C until further use.

2.4 GC-MS analysis

Gas chromatography-electron ionization/mass spectrometry (GC-MS) analysis of phytochemical compounds present in fresh (FCCE) and dried (DCCE) Chinese chive leaves was carried out using Perkin

and DCCE powders were dissolved in dimethyl sulfoxide (DMSO) and centrifuged at 10,000 rpm for 10 min at 10 °C before the supernatant was subjected to GC-MS analysis. The Elite-5 capillary column ((5% biphenyl) 95% dimethylpolysiloxane), length 30 m 0.25 mm ID, and film thickness 250 m df were utilized for the GC-MS analysis. A 1 ml/min of helium was used as the carrier gas. The temperature at the injector and interface was 260 °C. The column temperature was programmed from 60 to 300 °C at an increasing rate of 10 min, where it was held for 6 min. The spectrums of the compounds were compared with standard spectra available in the Perkin Elmer GC-MS NIST library [13].

2.5 Antioxidant Activity Assays

The antioxidant activity assays were determined by 2,2-diphenyl-1-picrylhydrazyl (DPPH) and 2,2′-azino-bis-(3-ethylbenzothiazoline-6-sulfonic acid) (ABTS) radical scavenging assays of CCE in 96-well microtiter plates using the methods described below.

2.5.1. DPPH Assay

The antioxidant activity of the CCE was evaluated by DPPH radical scavenging. In brief, 180 µl of 0.1 mM DPPH solution in methanol were combined with 20 µl of FCCE, DCCE, or standard solution. A spectrophotometer was used to measure the absorbance at 517 nm after 30 minutes [14].

2.5.2 ABTS Assay

The ABTS stock solution was prepared by mixing 7.75 mM of potassium persulfate with 7.25 mM of ABTS and incubated at room temperature for 16 hours in the dark. The ABTS stock solution was diluted to a concentration of 107.14 µM ABTS solution until use. Then, 280 µl of 107.14 µM ABTS solution was combined with 20 µl of FCCE, DCCE, or standard solution. The plate was mixed and incubated in the dark at room temperature for 6 minutes, and then the absorbance at 734 nm was measured using a spectrophotometer (LUMIstar, BMGLABTECH, Ortenberg, Germany) [15].

2.6 Minimum inhibitory concentration (MIC) and minimum bactericidal concentration (MBC) assays

The MICs of FCCE and DCCE against all pathogens were determined by following the Clinical and Laboratory Standard Institute (CLSI) guidelines [16]. The tested isolates were cultured in Mueller–Hinton broth (MHB) supplemented with (for *Vibrio* spp.) or without 1% NaCl for 4 hours. Then, cells were adjusted with fresh media to 10^6 CFU/ml, and 100 µl of cell suspensions were added to 100 µl of FCCE or DCCE solution at final concentrations ranging from 1 to 16 mg/ml. After incubation for 18–20 hours at 30 °C (for *Vibrio* spp.) or for 16 hours at 37 °C (for other species), the MIC values were determined by adding 20 µl of a 0.1% resazurin solution to each well and incubating for 2 h at 30 or 37 °C. For MBC values, a liquid portion from each well that showed no growth was taken and cultivated on Tryptic Soy agar (TSA) with or without 1% NaCl and incubated at 30 °C or 37 °C for 18–24 h.

2.7 Statistical analysis

A completely randomized experimental design was used with three replicates each, and the means and standard deviations (S.D.) were used to present the results. A one-way analysis of variance (ANOVA) was performed to compare more than two means. Duncan's new multiple-range tests were employed to determine the significant differences between the means. Correlations between the DPPH and ABTS assays of antioxidant activity were calculated at a significance level of $p < 0.05$.

3. Results and Discussion

This study investigated the phytochemical components from aqueous extracts of fresh and dried Chinese chives by GC-MS analyses and examined their biological activities, including antioxidants and antibacterial properties.

3.1 The visual appearance and extraction yield of Chinese chive extracts

The visual appearance of Chinese chive extracts from fresh and dried leaves were dry greenish and brown powder, respectively (Figure 1). The extraction yield obtained by water extraction was 290.40 mg/g of dried matter and 37.70 mg/g of fresh weight, respectively (Table 1). As a result, the maximum yield was obtained

water content in dry leaves, which leads to a higher concentration of the desired compounds. Consequently, the extraction process becomes more efficient, resulting in an improved yield. Moreover, the use of dry leaves offers additional advantages. Dry leaves are less susceptible to enzymatic degradation and microbial growth, ensuring the preservation of the plant substances' integrity during extraction. Additionally, their lighter weight and manageable nature make them more convenient to handle during extraction [17, 18].

Figure 1. The visual appearance of Chinese chive extracts. (A) Extract obtained from fresh sample (FCCE) and (B) Extract obtained from dried sample (DCCE)

Table 1. The extraction yield of Chinese chive extracts obtained by water extraction.

Sample	Yield (mg/g)	Characteristics
Fresh leaves	37.70	Dark green powder
Dried leaves	290.4	Brown powder

3.2 GC-MS Analysis

The GC-MS analysis identified 108 and 156 compounds in FCCE and DCCE, respectively. Ten major compounds identified in FCCE (a total of 18.70 mg/g or 49.60% of the extraction yield) were 2-methoxy-4-vinyl phenol, dimethyl sulfone, n-hexadecanoic acid, butanoic acid, 1,2,3-propanetriyl ester2-propanone, 1,3-dihydroxy-, 2-hydroxy-gamma-butyrolactone, furaneol, 1-heptadecanecarboxylic acid, 2-furanmethanol, and pentanoic acid (Table 2). Among these, 8 of 10 were also identified as major compounds in DCCE. The 5 additional compounds among top 10 hits found in DCCE were 4H-pyran-4-one, 2,3-dihydro-3,5-dihydroxy-6-methyl-, glycerin, benzofuran, 2,3-dihydro-, 4H-pyran-4-one, 3,5-dihydroxy-2-methyl-, and 2,4(1H,3H)-pyrimidinedione, 5-methyl- (Table 2).

In this study, both FCCE and DCCE exhibited a high content of 2-methoxy-4-vinylphenol, a phenolic compound with antibacterial, antioxidant, anti-inflammatory, analgesic, and anti-germination properties [19-21]. From previous research, 2-methoxy-4-vinylphenol, a major compound in red cabbage, has strong antibacterial activity and possesses higher degrees of interaction with bacteria DNA gyrase, leading to high antimicrobial efficacy [19]. Dimethyl sulfone is an organosulfur compound that is a metabolite of DMSO and certain sulfur-containing amino acids. It is present in some natural green plants, fruits, and vegetables, such as tomatoes, corn, and apples [22]. Several reports provide *in vitro* evidence of the antioxidant, anti-inflammatory, antibacterial, antifungal, and antiviral activity of dimethyl sulfone [22-25]. Moreover, it was also found to inhibit *E. coli* and *S. enterica* serovar Kinshasa [26]. Previous studies showed that one of the organosulfur compounds, dimethyl trisulfide, in Chinese chives could involve its antibacterial activity [10]. The fatty acid n-hexadecanoic acid isolated from the *Canthium parviflorum* leaves exhibited antimicrobial activity against *S. aureus*, *E. coli*, *B. subtilis*, and *Candida albicans* [27]. Antibacterial activity of furaneol has been reported against human pathogens, including *S. aurues*, *S. epidermidis*, *E. coli*, and *Proteus vulgaris* [28]. Thus, these major compounds in FCCE and DCCE might significantly contribute to their antimicrobial activities.

In DFFC, several compounds can be found as major constituents. However, they are not seen as major constituents in FCCE. For example, 4H-pyran-4-one, 2,3-dihydro-3,5-dihydroxy-6-methyl- is the second top component found in the DCCE, which was not found in the extract of fresh Chinese chives (Table 2). The formation of this compound in heat-treated food or dried fruit has been reported due to the Maillard reaction, which lead to changes in the color of the extract from dark green to brown [29, 30].

The DPPH and ABTS assays were used to evaluate the antioxidant activity of Chinese chive extracts. At the highest concentration (16 mg/ml), extracts had a more significant scavenging effect against ABTS than DPPH radicals. FCCE and DCCE possessed free radical scavenging properties but varying degrees, with an IC50 ranging from 7.25 to 8.62 and 4.91 to 6.66 mg/ml for DPPH and ABTS methods, respectively (Table 3). The antioxidant activity of Chinese chive extract may be due to several phytochemical compounds. For example, sulfur compounds have been reported to contribute to various vegetables' antioxidant properties in the *Allium* species [31]. Lachman *et al*., 2003 also reported that polyphenolic compounds in different onions (*Allium cepa* L.) are effective antioxidants due to their potential to scavenge free radicals of fatty acids and oxygen [32]. Additionally, antioxidant activity was found in extracts from all organs of *Allium schoenoprasum* L., which leaves showing the highest antioxidant activity [33].

In a previous study, the IC50 of Chinese chives essential oil extract by turbo hydrodistillation showed an IC50 of 12.16 mg/ml, which showed a slightly higher IC50 value (indicating less potency) in the DPPH assay compared to the current study's extracts. This discrepancy could be due to differences in extraction methods or the presence of varying antioxidant compounds in the different extracts [31]. According to Parvu *et al*., 2010 p-coumaric acid, ferulic acid, isoquercitrin, and rutin are the main polyphenolic compounds found in chives [34]. In addition, the IC50 values for the extract of Chinese chives in water and ethanol were 822.92 g/ml, 735.96 g/ml, 757.0 g/ml, and 650.6 g/ml, respectively, according to the DPPH and ABTS assays. As a result, Chinese chive extract has strong antioxidant activity against the DPPH and ABTS radicals [35]. In this study, it was found that DCCE had a slightly lower antioxidant activity than FCCE. This suggested that treating the Chinese chive leaves at 40 ^{o}C may result in the loss of some antioxidant components. Therefore, the study demonstrated that Chinese chive extracts possess significant antioxidant activity against both DPPH and ABTS radicals, likely due to the presence of various phytochemical compounds with antioxidant properties. However, the specific antioxidant components and their concentration might vary depending on extraction methods and processing conditions.

3.4 Antibacterial activities

The antibacterial activity of Chinese chives extracts against 7 bacterial strains causing foodborne illnesses, including *B. cereus* PSU3874, *L. monocytogenes* PSU6205, *S. aureus* ATCC25923, *E. coli* ATCC25922, *Salmonella* sp. PSU411, *V. cholerae* PSU6072, and *V. parahaemolyticus* ATCC17802 were evaluated using MIC and MBC assays. The result demonstrates that both FCCE and DCCE could inhibit all tested bacteria at the same MIC values (8 mg/ml) (Table 4). All bacterial strains in this investigation had MBC values greater than 16 mg/ml. This was consistent with previous studies showing that Chinese chives have inhibitory effects on Gram-positive and Gram-negative bacteria [11, 19]. In this study, one of the major components present in FCCE and DCCE is 2-methoxy-4-vinylphenol. This compound has been found to interact with DNA gyrase required for DNA synthesis and lipoprotein of the bacterial cell wall [19]. Thus, the inhibition of these targets could contribute to the antibacterial efficacy of the extracts. Both FCCE and DCCE extracts contain very similar active compounds responsible for antibacterial activity. Consequently, if the active ingredients are consistently present in both extracts at similar concentrations, they would exert comparable inhibitory effects on the bacterial strains. The bacterial strains tested might share a similar sensitivity profile to the compounds in both FCCE and DCCE, resulting in similar MIC values. This suggests that Chinese chives may contain a relatively narrow range of compounds with antibacterial properties. The MIC values could be consistently the same if the extracts mainly consist of a few key active compounds effective against the tested bacterial strains [36, 37].

In a previous study, Chinese chives extracted from water could inhibit *E. coli*, *L. monocytogenes,* and *V. parahaemolyticus* with an inhibitory zone of 15, 10, and 14 mm, respectively. However, it could not inhibit *S. aureus* by a disc diffusion assay [38]. In addition, Chinese chives crude extract obtained by steam distillation for 2.5 hours at a concentration of 75 mg/ml could inhibit both Gram-positive and Gram-negative bacteria with the inhibitory zone of 0.688 ± 0.023 cm against *B. cereus* and *L. monocytogenes* [10]. Moreover, the antibacterial study of Chinese chives extract based on the serial double dilution method has indicated that both water and ethanolic extracts exhibited good efficacy against *E. coli* at a MIC value of 64 μg/ml [35]. Consequently, this study demonstrated the potential of Chinese chive extracts as an antibacterial agent against important food pathogenic bacteria.

Table 2. Major compounds identified in Chinese chives extracts.

			FCCE			DCCE		
No.	**Compound Name**	**Formula**	**Amount (mg/g of fresh matter)**	**Retention time**	**Match Factor**	**Amount (mg/g of dried matter)**	**Retention time**	**Match Factor**
1	2-Methoxy-4-vinyl phenol	$C_9H_{10}O_2$	2.88	34.81	95.82	32.20	34.82	96.20
2	Dimethyl sulfone	$C_2H_6O_2S$	2.50	28.55	98.84	7.83	28.38	98.84
3	n-Hexadecanoic acid	$C_{16}H_{32}O_2$	2.40	49.27	97.34	9.57	49.27	96.60
4	Butanoic acid, 1,2,3-propanetriyl ester	$C_{15}H_{26}O_6$	2.32	40.42	92.50			
5	2-Propanone, 1,3-dihydroxy-	$C_3H_6O_3$	1.84	32.32	86.76	3.51	32.26	78.70
6	2-Hydroxy-gamma-butyrolactone	$C_4H_6O_3$	1.60	34.24	93.42	8.46	34.21	85.70
7	Furaneol	$C_6H_8O_3$	1.55	31.23	96.61	17.19	31.22	97.70
8	1-Heptadecanecarboxylic acid	$C_{18}H_{36}O_2$	1.28	52.48	95.16	2.26	52.46	84.00
9	2-Furanmethanol	$C_5H_6O_2$	1.24	24.95	84.53	0.52	26.51	73.70
10	Pentanoic acid	$C_5H_{10}O_2$	1.09	25.00	67.27			
11	4H-Pyran-4-one, 2,3-dihydro-3,5-dihydroxy-6-methyl-	$C_6H_8O_4$				23.91	36.34	95.60
12	Glycerin	$C_3H_8O_3$				16.29	37.42	95.20
13	Benzofuran, 2,3-dihydro-	C_8H_8O				9.30	39.09	93.40
14	4H-Pyran-4-one, 3,5-dihydroxy-2-methyl-	$C_6H_6O_4$				4.32	36.84	90.50
15	2,4(1H,3H)-Pyrimidinedione, 5-methyl-	$C_5H_6N_2O_2$				4.12	55.26	79.80
	Total			18.70			133.19	

Note: For FCCE, only the top 10 major compounds are listed in this table.

Table 3. Antioxidant activity of Chinese chive Extracts.

Sample	**Antioxidant Activity**[1]	
	DPPH IC_{50} (mg/ml)	**ABTS IC_{50} (mg/ml)**
FCCE	7.25 ± 0.14*	4.91 ± 0.29*
DCCE	8.62 ± 0.02*	6.66 ± 0.03*
Trolox	0.0281 ± 0.78	0.2795 ± 0.69

[1] IC_{50} = half-maximal inhibitory concentration. The value indicates the mean ± SD for three independent experiments performed in triplicates;
* $p < 0.05$ compared between DPPH and ABTS.

Table 4. The MIC and MBC values of Chinese chive extracts against various food pathogenic bacteria.

Bacteria	MIC (mg/ml)		MBC (mg/ml)	
	FCCE	DCCE	FCCE	DCCE
Bacillus cereus PSU3874	8	8	>16	>16
Listeria monocytogenes PSU6205	8	8	>16	>16
Staphylococcus aureus ATCC25923	8	8	>16	>16
Escherichia coli ATCC25922	8	8	>16	>16
Salmonella sp. PSU411	8	8	>16	>16
Vibrio cholerae PSU6072	8	8	>16	>16
Vibrio parahaemolyticus ATCC17802	8	8	>16	>16

4. Conclusions

The study results indicate the good antibacterial and antioxidant properties of Chinese chive extracts, mainly due to phytochemical compounds. Therefore, the extracts from fresh or dried leaves could be applied as natural ingredients in functional food products. The study highlights that the promising activities of Chinese chive extracts could attributed to the presence of phytochemical compounds in the plant. These bioactive compounds, commonly found in plants, offer various health benefits. Furthermore, the study emphasizes the distinct culinary uses of fresh and dried Chinese chive leaves. Fresh leaves add vibrant color, crisp texture, and a strong flavor to dishes, while dried leaves offer a more concentrated and potent taste and an extended shelf life. Although the drying process may lead to a slight reduction in heat-sensitive vitamins, dried chives retain essential nutrients, making them a practical choice for enhancing the nutritional content of meals. The valuable properties of Chinese chive extracts, whether derived from fresh or dried leaves, hold potential as natural ingredients for functional food products. Utilizing these extracts in such applications can offer health benefits and enhance the overall flavor of foods.

5. Acknowledgements

We acknowledge resources and support from the Faculty of Science, Prince of Songkla University.

Author Contributions: Conceptualization, P.M.; methodology, P.M. and B.K.; formal analysis, B.K.; investigation, B.K.; resources, P.M.; writing—original draft preparation, P.M. and B.K.; writing—review and editing, P.M.; supervision, P.M.; funding acquisition, P.M. All authors have read and agreed to the published version of the manuscript.

Funding: This research was supported by a Thesis Research Grant for graduate students, Faculty of Science, Prince of Songkla University.

Conflicts of Interest: The authors declare no conflict of interest.

References

[1] Alizadeh, B.; Savalan, Ş.; Khawar, K. M.; Özcan, S. Micropropagation of garlic chives (*Allium tuberosum* Rottl. ex Sprang) using mesocotyl axis. *Journal of Animal and Plant Sciences,* 2013; *23*(2), 543-549.

[2] Bunchauy, P. (2022, November 7). Report of Chinese chives growing in Thailand. Department of Agricultural Extension. http://production.doae.go.th

[3] Park, B. G.; Jung, H. J.; Cho, Y. W.; Lim, H. W.; Lim, C. J. Potentiation of antioxidative and anti-inflammatory properties of cultured wild ginseng root extract through probiotic fermentation. *Journal of Animal and Plant Sciences,* 2013; *65*(3), 457-464. https://doi.org/10.1111/jphp.12004

[4] Oh, M.; Kim, S.-Y.; Park, S.; Kim, K.-N.; Kim, S. H. Phytochemicals in Chinese chive (*Allium tuberosum*) induce the skeletal muscle cell proliferation via PI3K/Akt/mTOR and smad pathways in C_2C_{12} Cells. *International Journal of Molecular Sciences,* 2021; *22*(5), 2296. https://doi.org/10.3390/ijms22052296

[5] Yabuki, Y.; Mukaida, Y.; Saito, Y.; Oshima, K.; Takahashi, T.; Muroi, E.; Hashimoto, K.; Uda, Y. Characterisation of volatile sulphur-containing compounds generated in crushed leaves of Chinese chive (*Allium tuberosum* Rottler). *Food Chemistry,* 2010; *120*(2), 343-348. https://doi.org/10.1016/j.foodchem.2009.11.028

[6] Rattanachaikunsopon, P.; Phumkhachorn, P. Diallyl Sulfide Content and Antimicrobial Activity against Food-Borne Pathogenic Bacteria of Chives (*Allium schoenoprasum*). *Bioscience, Biotechnology, and Biochemistry,* 2008; *72*(11), 2987-2991. https://doi.org/10.1271/bbb.80482

[7] Kumar, N.; Goel, N. Phenolic acids: Natural versatile molecules with promising therapeutic applications. *Biotechnology reports,* 2019; 24, https://doi.org/10.1016/j.btre.2019.e00370

[8] Han, X.; Shen, T.; Lou, H. Dietary polyphenols and their biological significance. *International journal of molecular sciences,* 2007; *8*(9), 950-988. https://doi.org/10.3390/i8090950

[9] Gizaw, Z. Public health risks related to food safety issues in the food market: a systematic literature review. *Environmental Health and Preventive Medicine,* 2019; *24*(1), 1-21. https://doi.org/10.1186/s12199-019-0825-5

[10] Asavasanti, S.; Lawthienchai, N.; Tongprasan, T.; Tangduangdee, C.; Yasurin, P. Effect of extraction methods on antibacterial activity and chemical composition of Chinese chives (*Allium tuberosum* Rottl. ex Spreng) extract. *KMUTNB IJAST,* 2017; 10, 97-106. http://doi.org/10.14416/j.ijast.2017.05.001

[11] Kudo, H.; Takeuchi, H.; Shimamura, T.; Kadota, Y.; Sugiura, T.; Ukeda, H. *In vitro* anti-*Helicobacter pylori* activity of Chinese chive (*Allium tuberosum*). *Food Science and Technology Research,* 2011; *17*(6), 505-513. http://doi.org/10.3136/fstr.17.505

[12] Hernández, C.; Ascacio-Valdés, J.; De la Garza, H.; Wong-Paz, J.; Aguilar, C. N.; Martínez-Ávila, G. C.; Castro-López, C.; Aguilera-Carbó, A. Polyphenolic content, in vitro antioxidant activity and chemical composition of extract from *Nephelium lappaceum* L.(Mexican rambutan) husk. *Asian Pacific Journal of Tropical Medicine,* 2017; *10*(12), 1201-1205. https://doi.org/10.1016/j.apjtm.2017.10.030

[13] Arulmozhi, P.; Vijayakumar, S.; Kumar, T. Phytochemical analysis and antimicrobial activity of some medicinal plants against selected pathogenic microorganisms. *Microbial Pathogenesis,* 2018; 123, 219-226. https://doi.org/10.1016/j.micpath.2018.07.009

[14] Mohamed, S. A.; Saleh, R. M.; Kabli, S. A.; Al-Garni, S. M. Influence of solid state fermentation by *Trichoderma* spp. on solubility, phenolic content, antioxidant, and antimicrobial activities of commercial turmeric. *Toxicology and Applied Pharmacology,* 2016; *80*(5), 920-928. https://doi.org/10.1080/09168451. 2015.1136879

[15] Re, R.; Pellegrini, N.; Proteggente, A.; Pannala, A.; Yang, M.; Rice-Evans, C. Antioxidant activity applying an improved ABTS radical cation decolorization assay. *Free radical biology and medicine,* 1999; *26*(9-10), 1231-1237. https://doi.org/10.1016/S0891-5849(98)00315-3

[16] Jorgensen, J. H.; Turnidge, J. D. Susceptibility test methods: dilution and disk diffusion methods. *Manual of Clinical Microbiology*, 2015; 1253-1273. https://doi.org/10.1128/9781555817381.ch71

[17] Stéphane, F. F. Y.; Jules, B. K. J.; Batiha, G.; Ali, I.; Bruno, L. N. Extraction of bioactive compounds from medicinal plants and herbs. *Natural Medicinal Plants*, 2021. http://dx.doi.org/10.5772/intechopen.98602

[18] Jones, W. P., &Kinghorn, A. D. (2005). Extraction of plant secondary metabolites. *Natural products isolation*, 323-351. https://doi.org/10.1007/978-1-61779-624-1_13

[19] Rubab, M.; Chelliah, R.; Saravanakumar, K.; Barathikannan, K.; Wei, S.; Kim, J.-R.; Yoo, D.; Wang, M.-H.; Oh, D.-H. Bioactive Potential of 2-Methoxy-4-vinylphenol and Benzofuran from *Brassica oleracea* L. var. *capitate f, rubra* (Red Cabbage) on Oxidative and Microbiological Stability of Beef Meat. *Foods,* 2020; *9*(5), 568. https://doi.org/10.3390/foods9050568

[20] Gatto, M. A.; Sergio, L.; Ippolito, A.; Di Venere, D. Phenolic extracts from wild edible plants to control postharvest diseases of sweet cherry fruit. *Postharvest Biology and Technology,* 2016; 120, 180-187. https://doi.org/10.1016/j.postharvbio.2016.06.010

[21] Haminiuk, C. W.; Maciel, G. M.; Plata-Oviedo, M. S.; Peralta, R. M. Phenolic compounds in fruits–an overview. *International Journal of Food Science & Technology,* 2012; *47*(10), 2023-2044. https://doi.org/10.1111/j.1365-2621.2012.03067.x

[22] Marañón, G.; Muñoz-Escassi, B. Manley, W. García, C. Cayado, P. de la Muela, M. S. Olábarri, B. León, R., &Vara, E. The effect of methyl sulphonyl methane supplementation on biomarkers of oxidative stress in sport horses following jumping exercise. *Acta Veterinaria Scandinavica,* 2008; *50*(1), 45. https://doi.org/10.1186/1751-0147-50-45

[23] Amirshahrokhi, K.; Bohlooli, S.; Chinifroush, M. M. The effect of methylsulfonylmethane on the experimental colitis in the rat. *Toxicology and Applied Pharmacology,* 2011; *253*(3), 197-202. https://doi.org/10.1080/09168451.2015.1136879

[24] Kim, J. H.; Shin, H. J.; Ha, H. L.; Park, Y. H.; Kwon, T. H.; Jung, M. R.; Moon, H. B.; Cho, E. S.; Son, H. Y.; Yu, D. Y. Methylsulfonylmethane suppresses hepatic tumor development through activation of apoptosis. *World Journal of Hepatology,* 2014; *6*(2), 98-106. https://doi.org/10.4254/wjh.v6.i2.98

[25] Kim, L. S.; Axelrod, L. J.; Howard, P.; Buratovich, N.; Waters, R. F. Efficacy of methylsulfonylmethane (MSM) in osteoarthritis pain of the knee: a pilot clinical trial. *Osteoarthritis Cartilage,* 2006; *14*(3), 286-294. https://doi.org/10.1016/j.joca.2005.10.003

[26] Poole, T. L.; Benjamin, R.; Genovese, K. J.; Nisbet, D. J. Methylsulfonylmethane exhibits bacteriostatic inhibition of *Escherichia coli*, and *Salmonella enterica* Kinshasa, *in vitro*. *Journal of Applied Microbiology,* 2019; *127*(6), 1677-1685. https://doi.org/10.1111/jam.14446

[27] Krishnan, K. R.; James, F.; Mohan, A. Isolation and characterization of n-hexadecanoic acid from *Canthium parviflorum* leaves. *Journal of Chemical and Pharmaceutical Research,* 2016; 8, 614-617. https://doi.org/10.4236/ajps.2017.810171

[28] Sung, W.-S.; Jung, H.-J.; Lee, I.-S.; Kim, H.-S.; Lee, D.-G. Antimicrobial effect of furaneol against human pathogenic bacteria and fungi. *Journal of Microbiology and Biotechnology,* 2006; *16*(3), 349-354.

[29] Čechovská, L.; Cejpek, K.; Konečný, M.; Velíšek, J. On the role of 2, 3-dihydro-3, 5-dihydroxy-6-methyl-(4 H)-pyran-4-one in antioxidant capacity of prunes. *European Food Research and Technology,* 2011; 233, 367-376. https://doi.org/10.1007/s00217-011-1527-4

[30] Somjai, C.; Siriwoharn, T.; Kulprachakarn, K.; Chaipoot, S.; Phongphisutthinant, R.; Wiriyacharee, P. Utilization of Maillard reaction in moist-dry-heating system to enhance physicochemical and antioxidative properties of dried whole longan fruit. *Heliyon,* 2021; *7*(5), 07094. https://doi.org/10.1016/j.heliyon.2021.e07094

[31] Mnayer, D.; Fabiano-Tixier, A.-S.; Petitcolas, E.; Hamieh, T.; Nehme, N.; Ferrant, C.; Fernandez, X.; Chemat, F. Chemical composition, antibacterial and antioxidant activities of six essentials oils from the *Alliaceae* family. *Molecules,* 2014; *19*(12), 20034-20053. https://doi.org/10.3390/molecules191220034

[32] Lachman, J.; Pronek, D.; Hejtmánková, A.; Dudjak, J.; Pivec, V.; Faitová, K. Total polyphenol and main flavonoid antioxidants in different onion (*Allium cepa* L.) varieties. *Horticultural Science,* 2003; *30*(4), 142-147. http://dx.doi.org/10.17221/3876-HORTSCI

[33] Štajner, D.; Čanadanović-Brunet, J.; Pavlović, A. *Allium schoenoprasum* L., as a natural antioxidant. *Phytotherapy Research,* 2004; *18*(7), 522-524. https://doi.org/10.1002/ptr.1472

[34] Parvu, M.; Toiu, A.; Vlase, L.; Alina Parvu, E. Determination of some polyphenolic compounds from *Allium* species by HPLC-UV-MS. *Natural Product Research,* 2010; *24*(14), 1318-1324. https://doi.org/10.1080/14786410903309484

[35] Sultana, F.; Mohsin, M.; Sah, A. In-vitro Antioxidant and Antimicrobial Activity of *Allium tuberosum* Rottler. ex Spreng. *International Journal of Advanced Research in Biological Sciences,* 2015; *2*(12), 178-187. http://s-o-i.org/1.15/ijarbs-2-12-20

[36] Nantarat, N.; Tragoolpua, Y.; Gunama, P. Antibacterial activity of the Mucus Extract from the Giant African Snail (*Lissachatina fulica*) and Golden Apple Snail (*Pomacea canaliculata*) against pathogenic bacteria causing skin diseases. *Tropical Natural History,* 2019; *19*(2), 103-112. https://doi.org/704761-1-10-20190930

[37] Gao, Q.; Li, X.-B.; Sun, J.; Xia, E.-D.; Tang, F.; Cao, H.-Q.; Xun, H. Isolation and identification of new chemical constituents from Chinese chive (*Allium tuberosum*) and toxicological evaluation of raw and cooked Chinese chive. *Food and Chemical Toxicology*, 2018; 112, 400-411. https://doi.org/10.1016/j.fct.2017.02.011

[38] Mau, J.-L.; Chen, C.-P.; Hsieh, P.-C. Antimicrobial effect of extracts from Chinese chive, cinnamon, and corni fructus. *Journal of Agricultural and Food Chemistry*, 2001; *49*(1), 183-188. https://doi.org/10.1021/jf000263c

ASEAN
Journal of Scientific and Technological Reports
Online ISSN:2773-8752

Research article

Efficient Conversion of Oil Palm Trunk and Frond to Bioethanol and Biogas Using Two-Stage Steam Explosion Pretreatment

Tussanee Srimachai[1,2,3], Chaiyoot Meengam[4], Prawit Kongjan[5], and Kiattisak Rattanadilok Na Phuket[1,2,3*]

[1] College of Innovation and Management, Songkhla Rajabhat University, Songkhla, 90000, Thailand; Tussnee.sr@skru.ac.th
[2] Community Innovation Learning and Transfer Center "Thung Yai Sarapee Model" Songkhla Rajabhat University, Satun campus, 91100, Thailand; Kiattisak.pa@skru.ac.th
[3] Microbial Resources and Utilization Center SKRU, Songkhla Rajabhat University, Songkhla, 90000, Thailand; panpong1@hotmail.com
[4] Faculty of Industrial Technology, Songkhla Rajabhat University, Songkhla, 90000, Thailand; Chaiyoot.me@skru.ac.th
[5] Faculty of Science and Technology, Prince of Songkhla University, Pattani, 94000, Thailand; Kprawit.kongjan@gmail.com
* Correspondence: Kiattisak.pa@skru.ac.th

Citation:
Srimachai, T., Meengam, C., Konjan, P., Rattanadilok Na Phuket, K. Efficient conversion of oil palm trunk and frond to bioethanol and biogas using two-stage steam explosion pretreatment. *ASEAN J. Sci. Tech. Report.* **2023**, *26*(4), 11-20. https://doi.org/10.55164/ajstr.v26i4.249622

Article history:
Received: May 26, 2023
Revised: August 16, 2023
Accepted: August 25, 2023
Available online: September 30, 2023

Abstract: Bioethanol and biogas production from oil palm trunk (OPT) and oil palm frond (OPF) investigated within a biorefinery concept. Firstly, bioethanol production from OPT and OPF pretreated two-stage steam explosion by comparing with enzyme hydrolysis and without enzyme hydrolysis in the SSF process, which used *S. cerevisiae* in fermentation. The amount of bioethanol increased rapidly, which was stable when the fermentation process entered 96 hrs, resulting in the highest amount of bioethanol produced from OPF and OPT equal to 0.31 and 0.40 g ethanol/g glucose of bioethanol yield, which was about 24.96% and 25.99% higher than the non-enzymatic fermentation of OPF and OPT. The total stillage from OPT and OPF distillation produced a methane yield of 164.38 ml/CH_4 g COD at 30 days of HRT and an organic loading rate (OLR) of 12.45 g COD/L-day. Biofuels in the biorefinery concept of OPF/OPT material at 1,000 kg produced bioethanol, biogas, and solid residue as 49 L at 95% bioethanol, 7,116 L at 63.05% of methane composition, and 13 kilograms of solid residue.

Keywords: Bioethanol; Biogas; Two-stage steam explosion; Biorefinery

1. Introduction

Problems arising from the use of renewable energy in the form of bioethanol are mainly problems such as raw material problems. Presently, bioethanol production mainly uses sugarcane and cassava, the main raw material that is a food source for humans [1]. Still, it would not be easy to use sugarcane and cassava to produce all bioethanol because it infringes on the food supply of people. It affects the food security of the country. Therefore, there should be new sources of raw materials to replace such raw materials to achieve food and energy security at the same time. Another exciting raw material is biomass from palm oil. The government has focused on promoting the planting area to 10 million rai by the year 2029 to increase the amount of palm bunch raw materials that will be supplied to the palm oil industry for crude oil for processing into biodiesel. The palm oil industry has a large amount of lignocellulose biomass waste. Significantly, the oil palm trunk is cut after the oil palm tree is over 25 years old and the oil palm leaf is cut down every 2

weeks or with the harvesting of the oil palm fruit. Each year, approximately 1,000 palm oil palms are cut down 20,000-45,000 rai with biomass from oil palm trunks of about 400,000-900,000 million trees and biomass from oil palm leaves of approximately 7,050,000 tons, which biomass not used maximizes the benefits in the industry. Considering the composition of biomass from different parts of oil palm trunk and oil palm fronds, it was found that the main constituents were cellulose 40-50%, hemicellulose 20-35%, and lignin 16-29% [2]. The hemicellulose content of palm oil palm trees is as high as 34%, with hemicellulose being an exciting part as its main constituents are pentose and hexose sugar. If processed or pretreated, it can be used as a substrate in the fermentation process to produce bioethanol. Biorefineries, which produce various products and co-products such as biofuels, heat, and electricity, have attracted attention in recent years [3]. Biorefineries can convert biomass into valuable biomaterials and energy carriers in an integrated manner. This maximizes the economic value of the biomass used while reducing the waste stream generated [4]. Developing several biofuel-based lignocellulosic biorefineries is a significant opportunity to increase material and energy efficiency and reduce the cost of biomass options to reduce greenhouse gas emissions [5]. However, the main problem of bioethanol production from lignocellulosic materials. is the problem of raw materials. There is also a problem with efficiency and the cost of the pretreatment process [6]. A good hydrolysis process will affect the bioethanol yield because good hydrolysis and pretreatment have the least amount of inhibitors to occur. Inhibitors in lignocellulosic hydrolysates consist of aliphatic acids (i.e., acetic, formic, and levulinic acid), for aldehydes (i.e., 5-hydroxymethylfurfural (HMF), and furfural), aromatic compounds (i.e.phenolics) and extractives; all of which affect ethanol fermentation [7]. These substances are toxic to fermenting microorganisms, resulting in decreased bioethanol yield. Jonsson and Matin [8] reported that the disadvantage of using sulfuric acid pretreatment was the formation of inhibitory by-products. Additionally, the advantage of hydrothermal pretreatment by controlling the pH around neutral values was the decreased amount of fermentation inhibitors [9].

In this experiment, the methods of conditioning and hydrolysis of oil palm biomass, including oil palm trunk and oil palm frond, were selected by the two-stage steam explosion, which is likely to be effective in destroying the structure of lignocellulose materials well and have less toxicity compared to other methods such as using acids or alkali pretreatment. In addition, this method is likely to cost less than using enzymes. Using two-step pretreatment can reduce the cost of the bioethanol production process.

2. Materials and Methods

2.1 Preparation of materials

Prepare raw materials from oil palm trunk (OPT) and oil palm frond (OPF) of fresh oil palm by OPTs are peeled and OPFs cut off leaves by using OPT and OPF aged 25-30 years from farmers in Khuan Kalong District, Satun Province. After that, it is cut into pieces about 50-100 cm be able to enter the chipper, which will obtain a sample size of about 2-4 cm. After that, the samples of OPT and OPF were squeezed by a screw press juicer. After that, the juice from the OPT and OPF is filtered and stored in a cold room at -20 °C for preservation. The residues or solids of OPT and OPF were dried at 103-105 °C for 24 hrs. The samples were stored in zipped plastic bags to prevent moisture.

2.2 Pretreatment method

Steam explosion pretreatment was performed in a 98 L capacity reactor with a maximum steam output of 12 bar. OPF and OPT samples amounting to 150 g were treated for the first and two steps by steam explosion pretreatment (Figure 1) by steam explosion conditions as in Table 1, then filtered to separate the solid from the solution to remove only the insoluble solids and washed with distilled water until the pH was neutral. The solids were then dried at 103-105°C for 24 hours to evaporate moisture. The samples were analyzed for cellulose, hemicellulose, and lignin content. Samples undergoing a 2-stage steam explosion are fed into the fermentation process for bioethanol. It will be divided into 2 parts to compare the use of enzymes and non-enzymes during fermentation.

Figure 1. Steam explosion equipment

Table 1. Conditions for pretreatment method using experiment

First-steam explosion pretreatment			Second- steam explosion pretreatment		
Temperature (°C)	Pressure (bar)	Time (min)	Temperature (°C)	Pressure (bar)	Time (min)
160	4	30	230	10	3

2.3 Inoculum

Yeast cultures were stored on YM agar medium at 4 °C (refrigerator). *Saccharomyces cerevisiae TISTR 5339* was transferred from a solid medium into a liquid medium (YM broth) and cultured at 37 °C for 48 hrs at a rate of 100 rpm. Then, it measured the turbidity at the absorbance (OD_{620}) using 10% (v/v) as the starter culture.

2.4 Simultaneous Saccharification and Fermentation (SSF) for bioethanol production

2.4.1 SSF without enzymatic hydrolysis

Take 10% by weight of the samples from section 2.2 (OPT and OPF) without enzymatic hydrolysis in a 250 ml flask, add 5 ml of 5M Citrate buffer (pH 4.8) and 85 ml of distilled water, and sterilize at 121 °C for 15 minutes. Set aside to cool to room temperature, 10% (v/v) *S. cerevisiae* and 1% (v/v) yeast extract (10.0 g/l) was added and shaken at 150 rpm for 72 hrs in a 250 ml flask. Samples were collected and analyzed at 0, 24, 48, 72, and 96 hrs for analysis of reducing sugar content and bioethanol content.

2.4.2 SSF using enzymatic hydrolysis

Take the sample from 10% by weight, put it in a 250 ml flask, and add 5 ml of 5M Citrate buffer (pH 4.8) and 85 ml of distilled water. Sterilized at 121 °C for 15 min, then 3% wt% of CellicR CTec2 (Cellulase + β-glucosidase) was added and incubated at 55 °C and shaken at 150 rpm for 72 hrs. Samples were analyzed at 0, 24, 48, 72, and 96 hrs. After that, 10% (v/v) *S. cerevisiae* and 1% (v/v) yeast extract (10.0 g/l) were added and stirred at 150 rpm for 48 hrs. Samples were collected and analyzed at 0, 24, 48, 72, and 96 hrs to explore reduced sugar and bioethanol content.

2.5 Biogas production

Take the total stillage from the bioethanol distillation process and operate the system with a 200-liter CSTR reactor for biogas production. The conditions will be studied in different HRTs as follows: 35, 30, 25, and 20 days to define the optimal conditions of the experiment in the highest biogas production.

2.6 Analytical methods

The Van Soest method determined the chemical composition (cellulose, hemicellulose, and lignin) [10]. The chemical composition of the distillery slop was analyzed using the Standard method [11]. The total sugars were analyzed by high-performance liquid chromatography (HPLC) with a refractive index detector at 50 °C. 5.0 µl of samples were injected into a column (SH1011, 8.0x300 nm, Shodex) with 0.04 N H_2SO_4 as the mobile phase (flow rate 0.8 ml/min). The running time of the samples was 20 min. The dichromate reagent

method determined the bioethanol concentration [12]. pH was measured by using a pH meter (Horiba, Japan). Chemical oxygen demand (COD), total solid (TS), volatile solid (VS), total nitrogen (TN), protein, carbohydrate, and fat were analyzed following the procedures explained in the Standard Method [11]. The volume of biogas was measured by water replacement and biogas composition was monitored by gas chromatograph GC-8APT with a thermal conductivity detector (TCD)[13]. Gas chromatograph GC-8APF analyzed the VFA with a flame ionization detector (FID) [13].

3. Results and Discussion

3.1 Effect of pretreated first-steam explosion

OPF (untreated) before conditioning contained cellulose hemicellulose and lignin were 35.83, 26.79, and 26.33 percent, respectively, and OPT (untreated), before pretreatment, had cellulose hemicellulose and lignin were 43.76, 29.53, and 21.64 %, respectively (Table 1) which cellulose after pretreatment of OPF and OPT increased as 44.17 and 53.82 %. Because the result of the first-steam explosion pretreatment caused internal swelling to increase the reaction surface area of cellulose was increased porosity, reduced crystallinity, and degraded macro polymerization (Figure 2), affecting the amount of cellulose increased. After pretreatment, hemicellulose of OPF and OPT was decreased by 18.35% and 20.62% due to the hemicellulose portion dissolving with steam when pretreated by steam explosion. Lignin after pretreatment of OPF and OPT increased to 35.00% and 23.77% due to the limitation of the steam explosion pretreatment. Degradation of lignin is often incomplete because the pressure used for first-steam explosion pretreatment was not high enough when reducing the pressure effect of lignin did not escape.

Table 1. Effect of two-stage steam explosion pretreatment on the chemical composition of OPT and OPF.

Pretreatment	Composition	Percent (w/w)		
		Raw material (Untreated)	First stream explosion	Second stream explosion
OPF	Cellulose	35.83 ± 1.53	44.17 ± 3.25	55.15 ± 1.27
	Hemicellulose	26.73 ± 1.32	18.35 ± 3.50	5.78 ± 1.50
	Lignin	26.33 ± 1.25	35.00 ± 2.17	38.44 ± 2.17
OPT	Cellulose	43.76 ± 1.05	53.82 ± 2.45	63.22 ± 2.14
	Hemicellulose	29.53 ± 1.28	20.62 ± 5.50	4.58 ± 1.25
	Lignin	21.64 ± 1.32	23.77 ± 3.82	31.08 ± 1.58

3.2 Effect of pretreated second-steam explosion

Take the sample in the first stream explosion for further conditioning with the second stream explosion (230 °C, pressure 10 bar, for 3 mins). The results showed that by steam explosion pretreatment in step 2, the cellulose content of OPF and OPT increased by 55.15% and 63.22% (Table 1). The second pretreatment resulted in a marked decrease in hemicellulose after the pretreatment of OPF and OPT to only 5.78% and 4.58%. The hemicellulose content decreased due to the dissolution of the hemicellulose by the second steam explosion pretreatment (Figure 3). The lignin content after the pretreatment of OPF and OPT increased to 38.44 and 31.08 percent because the condition of the steam explosion was more severe. Still, the second steam explosion pretreatment depolymerized lignocellulose polymer structures and breakage of crosslinking between macromolecules affecting the amount of cellulose enhanced.

SEM images of untreated OPF and OPT are shown in A1 and A2 in Figures 2 and 3. It observed that the structure of the tested sample remains intact and firmly connected. The untreated samples contain higher amounts of lignin, which protects cellulose and hemicellulose from degradation. Therefore, lignin removal in sugar recovery required pretreatment by steam explosion. After the second-steam explosion pretreatment, the structure mesocarp fiber of OPT and OPF was destroyed, and the wall of the fibers was ruptured entirely, as shown in B1 and B2 in Figures 2 and 3. Jacque et al. [14] reported that pretreated steam explosion is a thermo-mechanicochemical pretreatment that allows the destruction of lignocellulose structure by heating, the formation of organic acids in the process, and shearing forces resulting in the expansion of the moisture, resulting in

more surface area and higher effect to enhance the enzyme hydrolysis process, increased to produce reducing sugar in bioethanol production.

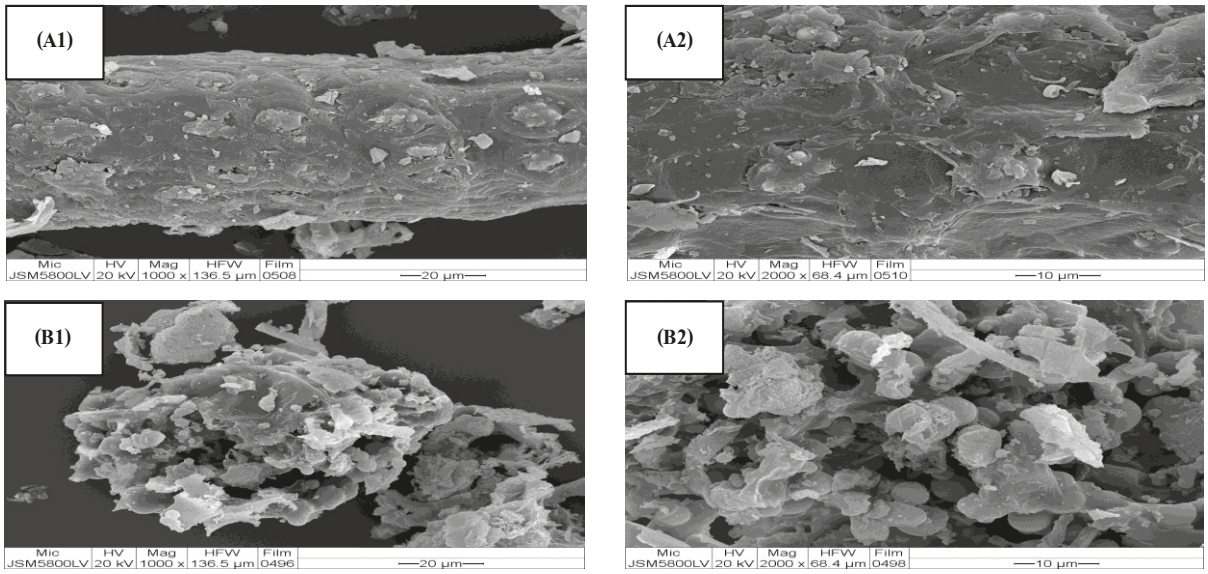

Figure 2. Morphology of OPT at 1,000 and 2,000 x magnification: (A1) and (A2) Untreated OPT, (B1) and (B2) Pretreated first-steam explosion

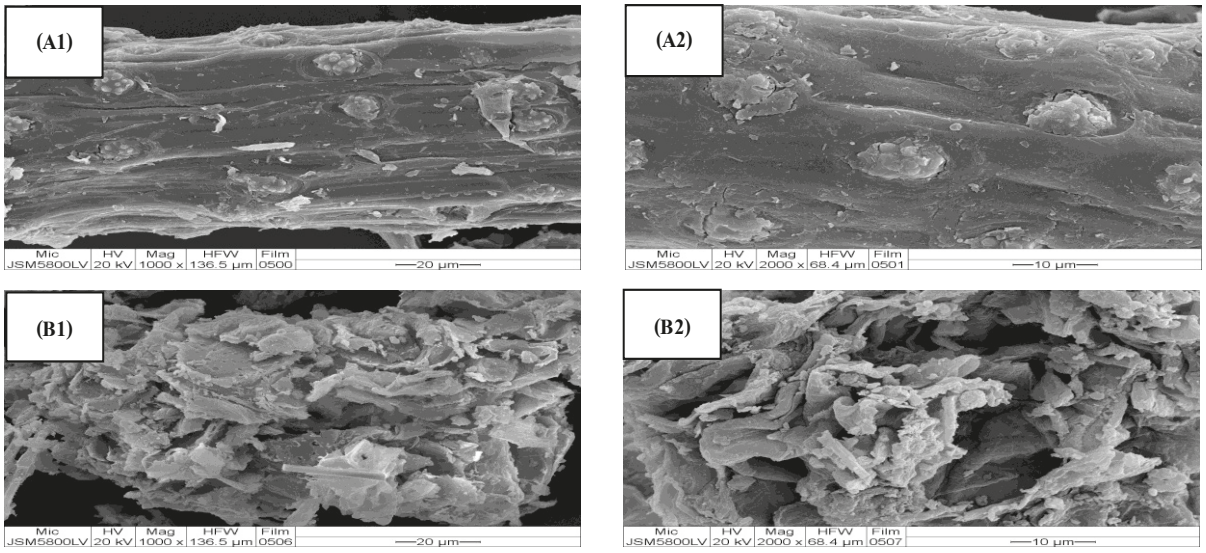

Figure 3. Morphology of OPF at 1,000 and 2,000 x magnification: (A1) and (A2) Untreated OPF, (B1) and (B2) Pretreatted second-steam explosion pretreatment

3.3 SSF without enzymatic hydrolysis to produce bioethanol

After a two-stage steam explosion, samples of OPF and OPT were studied in SSF by non-adding enzymatic to hydrolysis process for producing bioethanol. As a result of the two-stage steam explosion, the cellulose content explodes violently and breaks down to more glucose without the use of enzymes. The glucose contents of OPF and OPT after the two-stage steam explosion were 21.75 and 35.65 g/l, which the *S. cerevisiae* could use for bioethanol production. After 96 hours, 27.12 and 35.44 g/l of bioethanol (0.25 and 0.33 g ethanol/g glucose of bioethanol yield) from OPF and OPT could be produced without enzyme addition (Figure 4). The maximum bioethanol content of sugarcane bagasse was 21 g/l by H_2O_2 pretreatment using *S. cerevisiae* in SSF fermentation [15]. Zuo et al. [16] reported that corn stover could produce bioethanol 36.1 g/l by 1 % NaOH+8 % NH_4OH pretreatment using *Pichiastipitis* in SSF fermentation, similar to this experiment.

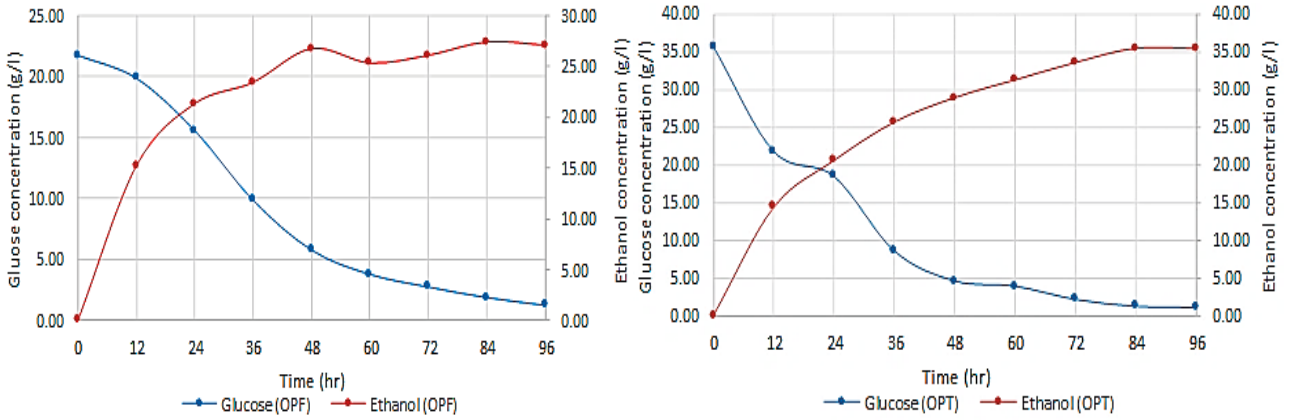

Figure 4. Glucose utilization and bioethanol production of OPF and OPT after the two-stage steam explosion (without enzyme)

3.4 SSF using enzymatic hydrolysis to produce bioethanol

Samples of OPF and OPT after a pretreated two-stage steam explosion were studied in SSF, in which enzymes are added to the hydrolysis process to produce bioethanol. Samples were collected and analyzed for glucose and bioethanol content at 0, 12, 24, 36, 48, 60, 72, 84, and 96 hrs. The experimental results showed cellulose was digested into glucose after adding an enzyme. The OPF glucose content increased from 21.75 to 35.76 g/l, and OPT increased from 35.65 to 46.88 g/l within 12 hours. After 12 hrs, the glucose decreased sharply because of the use of glucose by *S. cerevisiae* to produce bioethanol. As a result, the amount of bioethanol increased rapidly, which was stable when the fermentation process entered 96 hrs, resulting in the highest amount of bioethanol produced from OPF and OPT were 33.89 and 44.65 g/l (Figure 5) or 0.31 and 0.40 g ethanol/g glucose of bioethanol yield, which was about 24.96% and 25.99% higher than compared with the non-enzymatic fermentation (27.12 and 35.44 g/l of bioethanol) of OPF and OPT, respectively. Similarly, enzymatic hydrolysis and subsequent fermentation of cellulose yielded 0.41 g-ethanol/g-glucose from wheat straw[17].

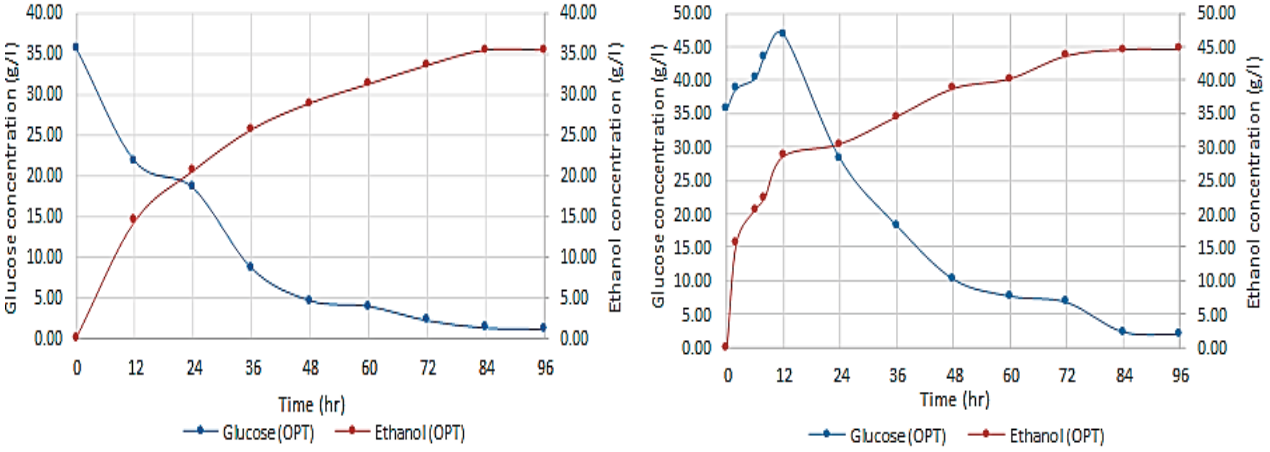

Figure 5. Glucose utilization and bioethanol production of OPF and OPT after the two-stage steam explosion (using enzyme)

3.5 Biogas production from total stillage

Total stillage is the total wastewater obtained after distillation of OPF and OPT of the bioethanol. The chemical characterization of the total stillage is shown in Table 2. The total stillage was operated in a CSTR reactor sizing 200 L to produce biogas in a continuous system. The operation was performed during the HRT as follows: 35, 30, 25, and 20 days, respectively. During 30 days of HRT, the daily methane production and maximum methane production were 116,000 ml CH_4/day (116 L CH_4/day) at 63.05 percent methane

concentration (Figures 6 and 7), followed by a hydraulic retention time of 35 days, with the highest daily methane yield and methane production rate of 88,000 ml CH_4/day (88 L CH_4/day) at 59.06% methane concentration. At 25 days of HRT, the maximum methane production was 64,000 ml CH_4/day (64 L CH_4/day) at 54.20% methane concentration. HRT at 20 days had the highest daily methane yield and methane production rate of 40,000 ml CH_4/day (40 L CH_4/day) at 52.87 % concentration of methane gas, respectively. Daily methane yield from continuous fermentation of distillery slop was studied using a 200-liter CSTR reactor. It found that day 63 yielded the highest daily methane yield. The 30-day of HRT yielded the highest daily methane yield of 164.38 ml/CH_4 g COD (Figure 7), which was calculated from the organic loading rate (OLR) of 12.45 g COD/L-day, followed by the hydraulic retention time of 35 days, 25, and 20 days, which result in the highest daily methane yield of 149.88 ml/CH_4 gCOD, 70.87 ml/ CH_4 gCOD and 32.07 ml/CH_4 g COD, calculated from organic loading rates (OLR) of 9.96, 16.44 and 24.90 g COD/L-day, respectively. At 30 days of HRT (optimal), the methane yield was 164.38 ml CH_4/g COD. Kaparaju et al. [17] reported that methane yield from the stillage of wheat straw fermentation was 381 ml CH_4/g VS-added.

Table 2. The chemical characterization of the total stillage

Chemical characterization	Total stillage	Stillage wheat straw [17]
pH	4.8	4.0
COD (g/L)	153	170.7
VFA (g/L)	5.25	0.37
TKN (g/L)	13.28	6.20
TS (g/L)	28	19.6
VS (g/L)	18	17.8
Protein (g/L)	10.54	38.80
Carbohydrate(g/L)	81.22	129.30
Lipids(g/L)	1.67	0.93
C/N ratio	13	-

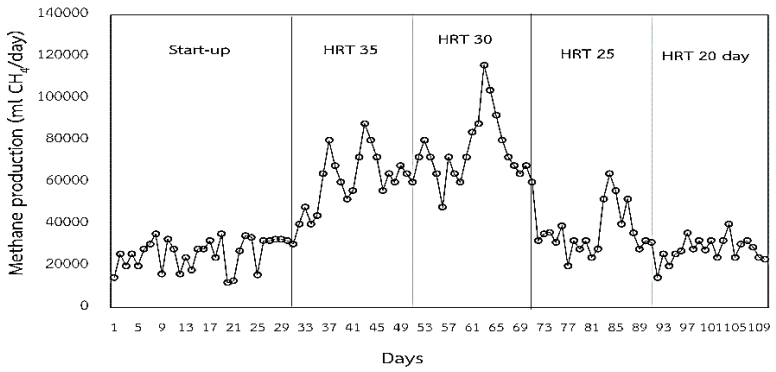

Figure 6. Methane production in a continuous system

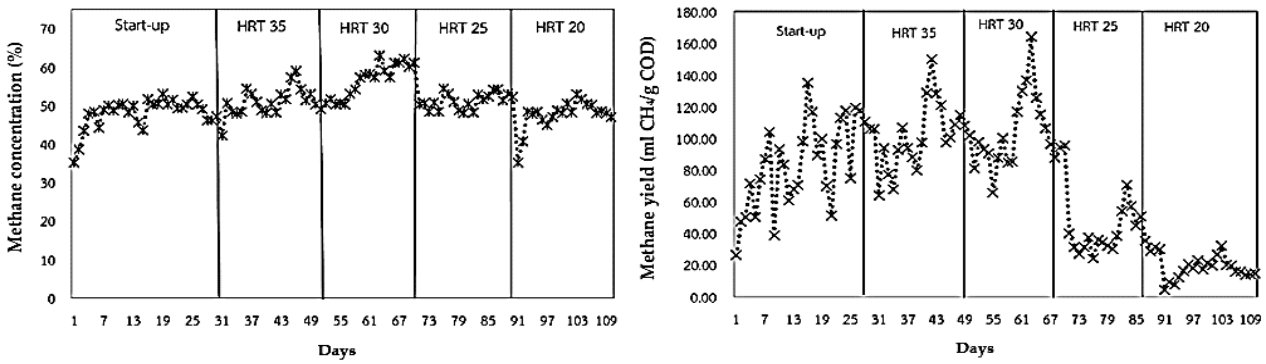

Figure 7. Methane concentration and methane yield in a continuous system

The volatile fatty acid (VFA) content study results showed that VFA composition increased with increasing organic matter input rate. The retention period was 30 days (maximum methane production). The VFAs in the system consisted of acetic and butyric acid as the major constituents, which ranged from 50-130 mg/l (Figure 8), indicating that methane-producing microorganisms were good efficiently for using volatile fatty acids to produce methane. There is no accumulation of volatile fatty acids in the system, which results in the pH value of the system being neutral. This corresponds to the pH in the 30-day retention period, which is 7.6-7.9 (Figure 8), indicating that the pH in the system is neutral. It is suitable for the growth of methane-producing microorganisms. The optimum pH range for methanogenesis in anaerobic systems is usually between 6 and 8 [18]. Franke Whittle et al. [19] noted that accumulation in most situations reflects an imbalance between acid producers and consumers. This leads to decreased pH within the system, inhibiting methanogen growth. Mass flow rates in the studied biorefinery concept were calculated based on the number of sugars and their conversion to various biofuels/products [17]. So, biofuels in the biorefinery concept of OPF/OPT material at 1,000 kg could produce bioethanol, biogas, and solid residue as 49 L at 95% bioethanol, 7,116 L at 63.05% of methane composition, and 13 kilograms of solid residue (Figure 9).

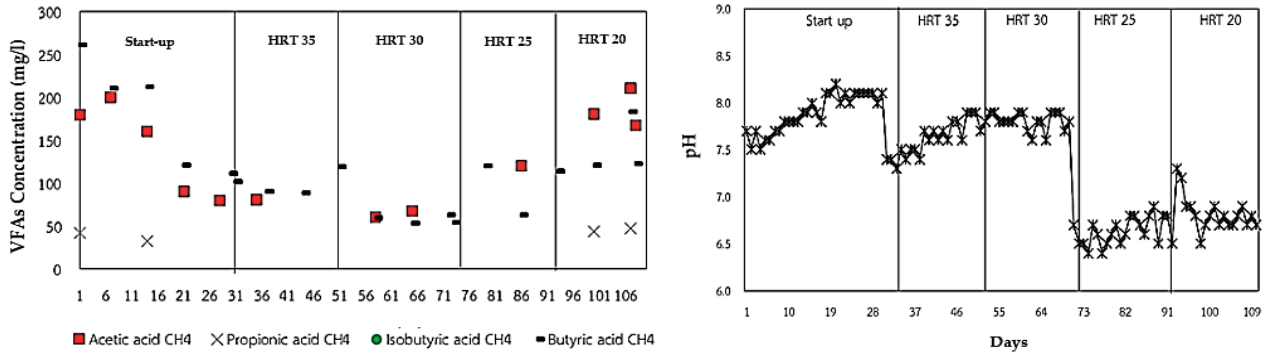

Figure 8. VFA concentration in a continuous system

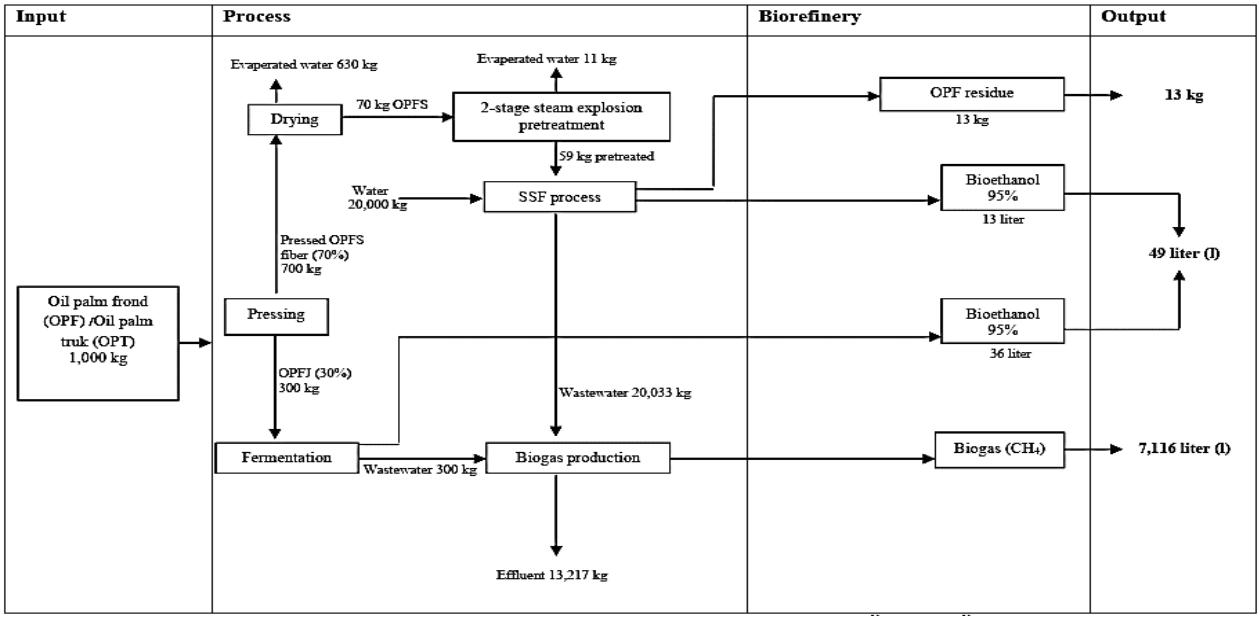

Figure 9. Mass flow in the biorefinery process

4. Conclusions

Two-stage steam explosion pretreatment of OPF and OPT could destroy the pores structure formed on the fiber when the lignin was solubilized and removed, resulting in more surface area and higher effect to enhance the enzyme hydrolysis process, increased to produce reducing sugar in bioethanol production. The optimization in bioethanol production compared between using enzyme and without enzyme SSF, without enzyme could produce maxed bioethanol from OPF and OPT was 27.12 (0.25 g ethanol/g glucose) and 35.44 g/l (0.33 g ethanol/g glucose) and with enzyme could produce maxed bioethanol 33.89 and 44.65 g/l (0.31 and 0.40 g ethanol/g glucose) of OPF and OPT which were 24.96 and 25.99 % higher than those of without enzymatic fermentation. Methane yield from total stillage in the CSTR reactor was 164.38 ml/CH_4 g COD. Increasing sugar content discharged from OPF and OPT by two-stage steam explosion pretreatment has produced biofuels (bioethanol and biogas) in production-based biorefineries.

5. Acknowledgements

The authors would like to thank Songkhla Rajabhat University and the Faculty of Science and Technology, Prince of Songkhla University (Pattani campus), for the opportunity to use the laboratory to do this research.

Author Contributions: Conceptualization, K.R.; methodology T.S. and K.R.; formal analysis, T.S.; investigation, P.K., and C.M.; writing—original draft preparation, K.R.; writing—review and editing, K.R.

Funding: The Energy Policy and Planning Office (EPPO) for funding this research.

Conflicts of Interest: The authors declare no conflict of interest.

References

[1] Shafiel, M.; Kabir, M.M.; Zilouei, H.; Horvath, I.H.; Karimi, K. Techno-economical study of biogas production improved by steam explosion pretreatment. *Bioresource Technology*. 2013; 148, 53–60. https://doi.org/10.1016/j.biortech.2013.08.111

[2] Zahari, M.A.K.M.; Zakaria, M.R.; Ariffin, H.H.; Mokhtar, M.N.; Salihon, J.; Shirai, Y.; Hassan, M.A. Renewable sugars from oil palm frond juice as an alternative novel fermentation feedstock for value-added products. *Bioresource Technology*. 2012; 110, 566–571. https://doi.org/10.1016/j.biortech.2012.01.119

[3] Zhang, Y. Reviving the carbohydrate economy via multi-product lignocellulose biorefineries. *Journal of Industrial Microbiology and Biotechnology*. 2008; *35*(5), 367–375. https://doi.org/10.1007/s10295-007-0293-6

[4] Thomsen, M. Complex media from processing of agricultural crops for microbial fermentation. *Applied Microbiology and Biotechnology*. 2005; *68*(5), 598–606. https://doi.org/10.1007/s00253-005-0056-0

[5] Sheehan, J.; Aden, A.; Paustian, K.; Killian, K.; Brenner, J.; Walsh, M.; Nelson, R. Energy and environmental aspects of using corn stover for fuel ethanol. *Journal of Industrial Ecology*. 2003; 7 (3–4), 117–146. https://doi.org/10.1162/108819803323059433

[6] Taherzadeh, M.J; Karimi, K. Enzyme-based hydrolysis processes for ethanol from lignocellulosic materials: a review. *Bioresource Technology*. 2007; 2, 707–738. https://doi.org/10.15376/biores.2.4.707-738

[7] Bellido, C.; Bolado, S.; Coca, M.; Lucas, S.; Gonzalez-Benito, G.; Garcia-Cubero, M.T. Effect of inhibitors formed during wheat straw pretreatment on ethanol fermentation by Pichiastipitis. *Bioresource Technology*. 2011; 102, 10868–10874. https://doi.org/10.1016/j.biortech.2011.08.128

[8] Jönsson, L.J.; Matin, C. Pretreatment of lignocellulose: Formation of inhibitory by-products and strategies for minimizing their effects. *Bioresource Technology*. 2016; 199, 103-112. https://doi.org/10.1016/j.biortech.2015.10.009

[9] Hu, F.; Ragauskas, A. Pretreatment and lignocellulosic chemistry.BioEnergy Research. 2012; 5, 1043–1066. https://doi.org/10.1007/s12155-012-9208-0

[10] Van Soest, P.J. Use of detergent in the analysis of fibrous feeds. A rapid method for the determination of fibre and lignin. *Journal of the Association of Official Analytical Chemists*. 1963; *46*(5), 829–835. https://doi.org/10.1093/jaoac/46.5.829

[11] APHA. *Standard methods for the examination of water and wastewater*. 21st ed. Washington DC: USA. 2012.

[12] William, M.B.; Reese, D. Colorimetric determination of ethyl alcohol. *Analytical Chemistry*. 1950; 22, 1556. https://doi.org/10.1021/ac60048a025
[13] O-Thong, S.; Hniman, A.; Prasertsan, P.; Imai, T. Biohydrogen production from cassava starch processing wastewater by thermophilic mixed cultures. *Int J Hydrogen Energy*. 2011; 36, 3409-3416. https://doi.org/10.1016/j.ijhydene.2010.12.053
[14] Jacque, N.; Maniet, G.; Vanderghem†, C.; Delvigne, F.; Richel, A. Application of steam explosion as pretreatment on lignocellulosic material: A Review. Industrial & Engineering Chemistry Research. 2015; *54*(10), 2593-2599. https://doi.org/10.1021/ie503151g
[15] Rabelo, S.C.; Carrere, H.; Filho, R.M.; Costa, A.C. Production of bioethanol, methane and heat from sugarcane bagasse in a biorefinery concept. *Bioresource Technology*. 2011; 102, 7887–7895. https://doi.org/10.1016/j.biortech.2011.05.081
[16] Zuo, Z.; Tian, S.; Chen, Z.; Li, J.I.; Yang, X. Soaking pretreatment of corn stover for bioethanol production followed by anaerobic digestion process. *Apply Biochemistry & Biotechnology*. 2012; 167, 2088–2102. https://doi.org/10.1007/s12010-012-9751-3
[17] Kaparaju, P.; Serrano, M.; Thomsen, A.B.; Prawit Kongjan, P.; Angelidaki, I. Bioethanol, biohydrogen and biogas production from wheat straw in a biorefinery concept. *Bioresour Technol*. 2009; 100, 2562–2568. https://doi.org/10.1016/j.biortech.2008.11.011
[18] Ward. A.J.; Hobbs, P.J.; Holliman, P.J.; Jones, D.L. Optimisation of the anaerobic digestion of agricultural resources. *Bioresour Technol*. 2008; 99, 7928-7940. https://doi.org/10.1016/j.biortech.2008.02.044
[19] Franke-Whittle, I.; Walter, A.; Ebner, C.; Insam, H. Investigation into the effect of high concentrations of volatile fatty acids in anaerobic digestion on mechanic communities. *Waste Manage*, 2014; 34, 2080-2089. https://doi.org/10.1016/j.wasman.2014.07.020

ASEAN
Journal of Scientific and Technological Reports
Online ISSN:2773-8752

Research article

Period Change Analysis of a W UMa-type Binary: V417 Aquilae

Supanee Maichandee[1], Torik Hengpiya[2], and Wiraporn Maithong[3]*

[1] Faculty of Science and Agricultural Technology, Rajamangala University of Technology Lanna, Chiang Mai, 50300, Thailand; supanee_j@rmutl.ac.th
[2] Regional Observatory for the Public, Songkhla, National Astronomical Research Institute of Thailand (Public Organization), Songkhla, 90000, Thailand; torik@narit.or.th
[3] Faculty of Science and Technology, Chiang Mai Rajabhat University, Chiang Mai, 50300, Thailand; wiraporn_mai@cmru.ac.th
* Correspondence: wiraporn_mai@cmru.ac.th

Citation:
Maichandee, S., Hengpiya, T., Maithong, W. Period change analysis of a W UMa-type binary: V417 aquilae. *ASEAN J. Sci. Tech. Report.* **2023**, *26*(4), 21-28. https://doi.org/10.55164/ajstr.v26i4.249516

Article history:
Received: May 16, 2023
Revised: September 5, 2023
Accepted: September 6, 2023
Available online: September 30, 2023

Abstract: Light curve analysis investigated the orbital period variations of the short period, overcontact eclipsing binary system, and V417 Aquilae (V417 Aql). The system was observed using a 0.70-meter telescope with a CCD photometric system using B and V filters at the Regional Observatory for the Public, Songkhla, Thailand, on 2 July 2021 UT. The light curve constructed by the photometric method for each filter was analyzed to find the period change of the system. It is found that the V417 Aql system is undergoing a long-term decrease of rate 0.00251 seconds/year. The reduction in the period showed that the distance between the stars was decreased according to Angular Momentum Loss (AML) theory. V417 Aql residuals tend to be periodic, indicating there might be a third body in the system. The calculation shows that the third body's distance, period, and mass function are about 1.97 AU, 47.7 years, and 0.19Mʘ, respectively.

Keywords: Binary stars; V417 Aql

1. Introduction

V417 Aql [$\alpha(2000) = 19^h\ 35^m\ 24.1219^s$, $\delta(2000) = +05°\ 50'\ 17.656''$] are classified as W Ursae Majoris (W UMa) binaries. They are over-contact eclipsing binary stars with short orbital periods. The effective temperatures of both components are very similar. The depth of the primary eclipse and the second one are close. There are two types of W UMa: A-type (the brighter and hotter star has a smaller size and mass) and W-type (the brighter and hotter star has a bigger size and mass). Some binary star systems can return between A-type and W-type.

The V417 Aql system has a short period that constantly changes. The eclipsing binary V417 Aql system was discovered by Hoffmeister [1]. In 1937, Soloviev [2-3] classified it as W UMa type with a period of 0.37 days. Koch [4] identified it as a strongly interacting solar-type binary system. Many studies indicate that their period is decreasing and a third body may be in the system. Samec [5] concluded that V417 Aql was a W-type W UMa system with a 25-minute time of constant light in the primary minimum. The system consisted of a GO V spectral type primary component and an F9 V spectral type secondary component with a mass ratio of q≈0.37 and might evolve into an A-type W UMa binary. Lu et al. [6] found that the spectroscopic mass ratio value q equals 0.362. By combining the photometric solution of Samec et al. with their radial velocity solution, the following absolute parameters could be derived: $a=2.68R_\odot$, side radii $R_1=1.29\ R_\odot$, and $R_2=0.80\ R_\odot$, and mass $M_1=1.40M_\odot$, $M_2=0.50M_\odot$.

The degree of contact was 19%. According to the study of Qian [7], a long-term period of V417 Aql was decreased with the value of dP/dt equal to -5.50×10^{-8} days/year. The long-term period variation was consistent with the study of Qian [8]. There is a suggestion of no third body in the system. The asymmetries in the light curve may be caused by the components' solar-type magnetic activity, and V417 Aql is an A-type in a deep contact configuration [9].

The objective of this study is to analyze the change in the period of V417 Aql. In this paper, the light curve is obtained from photometric observations in B and V wavelength bands.

2. Materials and Methods

2.1 Light curve analysis

An eclipsing binary normally consists of stars orbiting each other in space concerning the Earth. The light of one can be obscured behind the other. The total light observed from the earth could be decreased when the eclipse occurs. The light curve is temporal data that records a decrease or increase in light from the binary system over a complete light cycle. It has been widely used to study the characteristics of the binary star. The curve indicates the orbital orientation of the system observed on the Earth. If the brighter star orbits behind the lesser one, there will be a significant decrease in minimum light, called the primary minimum: Min I. Likewise, if a less brightness star is obscured, the light curve will reduce to minimum light with less volume than the primary minimum. This minimum is called the secondary minimum: Min II. For the W UMa binary, in which the depth of the primary and secondary eclipse is close to each other, Min I and Min II are not much different.

2.2 O-C

The time of the minimum of the light curve will vary according to the number of periods according to the Linear Ephemeris equation as follows:

$$HJD = HJD_0 + PE \tag{1}$$

The period change is achieved from the analysis of the O-C diagram, which can be described as follows:

$$O\text{-}C = (P - P_{est})\, E \tag{2}$$

O and C are observed, and the time of minimum light. At the same time, Pest and P are the orbital periods of a binary star system calculated from the ephemeris linear equation and observation, respectively. If the O-C diagram has a parabolic distribution, then

$$O\text{-}C = aE^2 + bE + c = (P - P_{est})E \tag{3}$$

$$\frac{dP}{dE}E + (P - P_{est}) = 2aE + b \tag{4}$$

So, the change in period dP/dE is equal to 2a. The value of "a" can be obtained from the quadratic polynomial fitting method.

2.3 Third body

Some binary star systems consist of more than two members, known as "multiple star systems." The third object could be a star or a planet. The existence of the third member affects some properties of the system. For example, the total mass comprises the masses of binary stars and the third body. The amount of light observed consists of the light from the three objects.

(The third body's light is considered constant). The small mass of the third body function can be calculated using the following equation.

$$f(m)=\frac{m_3^3}{m_1+m_2+m_3}\sin^3 i' = \frac{1}{P'^2}(a'\sin i')^3 \quad (5)$$

When m_1, m_2, and m_3 are the masses of the first, the second, and the third component, respectively. The i′ is the inclination, a′ is the distance of the third body from the binary system, and P′ is the orbital period of it.

3. Results and Discussion

V417 Aql was observed using a 0.70-meter telescope with a CCD photometric system using the standard B and V filters at the Regional Observatory for the Public, Songkhla, Thailand, on 2 July 2021 UT. The exposure time for each filter was 60 seconds.

The temporal flux of the binary archived from the observation using the standard B and V filters was plotted, as shown in Figure 1.

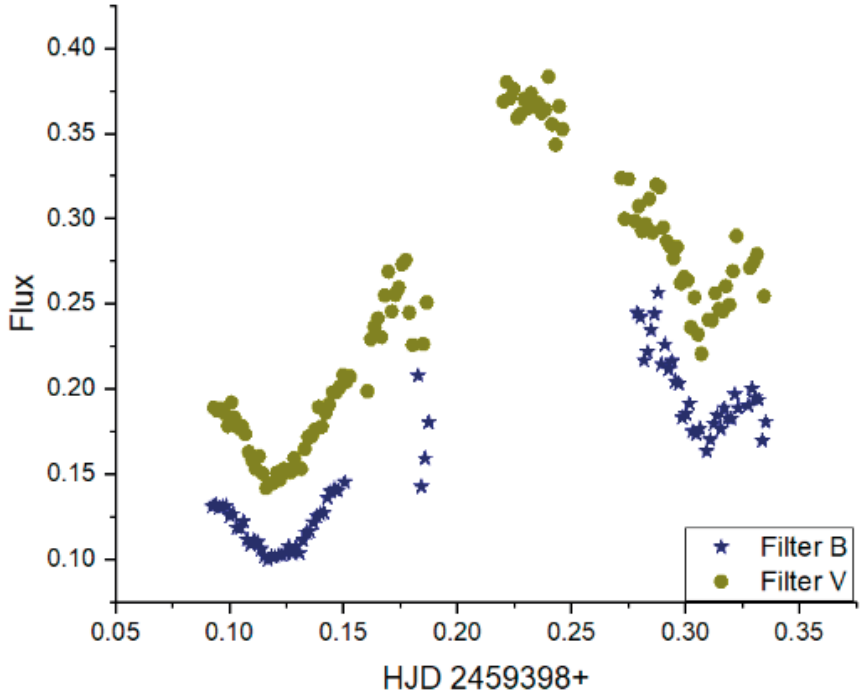

Figure 1. The light curve of V417 Aql in V filter (green dots) and B filter (blue dots)

The minimum time of V417 Aql can be obtained from the second-order ordinary differential equations. Each minimum is the average value of the minimum of B and V filters. The fittings of the light curve obtained from the observations using B and V filters considering only the first and secondary eclipse parts are shown in Figure 2.

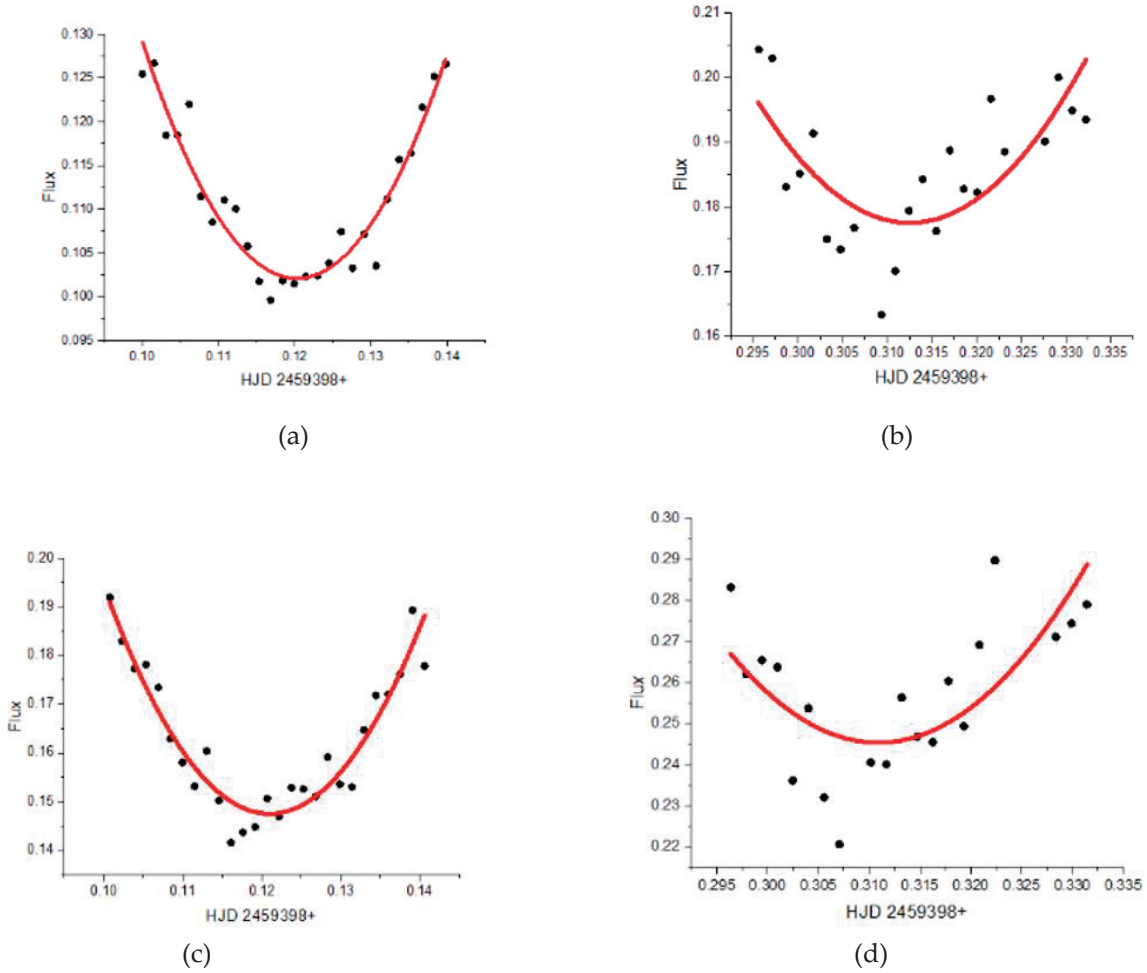

Figure 2. The ODE fits show the primary and secondary minimum eclipse depths obtained from the observation with B [(a) and (b)] and V [(c) and (d)] filters, respectively.

In the ordinary differential equation (ODE) from Figure 2, we got the average of the first time of minimum is equal to 0.120641822 and 0.311703 for the second one.

The following linear ephemeris (Eq.6) derived by Qian [7-8] along with the database of eclipsing binary O-C Files by Bob Nelson, AAVSO [10] was used to calculate the O–C values of all the times of minimum light.

$$\text{HJD Min} = 2449546.4983+0.37031178E \tag{6}$$

The corresponding O-C diagram is shown in Figure 3. The data during the secondary minimum seems to be very scattered; this could result from the existence of clouds along with the low transparency of the sky on the day of the observation.

The times of minimum light of V417 Aql are displayed in Table 1, and the O-C diagram is shown in Figure 3.

Table 1. The times of minimum light of V417 Aql.

HJD Min	Epoc	O-C	Source
2428427.127	-57031	-0.12017	CTAD 22
2428427.132	-57031	-0.11517	IBVS 6091
2428428.241	-57028	-0.11711	CTAD 22
2428429.165	-57025.5	-0.11889	Samec 1997
2428429.344	-57025	-0.12505	CTAD 22
2428430.266	-57022.5	-0.12882	Samec 1997
2428431.196	-57020	-0.1246	CTAD 22
2428460.253	-56941.5	-0.13708	Samec 1997
2428775.223	-56091	-0.11725	PZ 6.287
2428776.146	-56088.5	-0.12003	PZ 6.287
2430583.266	-51208.5	-0.12151	PZ 6.287
2430583.46	-51208	-0.11267	PZ 6.287
2431328.352	-49196.5	-0.10282	IODE 1.1.38
2431329.27	-49194	-0.11059	IODE 1.1.38
2431340.2	-49164.5	-0.10479	IODE 1.1.38
2431342.229	-49159	-0.11251	IODE 1.1.38
2431344.271	-49153.5	-0.10722	IODE 1.1.38
2431345.2	-49151	-0.104	IODE 1.1.38
2431346.306	-49148	-0.10894	IODE 1.1.38
2431347.232	-49145.5	-0.10872	IODE 1.1.38
2432385.409	-46342	-0.10079	IODE 1.1.41
2432392.441	-46323	-0.10472	IODE 1.1.41
2432415.399	-46261	-0.10605	IODE 1.1.41
2434922.819	-39490	-0.06711	AJ 61.47
2441135.405	-22713.5	-0.01668	BBSAG Bull...31
2441135.405	-22713.5	-0.01668	BBSAG Bull...31
2442990.498	-17704	-0.00055	BBSAG Bull.29
2443016.404	-17634	-0.01637	GCVS 4
2443016.414	-17634	-0.00637	BBSAG Bull.29
2443765.379	-15611.5	0.003053	BBSAG Bull.39
2444476.35	-13691.5	-0.02456	BBSAG Bull.49
2444486.367	-13664.5	-0.00598	BBSAG Bull.50
2444815.397	-12776	0.002001	BBSAG Bull.56
2444852.43	-12676	0.003823	BAVM 34
2444875.384	-12614	-0.00151	BAVM 34
2444878.347	-12606	-0.001	BAVM 34
2444885.383	-12587	-0.00093	BAVM 34
2445196.447	-11747	0.00128	Samec 1997
2445225.333	-11669	0.002861	BAVR 33.152
2445225.35	-11669	0.019861	IBVS 2344
2445542.689	-10812	0.002065	IBVS 2439
2445550.651	-10790.5	0.001762	IBVS 2439
2445554.723	-10779.5	0.000933	IBVS 2439
2445558.438	-10769.5	0.012415	BAVM 38
2445575.647	-10723	0.001717	IBVS 2439
2445583.434	-10702	0.01237	BAVR 33.157
2445605.642	-10642	0.001263	IBVS 2439
2445892.447	-9867.5	0.000189	BBSAG Bull.73
2445911.518	-9816	0.000132	BAVM 39

HJD Min	Epoch	O-C	Source
2445935.404	-9751.5	0.000623	Samec 1997
2445945.399	-9724.5	-0.0024	BAVM 39
2445962.622	-9678	0.001207	Samec 1997
2446263.13	-8866.5	0.001097	VSB 47
2446676.379	-7750.5	-0.01785	BBSAG Bull.81
2446679.347	-7742.5	-0.01234	BAVM 46
2446696.39	-7696.5	-0.00369	BBSAG Bull.82
2446702.311	-7680.5	-0.00767	BBSAG Bull.82
2446977.454	-6937.5	-0.00603	Samec 1997
2446982.457	-6924	-0.00304	BAVM 50
2447407.397	-5776.5	0.004697	BBSAG Bull.89
2447412.397	-5763	0.005488	BBSAG Bull.89
2447432.386	-5709	-0.00235	BBSAG Bull.90
2448163.382	-3735	-0.0018	BBSAG Bull.96
2448448.522	-2965	-0.00217	Samec 1997
2448476.49	-2889.5	0.007588	BAVM 60
2448490.365	-2852	-0.0041	BBSAG Bull.99
2448500.366	-2825	-0.00162	BAVM 60
2448500.366	-2825	-0.00152	Samec 1997
2448500.366	-2825	-0.00142	BAVM 60
2448843.46	-1898.5	-0.00139	BBSAG Bull.102
2449546.498	0	-0.0008	IBVS 4222
2449546.498	0	-0.0004	Samec 1997
2449546.498	0	0	IBVS 4222
2449568.531	59.5	-0.00055	IBVS 4222
2449568.531	59.5	-0.00045	IBVS 4222
2449568.531	59.5	-0.00045	Samec 1997
2449571.495	67.5	0.000655	BBSAG Bull.108
2449917.92	1003	-0.00102	Samec 1997
2449918.845	1005.5	-0.00139	Samec 1997
2449919.956	1008.5	-0.00143	Samec 1997
2449920.696	1010.5	-0.00195	Samec 1997
2449920.883	1011	-0.00091	Samec 1997
2449921.439	1012.5	-0.00048	IBVS 4383
2449921.808	1013.5	-0.00119	Samec 1997
2449922.918	1016.5	-0.00192	Samec 1997
2449959.382	1115	-0.01393	BBSAG Bull.113
2449962.361	1123	0.002571	BBSAG Bull.113
2450303.416	2044	-7.8E-05	IBVS 4472
2450312.488	2068.5	-0.00022	BBSAG Bull.114
2450315.451	2076.5	0.000389	IBVS 4472
2450315.452	2076.5	0.000989	IBVS 4472
2451016.453	3969.5	0.002489	IBVS 4711
2451378.435	4947	0.004724	BAVM 132
2451378.436	4947	0.005024	IBVS 5106
2451378.436	4947	0.005224	BAVM 132
2451388.435	4974	0.005706	IBVS 5106
2451747.453	5943.5	0.006236	IBVS 5296
2452448.457	7836.5	0.010136	IBVS 5594
2452469.377	7893	0.00802	IBVS 6158

HJD Min	Epoch	O-C	Source
2452469.563	7893.5	0.008565	IBVS 6158
2452470.488	7896	0.008085	IBVS 6158
2452489.376	7947	0.009764	IBVS 5594
2452489.376	7947	0.009784	IBVS 5594
2452498.078	7970.5	0.009558	VSB 40
2452498.449	7971.5	0.009946	IBVS 5364
2452504.378	7987.5	0.014357	IBVS 5438
2452511.41	8006.5	0.010733	IBVS 5364
2452847.469	8914	0.011693	IBVS 5676
2453194.083	9850	0.013367	VSB 43
2453222.412	9926.5	0.013916	IBVS 5741
2453547.174	10803.5	0.012785	VSB 44
2453584.022	10903	0.014363	VSB 44
2453601.057	10949	0.014921	VSB 44
2453910.452	11784.5	0.014829	IBVS 5802
2453910.452	11784.5	0.014829	IBVS 5802
2453933.414	11846.5	0.016698	IBVS 5761
2453971.001	11948	0.017953	VSB 45
2453973.037	11953.5	0.016538	VSB 45
2454297.431	12829.5	0.017918	IBVS 5801
2454299.467	12835	0.017104	IBVS 5801
2454307.432	12856.5	0.0201	IBVS 6089
2454317.062	12882.5	0.021894	VSB 46
2454326.504	12908	0.021644	BAVM 193
2454327.427	12910.5	0.018664	BAVM 193
2454607.201	13666	0.021915	VSB 48
2454706.445	13934	0.021957	BAVM 203
2454707.37	13936.5	0.021378	BAVM 203
2455028.06	14802.5	0.021277	VSB 50
2455041.392	14838.5	0.022752	IBVS 5918
2455056.389	14879	0.022025	IBVS 6088
2455385.414	15767.5	0.024809	IBVS 5984
2455418.371	15856.5	0.02426	IBVS 5984
2455418.557	15857	0.024405	IBVS 5984
2455795.535	16875	0.025213	BAVM 225
2456154.37	17844	0.028558	IBVS 6090
2456489.503	18749	0.028637	IBVS 6084
2456525.421	18846	0.027294	IBVS 6084
2456560.418	18940.5	0.029031	IBVS 6086
2456834.45	19680.5	0.030214	IBVS 6149
2456841.486	19699.5	0.03089	IBVS 6152
2456842.412	19702	0.03061	IBVS 6152
2456854.446	19734.5	0.030078	IBVS 6152
2456857.41	19742.5	0.030883	IBVS 6152
2456891.478	19834.5	0.03058	IBVS 6087
2456924.435	19923.5	0.030051	IBVS 6152
2456928.324	19934	0.030277	IBVS 6152
2456929.435	19937	0.030642	IBVS 6152
2459398.121	26603.5	0.032861	This work
2459398.312	26604	0.038805	This work

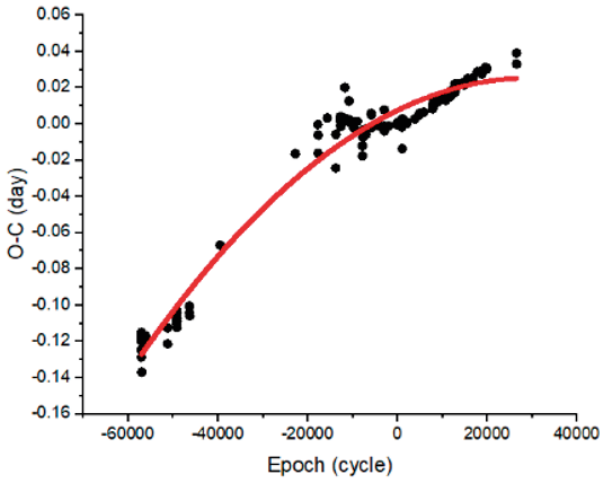

Figure 3. (O−C) diagram of V417 Aql constructed using the linear ephemeris in equation [6]

The quadratic fitting method in Figure 3 (red line), we got the corresponding equation as follows

$$O\text{-}C = [-2.02648\times10^{-11}(\pm1.39131\times10^{-12})]\ E^2 + [1.20521\times10^{-16}(\pm5.9625\times10^{-8})]\ E + 0.00723(\pm0.00087) \quad (8)$$

When compared with the O-C and E relation (Eq.4), we got the value of dP/dE, which is equal to 2a as:

$$\frac{dP}{dE} = 2\times(-2.02648\times10^{-11}) = -\ 0.00251 \text{ days/cycle}$$

The period of V417 Aql is decreasing with the rate -4.05296×10^{-11} days/cycle or -0.00251 second/year. The reduction of the period is according to the other studies [7-8]. The decrease in the period showed that the distance between the stars was decreased according to Angular Momentum Loss (AML) theory. Angular momentum loss through magnetic braking and mass transfer leads to a period decrease.

The residuals of V417 Aql are displayed in Figure 4. As shown in the figure, the plot reveals a cyclic variation.

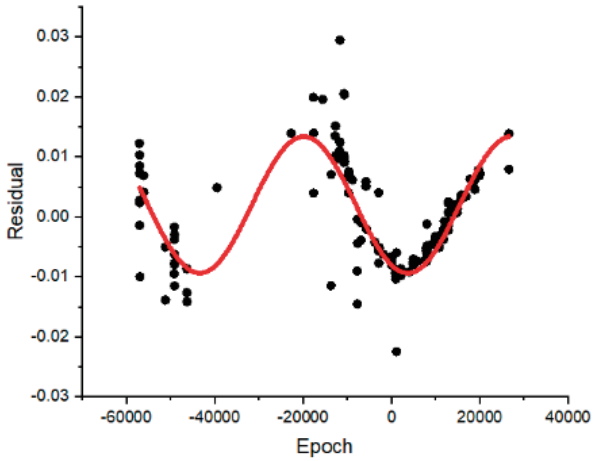

Figure 4. Residuals of V417 Aql

Residuals tend to be periodic. The probable causes of period oscillation might be from the light-time effect via the third body in the system. We can probably assume that a third body exists in the system and the period oscillation is caused by its existence. The best solution to the periodic oscillation is shown as follows:

$$\text{residual}=0.002+0.01139(\pm 0.00062)\ \sin\left(\pi \frac{\text{Epoch}-62475.65599}{2352.42087}(\pm 0.00897)\right) \quad [7]$$

According to equation [7], we can compute that the third body's distance and period are 1.966830392 AU and 47.70289105 years, respectively. A small mass function can be calculated using equation [7] along with the parameter archived from Lu et al. [6], then we got the mass function as 0.19121863MΘ. V417 Aql was observed using a 0.70-meter telescope with a CCD photometric system using the standard B and V filters at the Regional Observatory for the Public, Songkhla, Thailand, on 2 July 2021 UT. The exposure time for all filters was 60 seconds. The light cure obtained from B and V CCD photometric was analyzed. From the polynomial equation, we got the average of the first and second minimum times equal to 0.120641822 and 0.311703, respectively. The linear ephemeris derived by Qian [7-8], along with the database of eclipsing binary O-C Files by Bob Nelson, AAVSO [10] was used to calculate the O–C values of all the times of minimum light. The O-C diagram and quadratic and periodic fits are shown in Figure 5.

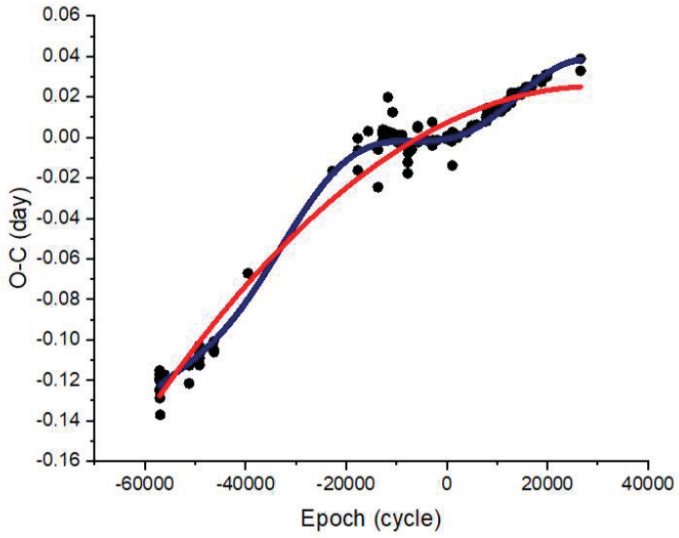

Figure 5. The O-C diagram and the solution for a binary system V417 Aql

The solution for the period change is as follows:

$$\text{O-C} = (-2.02648\times10^{-11})\ E^2 + (1.20521\times10^{-6})\ E + 0.00723 + 0.002 + 0.01139\ \sin\left(\pi \frac{\text{Epoch-62475.65599}}{2352.42087}\right) \quad [8]$$

The solution shows that the period of V417 ql is decreasing with the rate -4.05296×10^{-11} days/cycle or 0.00251 second/year. The decrease in the period showed that the distance between the stars was decreased according to Angular Momentum Loss (AML) theory. V417 Aql residuals tend to be periodic, indicating there might be a third body in the system. The sine-like term in equation [8] can fit the residuals so that we can assume the circular orbit of the third body. The calculation shows that the third body's distance, period, and mass function are about 1.97 AU, 47.7 years, and 0.19MΘ, respectively.

4. Conclusions

The comprehensive light curve analysis of V417 Aquilae (V417 Aql) has offered significant insights into the orbital variations of this short period, overcontact eclipsing binary system. Observations were meticulously conducted using a 0.70-meter telescope equipped with a CCD photometric system employing B and V filters at the Regional Observatory for the Public, Songkhla, Thailand, on 2 July 2021 UT. The detailed analysis of the constructed light curve for each filter provided an understanding of the period change of the V417 Aql system, revealing a notable long-term decrease at a rate of 0.00251 seconds/year. This consistent

reduction in the period underscores the diminishing distance between the stars, a phenomenon aligning with the Angular Momentum Loss (AML) theory. Furthermore, the analysis of V417 Aql residuals indicates a potential periodic tendency, suggesting the possible presence of a third body within the system. Calculations estimate the third body's distance, period, and mass function at approximately 1.97 AU, 47.7 years, and 0.19MΘ, respectively, reinforcing the hypothesis of its existence within the V417 Aql system. This extensive investigation augments our understanding of the V417 Aql system and contributes to the broader knowledge of orbital period variations and third-body influences in eclipsing binary systems. The findings pave the way for further research and observation, providing a foundation for exploring similar celestial systems' intricate dynamics and characteristics.

5. Acknowledgements

This research was funded by the Thailand Science Research and Innovation (TSRI) through Chiang Mai Rajabhat University, fiscal year 2023.

Author Contributions: Conceptualization, methodology, investigation, formal analysis, S.M. and W.M., writing—original draft preparation, S.M.; Observation, T.H., writing—review and editing and project administration, W.M.

Funding: Thailand Science Research and Innovation (TSRI) through Chiang Mai Rajabhat University, Fiscal Year 2023.

Conflicts of Interest: The authors declare no conflict of interest.

References

[1] Hoffmeister, C. *Astronomische Nachrichten*. 1935; 255, 401.
[2] Soloviev, A. *Tadjik Obs. Circ.* 1937; 22, 1.
[3] Soloviev, A. *Tadjik Obs. Circ.*1937; 25, 7.
[4] Koch, R. H. Blue CN-absorption measurements of close binary stars. *Astronomical Journal*. 1974; 79, 34.
[5] Samec, R. G.; Pauley, B. R.; Carrigan, B. J. U, B, V light curves of the short-period solar-type eclipsing binary, V417 Aquilae. *Astronomical Journal.* 1997; 113, 401.
[6] Lu, W.; Rucinski, S. M. Radial Velocity Studies of Close Binary Stars. I. *The Astronomical Journal*I. 1999; 118, 515.
[7] Qian, S. A period investigation of the overcontact binary system V417 Aquilae. *Astronomy & Astrophysics.* 2003; *400*(2), 649-653. https://doi.org/10.1051/0004-6361:20030018
[8] Qian, S. A possible relation between the period change and the mass ratio for W-type contact binaries. *Monthly Notices of the Royal Astronomical Society.* 2001; *328*(2), 635-644.
[9] Gazeas, K. D.; Baran, A.; Niarchos, P.; Zola, S.; Kreiner J. M.; Ogloza, W.; Drozdz, M. Physical parameters of components in close binary systems: IV. *Acta Astronomica.* 2005; 55,123-140.
[10] Bob Nelson's Database of Eclipsing Binary O-C Files, AAVSO. https://www.aavso.org/bob-nelsons-o-c-files

ASEAN
Journal of Scientific and Technological Reports
Online ISSN:2773-8752

Research article

The Off-cardinal Alignment of Chiang Mai City Plan in Relation to the Orion Belt

Chayapon Iemsonthi[1], Seksit Lorwilai[2], Panuwit Sankaokam[3], Orapin Riyaprao[4*], and Cherdsak Saelee[5*]

[1] Science Classroom Affiliated School Project, Chiang Mai University Demonstration School, Chiang Mai, 50200, Thailand; chayapon.i@satitcmu.ac.th
[2] Science Classroom Affiliated School Project, Chiang Mai University Demonstration School, Chiang Mai, 50200, Thailand; seksit.l@satitcmu.ac.th
[3] Science Classroom Affiliated School Project, Chiang Mai University Demonstration School, Chiang Mai, 50200, Thailand; panuwit.s@satitcmu.ac.th
[4] National Astronomical Research Institute of Thailand (Public Organization), Chiang Mai, 50180, Thailand; orapin@narit.or.th
[5] Faculty of Science, Chiang Mai University, Chiang Mai, 50200, Thailand; cherdsak.s@cmu.ac.th
* Correspondence: cherdsak.s@cmu.ac.th, orapin@narit.or.th

Citation:
Iemsonthi, C., Lorwilai, S., Sankaokam, P., Riyaprao, O., Saelee, C. The off-cardinal alignment of Chiang Mai city plan in relation to the Orion belt. *ASEAN J. Sci. Tech. Report.* **2023**, *26*(4), 29-37. https://doi.org/10.55164/ajstr.v26i4.249720.

Article history:
Received: June 5, 2023
Revised: September 11, 2023
Accepted: September 12, 2023
Available online: September 30, 2023

Abstract: Chiang Mai, the largest city in northern Thailand, was once the capital of the ancient Lanna kingdom, founded by King Mangrai on 19 April 1296 (Gregorian). The historic city plan, which may have been influenced by Vaastu Shastra (an ancient Hindu knowledge of architecture), features almost a square shape with each side length ranging from 1.52 -1.57 kilometers, bordered by four walls facing the cardinal directions. However, a careful examination reveals that the east-west orientation of the city plan is tilted southeastward with an azimuth of 92.5°, prompting further investigation as to which method was used in the city's orientation. Historically, two ways to lay out the directions were via the gnomon, such as the shortest shadow and the Indian circle methods, and via fixed stars. In this work, we carried out year-long measurements of the shortest shadow and the Indian circle methods and discovered that neither resulted in an error greater than 0.7°, allowing us to consider the orientation method as being associated with specific fixed stars. A theodolite and a GPS were used to identify the orientation axis along the northern city wall, calibrated using the positional astronomy program *Stellarium*. Using precession-corrected *Stellarium*, the ancient sky can be simulated to uncover the aligned star at the same azimuth as Mintaka (δ Ori) in the Orion's Belt at a height of 4° and possibly Alnilam (ε Ori) at a height of 1.5° (under an apparent sky condition) during the period between 1292 and 1296, which is close to when King Mangrai founded the city.

Keywords: Chiang Mai City Planning; Gnomon; Orion's Belt; Lanna Kingdom

1. Introduction

The capital of the Lanna kingdom, "Chiang Mai" (as it is now known), was established by King Mangrai in AD 1296. The Lanna inscriptions and historical data, including the Chiang Mai Chronicle (CMC) [1], all concur that King Mangrai entered the site on Thursday of the 8th Lanna lunar month, which is equivalent to the 5th Thai lunar month, 654 Culasakaraj (CS), which is equal to a Gregorian date as 3 April 1292. It was recognized as the starting date of the construction of his temporary residence, which was near the northeast corner of the Chiang Mai City Plan (now it is Wat Chiang Man; see the white circle in Figure 1: Top), where he would use to work on the city planning.

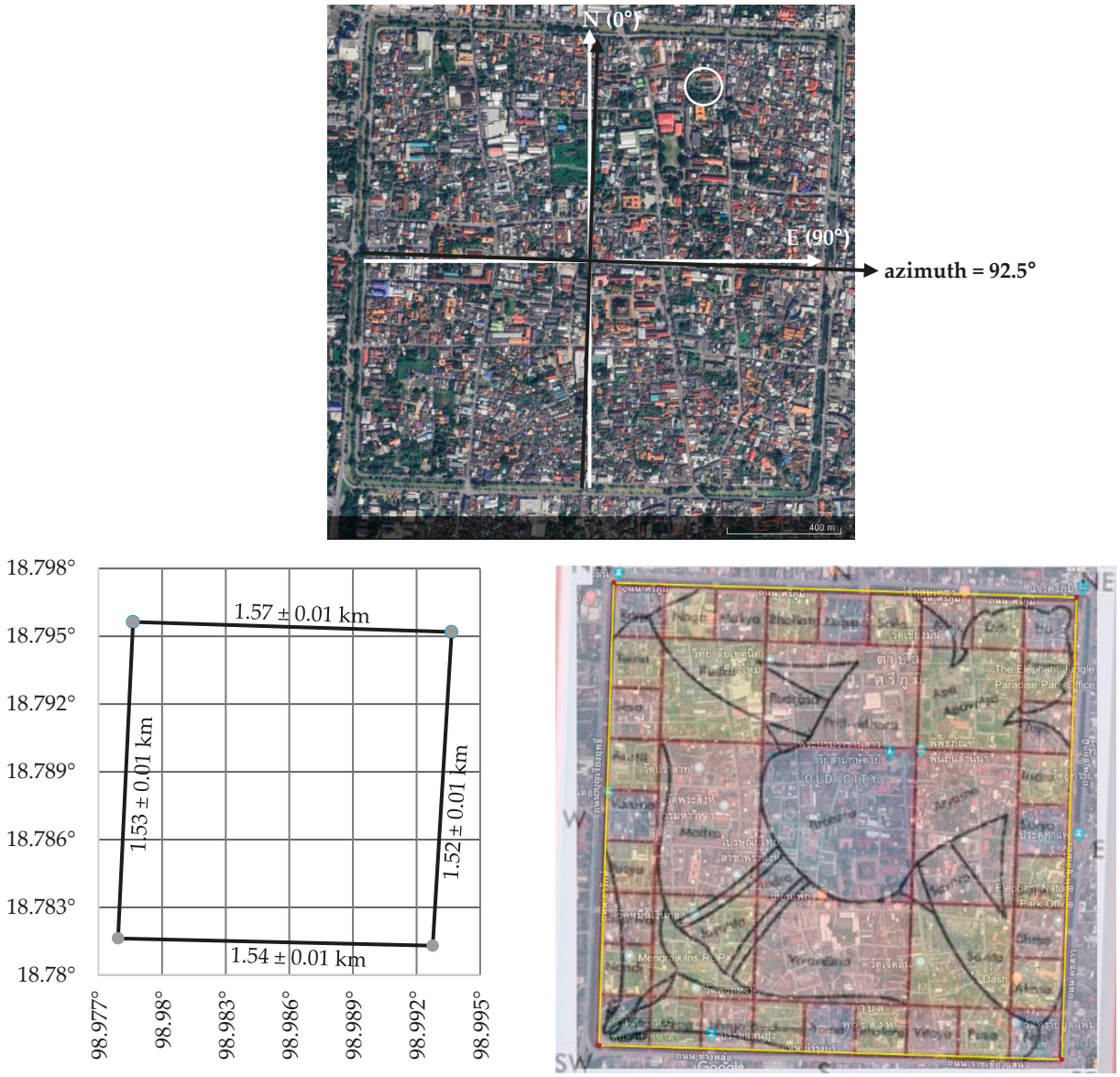

Figure 1. Top: The satellite image of the Chiang Mai old city surrounded by a moat with the east-west orientation of the city plan is tilted southeastward with an azimuth of 92.5° (image: from Google Earth). Bottom Left: Plotting of a geographic coordinate, i.e., latitude and longitude, for the GIS position collected on each of the four corners of the Chiangmai city wall and showing each side length calculated from these GPS positions. Bottom Right: Chiang Mai city site of square shape conforms well with the 9 ⊚ 9 grids of Paramasayika Mandala (image: modified after Saelee *et al*. [3])

According to the CMC, it took 4 years to plan the city before groundbreaking and installing Chiang Mai's main post on the full moon of the 8th Lanna lunar month, 658 CS. The Wat Chiang Man inscription [2] (Database of Inscriptions in Thailand | Wat Chiang Man Stale), however, was recorded otherwise on the waxing moon on the 8th day of the 8th Lanna lunar month, 658 CS, or 19 April 1296. Four months later, King Mangrai ordered to begin plowing the site from his sleeping chamber (presently Chiang Man Temple) to the northeastern corner known as the Sri Bhumi Corner, followed by the construction of four city walls and the five city gates. King Mangrai then ordered the construction of a perimeter wall and a moat, which were laid out in a rectangular shape of 900 *wa* by 1,000 *wa* (or 1.44 km by 1.6 km as 1 *wa* » 1.6 m) in the record. Once completed, the city hosted a festive celebration for three days and nights, naming it Nop Buri Sri Nakorn Ping [1].

Contrary to the record of the chronicle, the measurement of the actual size reported by Saelee *et al.* reveals a square shape with almost equal lengths in the 1.52 – 1.57 kilometers range [3], as shown in Figure 1: Bottom Left. The city plan is regarded as confidential information that could jeopardize national security if it leaks, which may be why the size differs from the CMC record. Saelee *et al*. [3] also suggest that the city planning may have been influenced by Vaastu Shastra, an ancient Hindu knowledge of architecture found in the book "Brihat Samhita" by Varaha Mihira [4]. The detailed comparison shows that the city planning followed Vaastu principles, i.e., selecting the site and selecting an auspicious day for site-plowing, which was determined by astronomical observation. The next step in Vaastu principles is to set the cardinal directions, which historically could be either using a gnomon or a fixed star, followed by the fixation of Vaastu-Purusha-Mandala, the metaphysical planning of the site. According to the analysis in the paper, the Chiang Mai city site, a square shape, bounded by moats and walls facing the cardinal directions on all four sides, conforms well with the 9 ⊚ 9 grids of *Paramasayika Mandala* [3] as illustrated in Figure 1: Bottom Right. In this work, we investigate further into the method of orientation, which has not been documented in the existing records after we have discovered that the east-west direction of the city plan is tilted southeastward with an azimuth of 92.5°.

In the literature, Yano [5] summarizes two methods for determining cardinal directions in ancient times: the gnomon method, such as the Indian circle, and the fixed-star method. The Indian circle yields four results: due east, west, north, and south. Furthermore, Kramrisch [6] concludes that Hindu temples exhibit three types of temple orientations: facing the rising sun or the cosmic orientation with reference to the sun (this implies the use of a sun shadow or a fixed star); meeting the center of man's settlement; and facing God (Vastu Purusha), where each God is related to a specific star. Since India inspired many ancient temples and monuments in Thailand's ancient kingdoms. However, several ancient temples or structures in Thailand do not face east, west, north, or south. For example, Prasat Hin Phanom Rung [7], Prasat Hin Pimai, and Wat Prathat Doi Suthep [8]. The cause of these temples' tilted orientation from the cardinal direction must have come from one of these two methods.

Given that we are uncertain of the orientation method utilized in the Chiang Mai city plan, we propose two possibilities. If the Gnomon method was applied, measurement inaccuracies could contribute to the 2.5° shift from cardinal directions. If the fixed star method was used on purpose, one star must have aligned with the city plan during construction. To test our hypotheses, we replicate the processes of the two methods to determine which produces results consistent with the city's orientation.

2. Materials and Methods

We first validated the tilting with an azimuth of 92.5° (2.5° south of east) using a theodolite and a GPS to measure the horizontal and vertical positions of the selected stars with time along the northern city wall. We then calibrated the measured positions with the positional astronomy software package *Stellarium* (version 0.21.3 with the time correction $\circledcirc T$—the difference between Terrestrial Dynamical Time and Universal Time [9]—using the default "Espenak and Meeus (2006)" model [10], accounted for atmospheric refraction and extinction, and a proper motion). The package, a free GPL software that renders realistic skies in real time with OpenGL, was used to calculate all astronomical coordinates of celestial objects in the ancient atmosphere. The Stellarium corrects the precession based on present knowledge that the equinox moves with a precessional period of approximately 26,000 years or 1° every 72 years. This work carried out two methods of orientation—using a gnomon and the fixed star—to answer why the Chiang Mai city plan is tilted.

For the gnomon method, there are two approaches called "the shortest shadow" and "the Indian circle." The shortest shadow refers to the shadow of the gnomon obtained around noon as the Sun crosses the meridian, an imaginary line along the North-South pole that divides the sky equally to the western and eastern sky. Therefore, the shortest shadow's direction points along the north-south axis, and a perpendicular line is drawn to obtain the east-west axis. This approach requires close monitoring from an observer to ensure that the shadow is the shortest. As for the Indian circle approach, the circle is drawn around the gnomon with a radius equal to the length of two shadows: one obtained in the late morning and the other in the afternoon. The east-west axis is established by connecting two points where the two shadows touch the circle. The Indian circle is preferable to the shortest shadow because it generates less human error. Therefore, the Indian circle

was the method of choice for aligning temples and cities with the cardinal directions, particularly the east direction, or with the four major astronomical dates, namely the two equinoxes and the two solstices [11].

For the fixed star method, a star of choice will be observed as it rises or falls at the horizon during sunrise or sunset. The star is chosen for its connection to the Sun or the Vaastu-Purusha-Mandala or the important person of the site. The primary axis of orientation will be the azimuth angle of the star. This method is often found in ancient areas that are not oriented along the cardinal directions, the four major astronomical dates, or towards the center of the town. Our procedures for the two methods are as follows:

1. For the gnomon method, we need to assess whether the measurement error resulting from this approach might cause the shift of 2.5° from cardinal directions. To carry out two gnomonic approaches, i.e., the shortest shadow and the Indian circle, within four days of two historical dates and 4 dates of astronomically significant dates. These dates are the vernal equinox (21 March), the autumnal equinox (23 September), the date King Mangrai entered the site (3 April), the founding date (19 April), summer solstices (22 June), and winter solstice (21 December), leading to the total of 24 measurement days in 2022.

2. For the fixed star method, we need to simulate the ancient sky using the precession-corrected *Stellarium* software to trace back in time to uncover which star aligned with the azimuth of 92.5° and to what extent the star impacted the city. We referenced the orientation axis along the northern city wall because the planning should be along the east-west direction, according to Brihat Samhita [4]. In addition, the CMC indicates that the construction started from the Sri Bhumi northeast corner; therefore, the axis along the northern city wall is the most appropriate reference. We employed a theodolite to measure the azimuth of the north wall concerning Polaris and Alnitak in Orion's belt. We could observe Orion's belt rising near the northern wall axis.

3. Results and Discussion

We checked the city plan's east-west orientation using a theodolite and GPS along the northern city wall, measuring to Polaris and the other star, calibrating with *Stellarium* (version 0.21.3) afterward. This verified the tilting with an azimuth of 92.5° (2.5° south of east).

3.1. The Gnomic Approach

Due to poor weather conditions, insufficient sunlight to identify a clear shadow and accidental removal of the gnomon, we obtained only eight days out of the intended 24 days of measurements, giving just eight data for the shortest shadow and six data from the Indian circle method. As summarized in Table 1, the Indian circle method yields a more precise orientation angle to the actual directions than the shortest shadow method. However, neither method produces an average deviated rise more significant than 0.7°, far less than the 2.5°-tilted city wall. The error might have been even lower if performed by the skilled Brahmin who planned the city. As a result, it is more plausible that the fixed star method was the orientation method than the sun-shadow method. It is worth noting that the gnomic shadow method for determining the cardinal direction can be employed on any day of the year; however, the condition of sunlight, depending on weather or terrain, can be a limiting factor for this method.

3.2. The Fixed Star Method

We need to investigate the azimuths of stars consistent with the orientation axis during construction, from 3 April 1292 – 19 April 1296. In Figure 2, the rising azimuths after precession correction of several prominent stars obtained by the *Stellarium* software were plotted from the year 0 to 2000 A.D. for the northeast corner, 18° 47′ 42.323″ N; 98° 59′ 36.773″ E) Only the azimuths of Spica and the Orion's Belt, namely Mintaka (δ Orionis) and Alnilam (ε Orionis), are near the city alignment of 92.5°. Still, the latter was associated with the city's founding time.

Table 1. Measured azimuth angles from the orientation axis constructed *via* the sun shadow method.

Events	No.	Date in 2022	Measured Azimuth /°			
			Shortest shadow		Indian circle	
			N (0°)	E (90°)	N (0°)	E (90°)
Vernal equinox	1	19 Mar	0.0	91.0	0.0	90.0
	2	20 Mar	*na.*	*na.*	*na.*	*na.*
	3	21 Mar	-1.0	89.0	0.0	91.0
	4	22 Mar	*na.*	*na.*	*na.*	*na.*
The date that	5	2 Apr	*na.*	*na.*	*na.*	*na.*
King Mangrai entered	6	3 Apr	1.0	91.0	0.0	90.0
to the site	7	4 Apr	1.0	92.0	1.0	92.6
	8	5 Apr	-0.3	88.0	-1.4	88.0
The date that	9	17Apr	*na.*	*na.*	*na.*	*na.*
King Mangrai began	10	18Apr	*na.*	*na.*	*na.*	*na.*
to build the city	11	19Apr	*na.*	*na.*	*na.*	*na.*
	12	20Apr	*na.*	*na.*	*na.*	*na.*
Summer solstice	13	20 Jun	*na.*	*na.*	*na.*	*na.*
	14	21 Jun	*na.*	*na.*	*na.*	*na.*
	15	22 Jun	*na.*	*na.*	*na.*	*na.*
	16	23 Jun	*na.*	*na.*	*na.*	*na.*
Autumnal equinox	17	20 Sep	0.3	90.3	*na.*	*na.*
	18	21 Sep	2.0	92.0	1.0	91.0
	19	22 Sep	1.0	92.0	*na.*	*na.*
	20	23 Sep	*na.*	*na.*	*na.*	*na.*
Winter solstice	21	19 Dec	*na.*	*na.*	*na.*	*na.*
	22	20 Dec	*na.*	*na.*	*na.*	*na.*
	23	21 Dec	*na.*	*na.*	*na.*	*na.*
	24	22 Dec	*na.*	*na.*	*na.*	*na.*
		Average	0.5	90.7	0.1	90.4

na. -not available noticed for incomplete data collection.

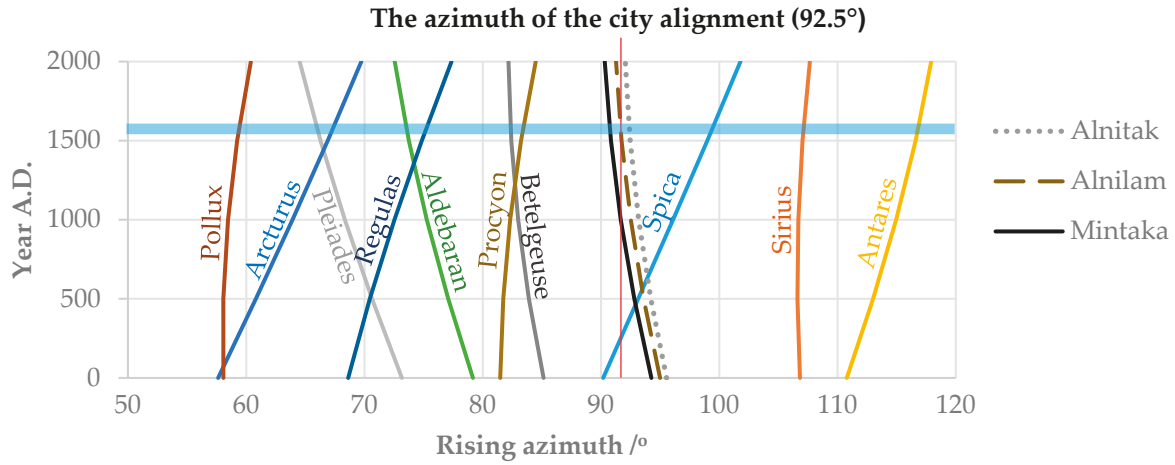

Figure 2. Observing at Sri Poom Corner (the northeast corner, 18° 47′ 42.323″ N; 98° 59′ 36.773″ E; altitude 312 m), the changing azimuths of the stars when rising on the eastern horizon over two millenniums, due to the precession of the equinoxes. The red hairline (at 92.5°) indicates the azimuth of the city alignment, and the light blue strip illustrates the city planning period during 1292 – 1296 A.D.

The stars that might be candidates for aligning the city's orientation are Mintaka (δ Ori), Alnilam (ε Ori), and Alnitak (ζ Ori), three lined-up stars that represent the belt of a famous hunter in Greek mythology. Still, the Orion constellation looks like a turtle for Thai people (see Figure 3: Top). This constellation is of great use in finding the positions of other stars. Tracing a line from Orion's belt to the southeast, we will find Sirius in the Canis Major constellation; in the opposite direction, towards the northwest, we can locate Aldebaran. A straight line that draws across both shoulders of Orion to the east will point to Procyon in Canis Minor. If one draws from Rigel to Betelgeuse, it will mean to the positions of Pollux and Castor. From all the stars mentioned, the Pollux, Castor, Procyon, and Sirius stars, which together resemble the Chinese Junk Boat images (see Figure 3: Top), are stars of the Punavasu Nakshatra. When the moon was in this nakshatra on 3 April 1292 and 19 April 1296, it set the auspicious date and time for the ceremony of entering the new site and starting the construction, respectively. During the year of planning the Chiang Mai City Wall, as can be seen as visualized in Figure 4 and Figure 5, Mintaka rose at a height of 4° and Alnilam at a height of 1.5°; these two stars had the closest rising azimuth at 92.5°.

In Figure 5, only Mintaka and Alnilam have azimuths corresponding with the azimuth of the northern city wall but at different altitudes; the apparent brightness of these two stars is a magnitude of 2.23 and 1.7, respectively. To the Rule of Thumb, the star can be observed with the naked eye at least at its critical altitude, which can be regarded as its magnitude [13]. Therefore, the Mintaka at 4.0° altitude would be seen. In contrast, the Alnilam at 1.5° altitude (close to its critical altitude of 1.7°) could also be seen under the apparent sky condition.

We also investigate the significance of choosing this star for the city's orientation. According to the literature, Orion was used in an ancient harvest calendar in Indonesia [13]. To the Indonesians, this constellation resembles the Javanese plow (see Figure 3: Bottom) and marks the harvest season's start. For Thai people, this constellation is also known as a plowing star, which has long been considered a promising star for agriculture. King Mangrai chose the location of Chiang Mai based on the seven good omens that valued the fertility of soil, land, and plant varieties [3]. Therefore, it is possible that Orion was chosen for its auspiciousness in agriculture.

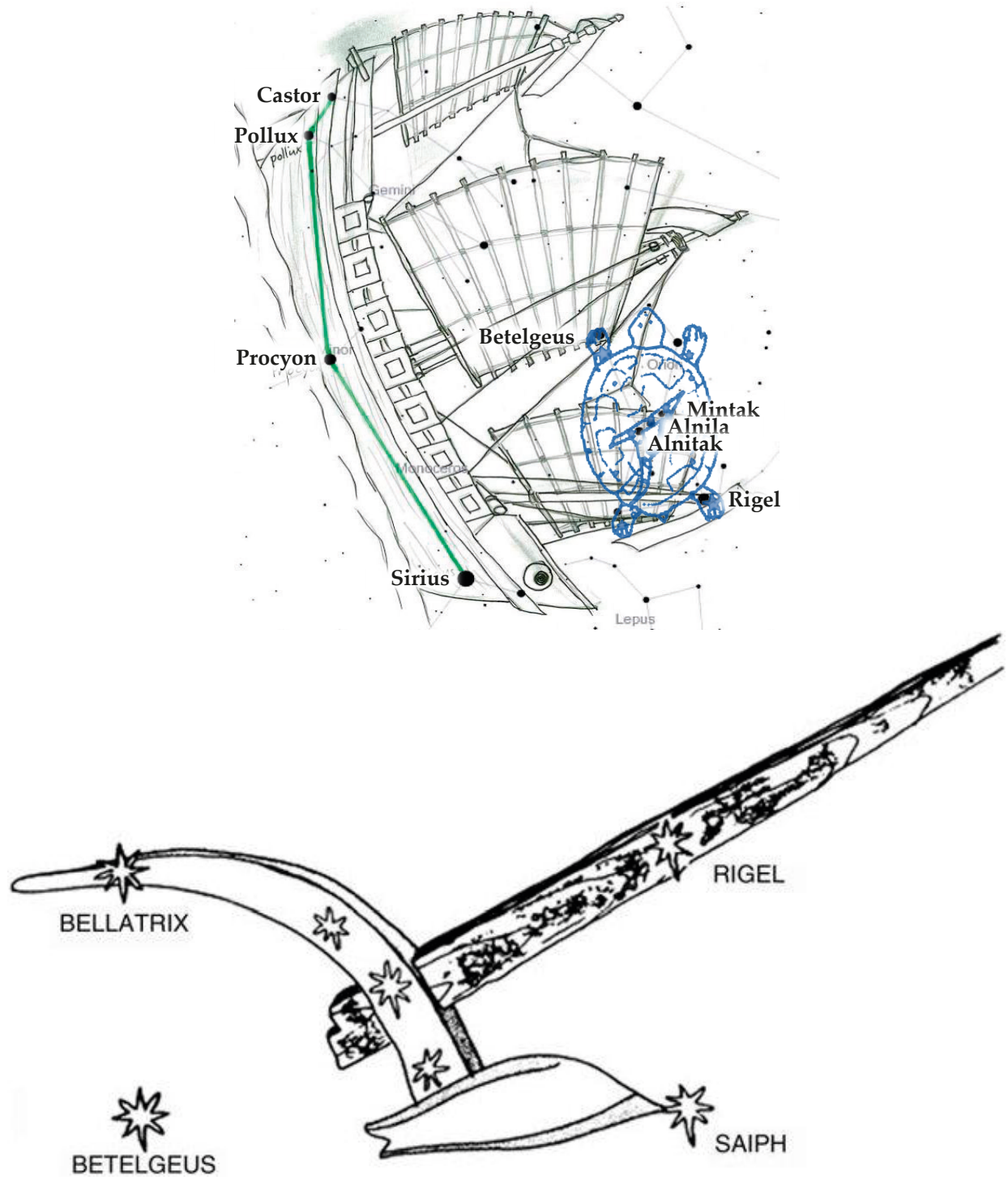

Figure 3. Top: The Orion Constellation appears to the native Thais as a turtle, and the Orion's Belt is imagined as a plow. The stars of the Punavasu Nakshatra are Pollux, Castor, Procyon, and Sirius, which resemble Chinese Junk Boat imagery (Drawing by Pisit Nitiyanant). Bottom: Illustration of the rising of Orion, which is also known as the Waluku (a traditional Javanese plough; an asterism in the constellation Orion) to indicate the start of the harvest season in Java (Drawing after Ammarell and Tsing [12]; Fig. 212.1, p. 2210)

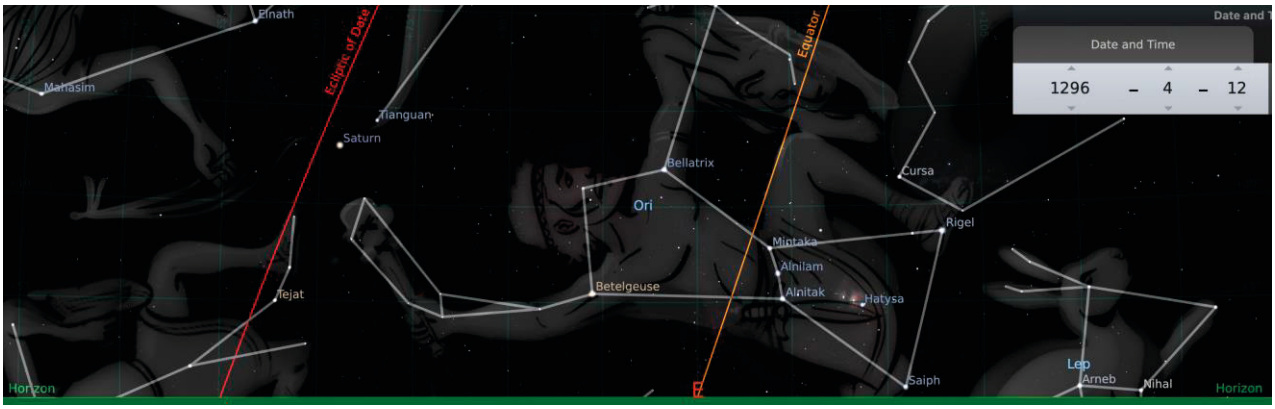

Figure 4. The visualized ancient eastern sky on the auspicial founding date, 19 April 1296 (note: the date labeled in the figure is used as Julian in the software), showing how the Orion Constellation appears to be rising on the horizon (Image generated by the *Stellarium* software, version 0.21.3)

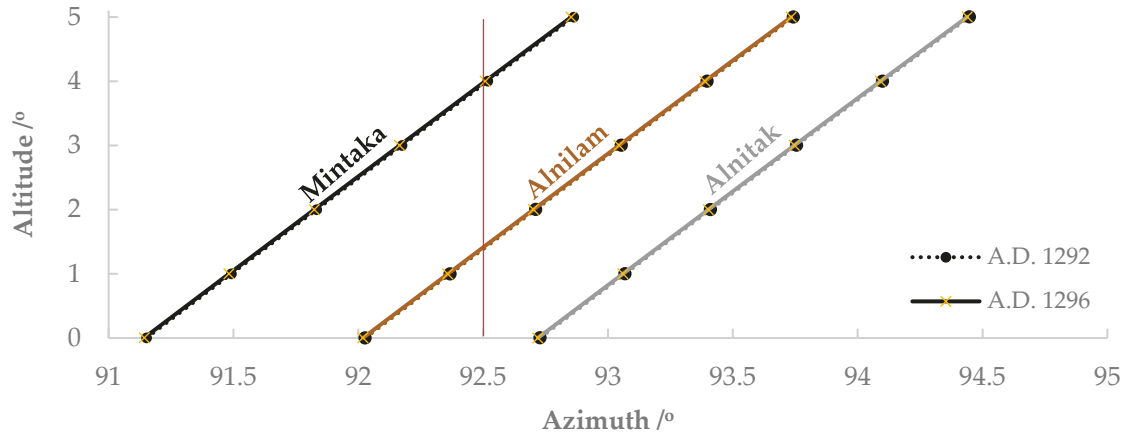

Figure 5. The azimuths and altitudes of Orion's belt stars in the year 1292 when the new site was to be chosen (dotted lines with a circle marker), and in the year 1296 when the ancient Chiang Mai city was being constructed (solid lines with a cross marker). The red hairline indicates the azimuth of the city alignment.

4. Conclusions

We find that the orientation method for the Chiang Mai city plan may have been the fixed star rather than the gnomon, like the Indian circle method or the shortest shadow method. The results of this investigation suggest that the orientation of Chiang Mai's old city wall might be aligned to the rising of the Mintaka star in Orion's belt at a height of 4° and possibly the Alnilam start at a height of 1.5° (under a very clear sky condition) between 1292 and 1296. The star may have been selected because of its optimistic role in agriculture, which was highly valued in the founding of Chiang Mai city for King Mangrai.

5. Acknowledgements

The research team wishes to express gratitude to Assoc. Prof. Smai Yodintra, Asst.Prof. Mullika Tawonatiwas, and Assoc.Prof. Snan Supasai, the pioneer of holistic learning and co-founder of the SCiUS CMU, and Dr. Sakda Swathanan, the present director. Special thanks to Mr. Theerawat Bunfong, Mr. Aekkarin Kadta, and all the project staff for providing related academic support. Finally, we thank the History and Heritage in Astronomy Group of the National Astronomical Research Institute of Thailand for their assistance and advice.

Author Contributions: Conceptualization and methodology, CI, SL, PS, CS, and OR; collected and organized relevant historical documents, OR; data survey, CI, SL, and PS; data analysis, CI, SL, PS, and CS; astronomical interpretation, CI and CS; writing—original draft preparation, CI, SL, and PS; writing—review and editing, CS and OR. All authors read and approved the final manuscript.

Funding: This research was funded by the National Astronomical Research Institute of Thailand and the Physics and Astronomy Research Group, Chiang Mai University. The costs were partially granted by Thailand Science Research and Innovation, Grant ID 2526292, and the funding for the Science Classroom at the University Affiliated School (SCiUS) is provided by the Ministry of Higher Education, Science, Research, and Innovation.

Conflicts of Interest: The authors declare that they have no competing interests.

References

[1] Wichienkaeo, A.; Wyatt, D. K. *The Chiang Mai Chronicle*. Chiangmai: Silkworm Books; 1995. (in *Thai*)

[2] Princess Maha Chakri Sirindhorn Anthropology Centre. *Wat Chiang Man Inscription Face I* 2021. https://db.sac.or.th/inscriptions/inscribe/image_detail/26515 (accessed June 4, 2023).

[3] Saelee, C.; Riyaprao, O.; Komonjinda, S.; Sriboonrueang, K. An archaeoastronomical investigation of vaastu shastra principles (vedic architecture) implemented in the city planning of ancient Chiang Mai. In: Orchiston, W.; Vahia, M. N., editors. *Exploring the History of Southeast Asian Astronomy: A Review of Current Projects and Future Prospects and Possibilities*, Cham: Springer, 2021; 461–485. https://doi.org/10.1007/978-3-030-62777-5_13.

[4] Sastri, V. S.; Bhat, W. M. R. *Varahamihira's Brihat Samhita: with an english translation and notes*. Bangalore: V.B. Soobbiah & Son; 1946.

[5] Yano, M. Knowledge of Astronomy in Sanskrit Texts of Architecture (Orientation Methods in the īśāna śiv a gurudev apaddhati). *Indo-Iranian Journal*, 1986; 29. https://doi.org/10.1163/000000086790082163.

[6] Kramrisch, S. *The hindu temple: volume one*. Delhi: Motilal Banarsidass Publ.; 1976.

[7] Komonjinda, S.; Riyaprao, O.; Sriboonrueang, K.; Saelee, C. Relative orientation of Prasat Hin Phanom Rung Temple to Spica on New Year's Day: the chief indicator for the intercalary year of the luni-solar calendar. *Proceedings of the International Astronomical Union*, 2019; 15, 260–264. https://doi.org/10.1017/S1743921321001034.

[8] Riyaprao, O.; Sriboonrueang, K.; Komonjinda, S.; Saelee, C. Astronomical Orientation of Phra That Doi Suthep Temple in Relation to Acronychal Rising of Corona Borealis and Visakha Bucha Day. *Journal of Astronomical History and Heritage* 2023; (in press).

[9] Espenak, F. *Delta T (ΔT) and Universal Time*, 2011. https://eclipse.gsfc.nasa.gov/SEhelp/deltaT.html (accessed September 10, 2023).

[10] Espenak, F.; Meeus, J. *Five Millennium Canon of Solar Eclipses: -1999 to +3000*, 2006. https://eclipse.gsfc.nasa.gov/SEpubs/5MCSE.html (accessed September 9, 2023).

[11] Burgess, E. *Translation of the Surya Siddhanta*. Delhi: Indological Book House; 1977.

[12] Ammarell, G.; Tsing, A. L. Cultural Production of Skylore in Indonesia. *Handbook of Archaeoastronomy and Ethnoastronomy*, New York, NY: Springer New York; 2015; 2207–2214. https://doi.org/10.1007/978-1-4614-6141-8_236.

[13] Thom, A. *Megalithic Sites in Britain*. Oxford: Clarendon Press; 1967.

[14] Gislén, L.; Eade, J. C. The Calendars of Southeast Asia. 4: Malaysia and Indonesia. *Journal of Astronomical History and Heritage*, 2019; 22, 447–57.

ASEAN
Journal of Scientific and Technological Reports
Online ISSN:2773-8752

Research article

Comparison of Different Extraction Methods for Bioactive Compounds from Kao-Kum Doi-Saket (*Oryza sativa* L.)

Sureewan Rajchasom[1*], Pornsawan Sombatnan[2], Janyawat Tancharoenrat Vuthijumnonk[3] and Phanida Suphiratwanich[4]

[1] College of Integrated Science and Technology, Rajamangala University Technology of Lanna, Chiang Mai, 50300, Thailand; sureewan@rmutl.ac.th
[2] College of Integrated Science and Technology, Rajamangala University Technology of Lanna, Chiang Mai, 50300, Thailand; pornsawan.sbtn@gmail.com
[3] College of Integrated Science and Technology, Rajamangala University Technology of Lanna, Chiang Mai, 50300, Thailand; vjanyawat@hotmail.com
[4] Faculty of Pharmacy, Payap University, Chiang Mai, 50000, Thailand; phanthong73@gmail.com
* Correspondence: sureewan@rmutl.ac.th

Citation:
Rajchasom, S., Sombatnan, P., Vuthijumnonk, J., Suphiratwanich P. Comparison of different methods for bioactive compounds from Kao-Kum Doi-Saket (*Oryza sativa* L.). *ASEAN J. Sci. Tech. Report.* **2023**, *26*(4), 38-46. https://doi.org/10.55164/ajstr.v26i4.249961

Article history:
Received: June 20, 2023
Revised: September 18, 2023
Accepted: September 19, 2023
Available online: September 30, 2023

Abstract: Kao-Kum Doi-Saket is one type of purple rice known for its high content of anthocyanin and its ability to resist free radicals. Anthocyanin extracts can be utilized in various applications, including food coloring, nutritional supplements, natural medicine, and cosmetics. There are several methods for extracting anthocyanin from Kao-Kum Doi-Saket. This research aims to compare the effects of extraction methods, including Conventional extraction (CE), Pulse electric field extraction (PEF), and Ultrasonic assisted extraction (UAE) on total anthocyanin content and antioxidant activity in Kao-Kum Doi-Saket. It was found that the UAE method resulted in the highest total anthocyanin content of 57.05 ± 4.27 mg/L, which was significantly different from the other two methods ($p<0.05$). Kao-Kum Doi-Saket extracts from the UAE method also showed the highest DPPH inhibition (88.32 ± 1.83%) compared to the CE and PEF methods. Therefore, these findings suggest that UAE is the most effective method for extracting anthocyanin and antioxidant activity from Kao-Kum Doi-Saket and could be beneficial for developing processed products from Kao-Kum Doi-Saket in the future.

Keywords: Purple rice; Pulse electric field; anthocyanin; antioxidant activity

1. Introduction

Kao-Kum (*Oryza sativa* L.) is commonly grown in Thailand, particularly in the northern region of Thailand. Kao-Kum Doi-Saket is the name of planting area of this rice since it is popularly cultivated in Doi Saket District, Chiang Mai Province. Kao-Kum Doi-Saket is red to dark purple due to anthocyanin pigments in the rice grain. Kao-Kum is, therefore, called purple rice. Base on the study of Leelawat et al. [1] found that Kao-Kum Doi-Saket contains cyanidin-3-glucoside and peonidin-3-glucoside and Zhang et al. [2] also found that anthocyanin in purple rice has antioxidant properties.

In general, anthocyanin compounds can be extracted using water as a conventional method (CE). However, this method has limitations regarding low anthocyanin yield and lengthy extraction time [3]. Therefore, there have been developments in extraction techniques that consider the stability of anthocyanins under heat, light, and pH conditions [4]. The current popular

extraction techniques include Pulse electric field extraction (PEF), Ultrasonic-assisted extraction (UAE), and Microwave Extraction (ME) [5]. Apart from the extraction methods, the choice of solvent used for extraction is also a factor to be considered. Solvents for anthocyanin extraction include methanol, ethanol, hydrochloric acid, and water. Water-based extraction methods are currently preferred due to the potential health and environmental impacts of other solvents on consumers [6].

Using new techniques for extracting bioactive compounds from plant promotes environmentally friendly extraction methods, known as "Green extraction," following the plan of the United Nations for 2030. These techniques are based on six principles as follows: (1) Sourcing diverse raw materials that can be reused; (2) Reducing the use of organic solvents for extraction by utilizing alternative solvents; (3) Minimizing energy consumption during the extraction process; (4) Achieving efficient and high-value yields (5) Decreasing extraction processes and enhancing safety (6) Focusing on environmentally friendly and toxin-free extraction methods [7].

The PEF method is widely used for extracting anthocyanins from various plant sources because it is an un-thermal extraction process in which technology helps reduce environmental impacts and amounts of solvent and enhances the energy efficiency of the processes [8]. This method utilizes electroporation, which applies electrical pulses to the plant cell walls. The pore from electric pules on the plant cell wall allows extraction even at room temperature (Figure 1). PEF extraction has gained popularity for anthocyanin extraction because it can effectively overcome the limitations associated with the heat sensitivity of anthocyanins [9]. A study by Drosou et al. [10] found that PEF extraction significantly increased the quantity of anthocyanins in grape wine compared to conventional extraction methods.

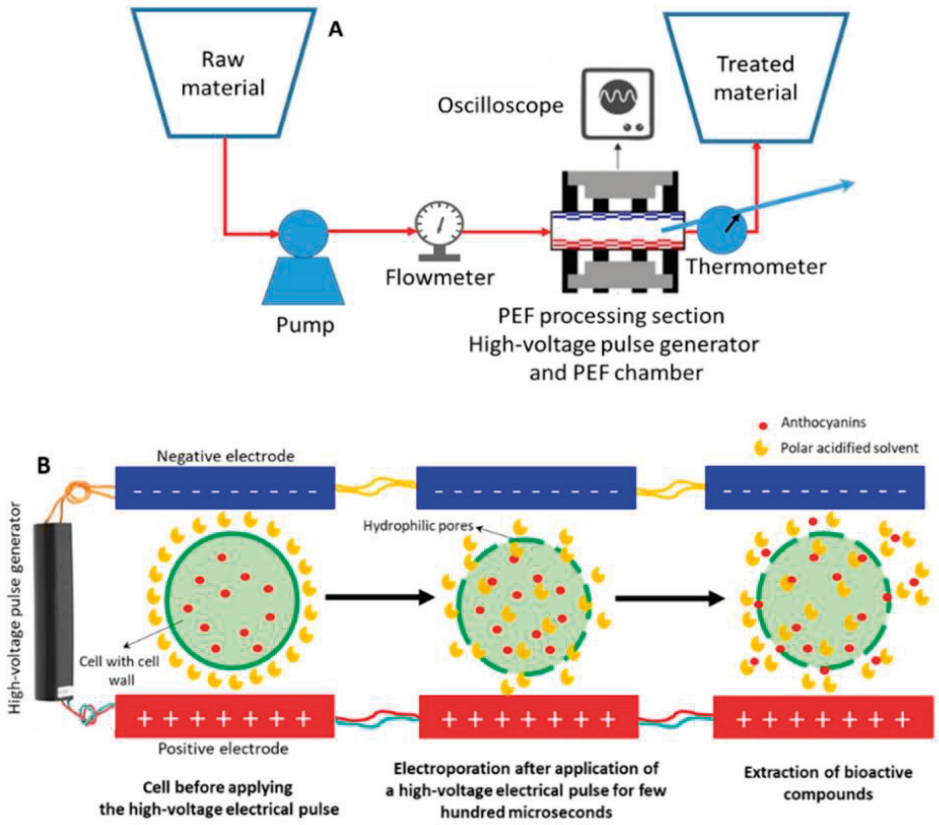

Figure 1. The diagram and general principles of the pulsed electric field extraction process [11].

The UAE method is another popular extraction technique used nowadays. It is a novel, clean, and safe method for extracting biomaterial molecules such as polysaccharides, essential oils, proteins, and pigments

[12]. The UAE principle involves applying ultrasound waves that induce vibration, resulting in a cavitation phenomenon. The cavitation phenomenon leads to the formation of air bubbles within the liquid, and when these bubbles collapse, they cause cell wall disruption in plants [13] (Figure 2). This extraction technique has proven highly efficient, cost-effective, and environmentally friendly. It is suitable for extracting bioactive compounds from plants, including anthocyanins, phenolic compounds, rutin, quercetin, and others [14-16].

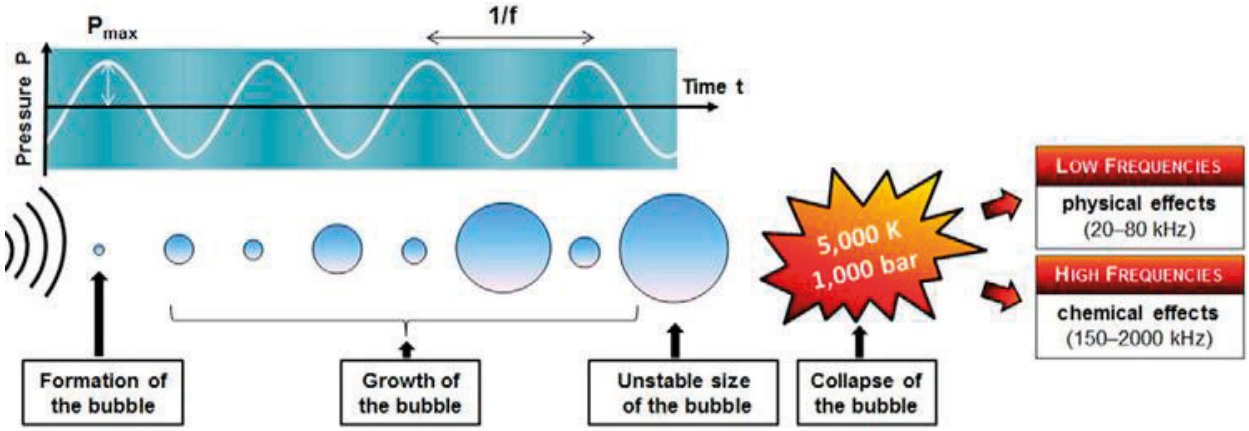

Figure 2. The cavitation phenomenon in the Ultrasonic process [17].

Based on the aforementioned nutritional properties of Kao-Kum Doi-Saket with high nutritional value, there has been an interest in studying extraction methods to utilize Kao-Kum Doi-Saket to produce health products. No suitable extraction technique can preserve essential compounds for this particular Kao-Kum strain. Therefore, this research aims to compare the extraction techniques of Kao-Kum Doi-Saket in terms of CE, PEF, and UAE methods for their ability to extract anthocyanins and antioxidant properties.

2. Materials and Methods

2.1 Materials

The local farmers from Doi Saket Chiangmai, Thailand, supplied the purple rice (*Oryza sativa* L.) or Kao-Kum Doi-Saket. The harvesting period was from November to December, vacuum-sealed using air-vacuum plastic bags to prevent moisture and stored at room temperature in a controlled humidity environment. The chemicals were purchased from Northern Chemical Co., Ltd. and Union Science Co., Ltd. All are analytical grade.

2.2 Extraction method

2.2.1. Conventional extraction method

CE method of Kao-Kum Doi-Saket was performed by soaking Kao-Kum Doi-Saket in distilled water with a ratio of 1 kg of rice to 2 L of water and left overnight for 24 hours at room temperature without stirring. The extracts were filtered using a white cloth, and the samples were stored in an amber glass vial for further analysis.

2.2.2 Pulse electric field extraction method

PEF method was used following the technique of Rajchasom et al. [18]. The extraction ratio was 1 Kg of rice to 2 L of water. The electric field level was generated at 6 kV/cm and the number of pulses was varied at 1,000, 3,000, 4,000, and 5,000 pulses (each pulse lasting 0.078 seconds). The extracts were filtered using a white cloth, and the samples were stored in amber glass vials for further analysis.

2.2.3 Ultrasonic assisted extraction method

The extraction method of Kao-Kum Doi-Saket using the UAE method was adopted from the study conducted by Rajchasom et al. [19]. Kao-Kum Doi-Saket samples were extracted using an ultrasonic device

(Model GT Sonic-D6, China) with a fixed frequency of 40 kHz and electrical power of 150 W at a ratio of 1 kg of rice to 2 L of water. The extraction process was conducted at 30, 50, and 70 °C for 60 minutes (UAE1, UAE2, and UAE3, respectively). The extracts were filtered using a white cloth, and the samples were stored in amber glass vials for further analysis.

2.3 Chemical analysis of Kao-Kum Doi-Saket extraction

2.3.1 Determination of total anthocyanin content

The total anthocyanin content of Kao-Kum Doi-Saket extracts was analyzed using the pH differential method. A sample of Kao-Kum Doi-Saket extract (1 mL) was diluted with distilled water to a volume of 10 mL. Then, the solution was shaken using a centrifuge device (Hettich zentrifugen, EBA 20) at 6,000 rpm for 8 minutes. Afterward, 3 mL of the supernatant solution was pipetted and mixed with buffer solutions, including potassium chloride pH 1 and sodium acetate pH 4.5, to a final volume of 30 mL. Afterward, the sample was left to incubate for 30 minutes in the darkroom conditions and at ambient temperature. Each mixture sample's light absorption (A) was measured using a UV-Vis spectrophotometer at 510 and 700 nm (Spectrum Instruments, SP-UV 200 spectrophotometer). Equation (1) was used to calculate the total anthocyanin content [20] .

$$\text{Total anthocyanin content (mg/L)} = \frac{A_{diff} \times M_w \times df \times 1000}{\varepsilon} \quad (1)$$

Where A_{diff} represents the absorbance value (510 nm -700 nm) pH1 - (510 nm -700 nm) pH4.5, M_w is the molecular weight of Cyanidin-3-glucoside (449.2 g/mol), ε is the molar absorptivity (26,900 $M^{-1}cm^{-1}$), df represents the dilution factor, which is 10.

2.3.2 Determination of antioxidant activity

The antioxidant activity of Kao-Kum Doi-Saket extracts was analyzed using the DPPH radical scavenging assay. A sample of Kao-Kum Doi-Saket extract volume of 200 µL was taken and mixed with 1.8 mL of methanol. Then, 2 mL of 2,2-diphenyl-1-picrylhydrazyl (DPPH) solution with a concentration of 0.12 mM was added to the sample. For the control sample, 2 mL of methanol and 2 mL of DPPH solution were added. The blank sample was prepared using 4 mL of methanol [21]. The antioxidant activity was then calculated using the following Equation (2).

$$\text{\% DPPH inhibition} = \frac{(A517_{control} - A517_{sample}) \times 100}{A517_{control}} \quad (2)$$

Where $A517_{control}$ represents the absorbance value at 517 nm of the control sample (Control DPPH), $A517_{sample}$ represents the absorbance value at the nanometer of the experimental sample.

2.4 Statistical analysis

Statistical analysis was performed on the experimental data using MINITAB statistic software version 20. The data was analyzed by calculating the mean ± standard deviation (mean ± SD). The data was further compared using Analysis of Variance (ANOVA) and the mean values were compared using Duncan's test at a confidence level of 95%. The entire experiment was conducted in triplicate.

3. Results and Discussion

3.1 Effect of various extraction methods on total anthocyanin content of Kao-Kum Doi-Saket extract

The study was conducted to compare the effects of different extraction methods,, CE, PEF, and UAE methods, on the total anthocyanin content of Kao-Kum Doi-Saket extract. The results of the total anthocyanin content of the extracted solutions conducted using various extraction techniques are shown in Table 1.

Table 1. Total anthocyanin content (mg/L) and % DPPH inhibition of Kao-Kum Doi-Saket extracts using various extraction methods.

Extraction methods	Conditions	Total anthocyanin content (mg/L)	%DPPH inhibition
PEF1	6 kV/cm, 1,000 pulses	16.09 ± 0.77^{f}	67.74 ± 1.88^{b}
PEF2	6 kV/cm, 3,000 pulses	24.99 ± 0.92^{e}	60.97 ± 0.64^{bc}
PEF3	6 kV/cm, 4,000 pulses	27.66 ± 1.09^{de}	43.50 ± 1.26^{de}
PEF4	6 kV/cm, 5,000 pulses	32.84 ± 1.84^{cd}	33.24 ± 0.43^{e}
UAE1	30°C, 60 min	38.02 ± 1.21^{c}	83.82 ± 9.22^{a}
UAE2	50°C, 60 min	57.05 ± 4.27^{a}	88.32 ± 1.83^{a}
UAE3	70°C, 60 min	47.65 ± 1.90^{b}	83.20 ± 3.67^{a}
CE	24 hr.	9.30 ± 1.11^{g}	51.27 ± 8.60^{cd}

Note: Values are the means of three replicates experimental (mean ± SD). Different superscript letters indicate statistically significant differences at $p \leq 0.05$ for values within the same column**.**

It was found from Table 1 that the extraction using the UAE method yielded a higher total anthocyanin content of the extracts compared to the PEF and CE methods, and the UAE and PEF produced 6 and 2 times anthocyanin contents in the extracts higher than the CE method. The UAE2 (50°C, 60 min) yielded the significantly highest anthocyanin content of the extracts (57.05±4.27 mg/L), and there was a significant difference ($p<0.05$) among them. This was because the low temperature of the UAE1 condition (30°C, 60 min) did not effectively promote extraction efficiency, and the high temperatures of the UAE3 condition (70°C, 60 min) caused the breakdown of phytochemicals. Similar to the results of He et al. [22] and Figueiredo et al. [23] suggested that anthocyanin could be oxidized at exceeding 50°C of extraction temperature. On the other hand, UAE1 (30°C, 60 min) and UAE3 (70°C, 60 min) produced lower anthocyanin content in the extracts (38.02±1.21 and 47.65±1.90 mg/L, respectively) because the exceeded extraction temperature had a damaging effect on the total anthocyanin content of Kao-Kum Doi-Saket extracts [24] and at low extraction temperature with short period of extraction time could not provoke the releasing of total anthocyanin content from Kao-Kum Doi-Saket extracts [25]. The total anthocyanin content of Kao-Kum Doi-Saket extracts using the PEF method increased with an increasing number of pulses, with values of 16.09±0.77, 24.99±0.92, 27.66±1.09 and 32.84±1.84 mg/L for 1,000, 3,000, 4,000 and 5,000 pulses, respectively [18]. However, these values of anthocyanin extracted using the PEF method were lower than those of the UAE method. The temperature of the PEF method in this study was between 50 - 60°C, similar to that of the UAE method. It can be assumed that the temperature of the process was not the main effect on the anthocyanin content when compared between these 2 methods. Still, the extraction mechanism may have more influence. On the other hand, the CE method provided the lowest total anthocyanin content of the extracts (9.30±1.11 mg/L) when compared with the other 2 methods. The reason for this is that the PEF and UAE methods can disrupt the cell walls, which promote the release of anthocyanin pigment by transferring it from the moisture mass within the cellular structure of the sample. As a result, the dissolution of phytochemical compounds in the extract of Kao-Kum Doi-Saket is enhanced without affecting its essential components. Similarly, Zhou et al. [26] investigated the extraction of anthocyanins from the remaining extracts of blueberries using PEF and UAE methods. They found that PEF and UAE methods were more effective in extracting anthocyanins than the CE method. Likewise, Manzoor et al. [27] studied the extraction of anthocyanins from almond seeds (*Prunus dulcis*) using PEF and UAE methods. They found that PEF and UAE methods yielded higher anthocyanin content in the extracts. The UAE yielded the highest total anthocyanin content, 6.14 times greater than the CE method. The result aligns with the findings reported by Lertkaeo et al. [28], who conducted a comparative study on the extraction of anthocyanins from Hom Mali black glutinous rice using CE and UAE methods. The study found that the UAE method resulted in a significantly higher amount of anthocyanins than the CE method, with an increase of 15.49%. Moreover, from the results of this study on the Kao-Kum Doi-Saket extraction, another reason can explain the experimental results that the UAE extraction method resulted in higher anthocyanin content than the PEF method was because a high concentration of anthocyanin compounds was found on the surface of the Kao-

Kum Doi-Saket rice grain. The UAE method utilizes sound waves, which create alternating high-pressure and low-pressure cycles within the sample. This phenomenon, known as cavitation, leads to tiny bubbles' formation and rapid collapse. The collapse of these bubbles generates intense local pressures and temperatures, disrupting cell walls or breaking molecular bonds, facilitating the release of desired compounds [13-16, 29]. Whereas the PEF method involved the use of electric current, caused structural changes in the cell membranes, and induced severe cracking in the cell walls of the Kao-Kum Doi-Saket. The electric field disrupts the cell membranes, creating temporary pores or openings, causing the pigment to be extracted and more starch extracted compared to the UAE method [9-10]. Regarding energy and cost consumption, it was found that the UAE method can reduce extraction time, energy, and operating costs than the PEF method, which was suggested to be more suitable for community enterprises. Furthermore, it was found that the total anthocyanin content of Kao-Kum Doi-Saket or purple rice was higher than other rice species. Das et al. [30] extracted the anthocyanin content of purple and black rice using the UAE method of 30.40 and 35.56 mg C3G/L, respectively. Likewise, the report from Yamuangmorn and Prom-u-Thai [31] found that Kao-Kum Doi-Saket had total anthocyanin content higher than KJ CMU 107, Mamihunger, Kao Hom Nill, Kao Malinil Surin and (10, 3.5, 2 and 1.5 times, respectively).

3.2 Effect of various extraction methods on antioxidant activity of Kao-Kum Doi-Saket extract

Not only was the anthocyanin content of the extracts from Kao-Kum Doi-Saket, but antioxidant activity was also evaluated to compare the extraction efficiency of each method. The antioxidant activity of Kao-Kum Doi-Saket extracts using three different extraction methods, including CE, PEF, and UAE methods, was analyzed using the radical scavenging activity (% of DPPH inhibition) and shown in Table 1. The results show that the UAE method provided a higher percentage of DPPH inhibition (83.20±3.67 - 88.32±1.83%) [19] of Kao-Kum Doi-Saket extracts than that of the extracts using the PEF and CE methods. These values showed a statistically significant difference ($p<0.05$) compared to other extraction methods, but there was no significant difference among them in the UAE method. The highest percentage of DPPH inhibition of the extracts was determined by the UAE method at the condition of 50°C, 60 min. The PEF method produced a lower rate of DPPH inhibition than the UAE method, with values between 33.24±0.43 and 67.74±1.88%. Table 1 shows that the percentage of DPPH inhibition of the extracts using the PEF method decreased with an increase in the number of pulses. The PEF1 and PEF2 were acceptable extraction conditions by providing the extracts with the high antioxidant value of 67.74±1.88% and 60.97±0.64%, respectively. However, the other 2 PEF conditions (PEF3 and PEF4) yielded a deficient antioxidant activity (43.50±1.26% and 33.24±0.43%, respectively), which was lower than that of the CE method (51.27±8.60%) but insignificantly different. These experimental results were consistent with Madalão et al. [32], who studied the effect of extraction methods, CE and UAE methods, on the antioxidant capacity of anthocyanin extracts from palm (*Euterpe edulis M.*). The result showed that the UAE method yielded a significantly higher antioxidant capacity of the palm extracts than that of the CE method. It was also found from the results of this study (Table 1) that the antioxidant activity of the extracts using the PEF method did not correlate with the total anthocyanin content results. Increasing the pulse intensity resulted in a higher anthocyanin content while decreasing the antioxidant capacity. This can be explained by increasing the pulse number during extraction, resulting in more heat generation in the solution and effect in lower ability of antioxidant of the extracts since antioxidant activity was sensitive to high temperature [33]. This was also consistent with the research study on using the PEF method to extract *Moringa oleifera*, which indicated that increasing the pulse intensity led to a decrease in the antioxidant capacity of *Moringa oleifera* extracts since high pulse intensity not only produced high temperature but also consumed longer extraction time. Consequently, there was sufficient time for the antioxidant impact to decay [34]. Nevertheless, the high temperature in the UAE technique did not meaningfully yield any discernible effect on antioxidants. Although the temperatures of the UAE and PEF extraction conditions were similar, there was no effect on the extract's antioxidant content when extracted using the UAE method because the UAE method produced significantly higher amounts of extracts and anthocyanins. Therefore, it was possible to explain that other bioactive compounds in the extracts from the UAE method may result in a high level of antioxidant activity. Furthermore, a previous study on rice berry bran indicated additional antioxidative compounds were

present in purple rice besides anthocyanin, suggesting that anthocyanin may not be the primary antioxidative compound in purple rice [35]. Therefore, it was necessary to consider the extraction time, extraction temperature, and the mechanism of each method for enhancing the major bioactive compounds from Kao-Kum Doi-Saket.

4. Conclusions

In conclusion, it can be concluded that the UAE method was the most effective method for Kao-Kum Doi-Saket extraction. The UAE2 extraction condition (50°C, 60 min) yielded the highest total anthocyanin content (57.05±4.27 mg/L) and antioxidant capacity (88.32±1.83%). These values significantly differed from the CE and PEF methods ($p<0.05$). Therefore, it can be suggested from this study result that this extraction method and condition can be used as a guideline for extracting phytochemical compounds from Kao-Kum Doi-Saket and may be applied in other purple rice grains for developing nutritious commercial products.

5. Acknowledgements

This study was supported by the Institute of Research and Development and College of Integrated Science and Technology, Rajamangala University Technology of Lanna.

Author Contributions: Conceptualization, S.R. and J.V.; methodology, S.R., J.V., and P.S.; formal analysis, P.S.; investigation, S.R., and P.S.; resources, S.R. and J.V.; data curation, P.S.; writing—original draft preparation, P.S.; writing—review and editing, S.R.; visualization, S.R.; supervision, S.R.; project administration, S.R.; funding acquisition, S.R.

Funding: This research was funded by Thailand Science Research and Innovation (TSRI) in 2022.

Conflicts of Interest: The authors declare no conflict of interest.

References

[1] Leelawat, B.; Tilokkul, R.; Baikhunakon, M. Development of Kaimook from Purple Rice. *Thai Science and Technology Journal (TSTJ)*, 2018; *28*(3), 456–465.

[2] Zhang, X.; Shen, Y.; Prinyawiwatkul, W.; King, J. M.; Xu, Z. Comparison of the activities of hydrophilic anthocyanins and lipophilic tocols in black rice bran against lipid oxidation. *Food Chemistry*, 2013; *141*(1), 111–116.

[3] Srimoon, R.; Santimalai, S. Extraction of anthocyanin from Black plum (Syzygium cumini Skeels) using pulsed-electric field assisted. *KKU Science Journal*, 2018; *46*(4), 800–811.

[4] Pratiwi, R.; Purwestri, Y.A. Black rice as a functional food in Indonesia. *FFHD*, 2017; *7*(3), 182–194.

[5] Harun, N.F.; Hamid, F.H.A. An overview of the extraction methods of plant-based natural antioxidant. *Malaysian Journal of Chemical Engineering & Technology*, 2021; *4*(2), 73–89.

[6] Carpentieri, S.; Soltanipour, F.; Ferrari, G.; Pataro, G.; Donsì, F. Emerging Green Techniques for the Extraction of Antioxidants from Agri-Food By-Products as Promising Ingredients for the Food Industry. *Antioxidants*, 2021; *10*(9), 1417.

[7] Majid, I.; Khan, S.; Alade, A.; Dar, A.H.; Adnan, M.; Khan, M.I.; Awadelkareem, A.M.; Ashraf, S.A. Recent insights into green extraction techniques as efficient methods for the extraction of bioactive components and essential oils from foods. *CYTA – JOURNAL OF FOOD*, 2023; 21, 101–114.

[8] Barba, J.F.; Parniakov, O.; Pereira, A.S.; Wiktor, A.; Grimi, N.; Boussetta, N.; Saraiva, G.; Raso, J.; Martin-Belloso, O.; Witrowa-Rajchert, D.; Lebovka, N.; Vorobiev, E. Current applications and new opportunities for the use of pulsed electric fields in food science and industry. *Food Res*, 2015; 77, 773–798.

[9] Ranjha, M.M.A.N.; Kanwal, R.; Shafique, B.; Arshad, R.N.; Irfan, S.; Kieliszek, M.; Kowalczewski, P.Ł.; Irfan, M.; Khalid, M.Z.; Roobab, U. A Critical Review on Pulsed Electric Field: A Novel Technology for the Extraction of Phytoconstituents. *Molecules*, 2021; 26, 4893.

[10] Drosou, F.; Yang, E.; Marinea, M.; Dourtoglou, E.G.; Chatzilazarou, A.; Dourtoglou, V.G. An assessment of potential applications with pulsed electric field in wines. *40th World Congress of Vine and Wine*, 2017; 1–10.
[11] Tena, N. (2023, June 10). Extraction Methods for Anthocyanins. *Encyclopedia.* https://encyclopedia.pub/entry/19587
[12] Tiwary, K.B. Ultrasound: A clean, green extraction technology. *Trends Anal. Chem*, 2015; 71, 100–109.
[13] Vyas, S.; Ting, Y.P. A Review of the Application of Ultrasound in Bioleaching and Insights from Sonication in (Bio)Chemical Processes. *Resources*, 2018; *7*(3), 1–16.
[14] Herrera, M.C.; Luque de Castro, M.D.L. Ultrasound-assisted extraction for the analysis of phenolic compounds in strawberries. *Anal. Bioanal. Chem*, 2004; 379, 1106–1112.
[15] Li, H.; Chen, B.; Yao, S. Application of ultrasonic technique for extracting chlorogenic acid from Eucommia ulmodies Oliv. (E. ulmodies). *Ultrason. Sonochem*, 2005; 12, 295–300.
[16] Yang, Y.; Zhang, F. Ultrasound-assisted extraction of rutin and quercetin from Euonymus alatus (Thunb.) Sieb. *Ultrason. Sonochem*, 2008; 15, 308–313.
[17] Al-Hilphy, A.R.; Al-Temimi, A.B.; Al-Rubaiy, H.H.M.; Anand, U.; Delgado-Pando, G.; Lakhssassi, N. Ultrasound applications in poultry meat processing: A systematic review. *Journal of Food Science*, 2020; 1-11.
[18] Rajchasom, S.; Sombatnan, P.; Kantala, C.; Vuttijamnong, J.T. Effect of pulse electric field assisted extraction on anthocyanin content and antioxidant activity of purple rice. *SNRU Journal of Science and Technology*, 2022; *14*(2), 1–9.
[19] Rajchasom, S.; Sombatnan; Vuttijamnong, J.T. Effect of Ultrasonic Assisted Extraction Conditions on Phytochemical Content and Antioxidant Activity of Kao Kum Doi-Saket (*Oryza sativa* L. indica). *The 17th National and the 7th International Sripatum University Online Conference (SPUCON2022),* 2022; 489-501.
[20] Giusti, M.; Wrolstad, R.E. Characterization and measurement of anthocyanins by UV visible Spectroscopy, *CPFAC,* 2001; F1.2.1–F1.2.13.
[21] Sueaman, K.; Paksee, S.; Arpsuwan, A.; Chalongsuppunyoo, R.; Sam-ang, P.; Jannoey, P.; Pinwattana, K. Determination of antioxidant capacity of riceberry and khao dak mali 105 cultivars. *PSRU Journal of Science and Technology*, 2019; *4*(3), 95–108.
[22] He, S.; Lou, Q.; Shi, J.; Sun, H.; Zhang, M.; Li, Q. Water extraction of anthocyanins from black rice and purification using membrane separation and resin adsorption. *Journal of Food Processing and Preservation ISSN,* 2016; 1–8.
[23] Figueiredo, P.; Elhabiri, M.; Saito, N.; Brouillard, R. Anthocyanin Intramolecular Interactions. A New Mathematical Approach To Account for the Remarkable Colorant Properties of the Pigments Extracted from *Matthiola incana*. *Journal of the American Chemical Society*, 1996; 118, 4788-4793.
[24] Liu, Y.; Liu, Y.; Tao, C.; Liu, M.; Pan, Y.; Lv, Z. Effect of temperature and pH on stability of anthocyanin obtained from blueberry. *Journal of Food Measurement and Characterization*, 2018; 12, 1744–1753.
[25] Fernandes, F.; Pereira, E.; Prieto, M.A.; Calhelha, R.C.; Ciri´, A.; Sokovi´c, M.; Simal-Gandara, J.; Barros, L.; Ferreira, I. C. F. R. Optimization of the Extraction Process to Obtain a Colorant Ingredient from Leaves of *Ocimum basilicum* var. *purpurascens*. *Molecules*, 2019; 24, 1–18.
[26] Zhou, Y.; Zhao, X.; Huang, H. Effect of Pulsed Electric Fields on Anthocyanin Extraction Yield of Blueberry Processing By-Products. *Journal of Food Processing and Preservation*, 2015; 1-7.
[27] Manzoor, M.F.; Zeng, X.; Rahaman, A.; Siddeeg, A.; Aadil, R.M.; Ahmed, Z.; Li, J.; Niu, D. Combined impact of pulsed electric field and ultrasound on bioactive compounds and FT-IR analysis of almond extract. *J Food Sci Technol,* 2019; *56*(5), 2355–2364.
[28] Lertkaeo, P.; Yansakol, J.; Yoothit, K.; Kongputorn, S.; Promma, T. Comparison of traditional and ultrasonic-assisted extraction methods on anthocyanins, total phenolic compounds and antioxidant activity of Homdaeng ST.1 and Homdum ST.2 brown rice. *PSRU Journal of Science and Technology,* 2021; *6*(1), 109–122.
[29] Thakur, R.; Gupta, V.; Dhar, P.; Deka, S. C.; Das, A. B. Ultrasound-assisted extraction of anthocyanin from black rice bran using natural deep eutectic solvents: optimization, diffusivity, and stability. *Journal of Food Processing and Preservation,* 2022; *46*(3), e16309.

[30] Das, A.B.; Goud, V.V.; Das, C. Extraction of phenolic compounds and anthocyanin from black and purple rice bran (*Oryza sativa* L.) using ultrasound: A comparative analysis and phytochemical profiling. *Industrial Crops and Products*, 2017; 95, 332–341.

[31] Yamuangmorn, S.; Prom-u-Thai, C. The Potential of High-Anthocyanin Purple Rice as a Functional Ingredient in Human Health, *Antioxidants*, 2021; 10, 1–21.

[32] Madalão, M.C.M.; Lima, E.M.F.; Benincá, D.B.; Saraiva, S.H.; Carvalho, R.V.; Silva, P.I. Extraction of bioactive compounds from juçara pulp (Euterpe edulis M.) is affectedby ultrasonic power and temperature. *Food Science and Technology (Ciência e Agrotecnologia),* 2021; 45, eISSN 1981–1829.

[33] Bocker, R.; Silva, E.K. Pulsed electric field assisted extraction of natural food pigments and colorings from plant matrices. *Food Chemistry: X*, 2022; 15, 1–14.

[34] Bozinou, E.; Karageorgou, I.; Batra, G.; Dourtoglou, V.G.; Lalas, S.I. Pulsed Electric Field Extraction and Antioxidant Activity Determination of Moringa oleifera Dry Leaves: A Comparative Study with Other Extraction Techniques. *Beverages*, 2019; *5*(8), 1–13.

[35] Sirichokworrakit, S.; Rimkeeree, H.; Chantrapornchai, W.; Sukatta, U.; Rugthaworn P. The effect of extraction methods on phenolic, anthocyanin, and antioxidant activities of riceberry bran, *SSSTJ*. 2020; *7*(1), 7-13.

ASEAN
Journal of Scientific and Technological Reports
Online ISSN:2773-8752

Research article

Changing of Chlorophyll Contents in *Caulerpa lentillifera* After Five-Day Harvest

Bongkot Wichachucherd[1]*, Kattinat Sagulsawasdipan[2], and Eknarin Rodcharoen[3]

[1] Faculty of Liberal Arts and Science, Kasetsart University, Kamphaeng Saen, Nakorn Pathom 73140, Thailand; bongkot.w@ku.th
[2] Faculty of Science and Fisheries Technology, Rajamangala University of Technology Srivijaya, Trang 92150, Thailand; kattinat.s@gmail.com
[3] Faculty of Natural Resource, Prince of Songkla University, Hat Yai, Songkhla 90110, Thailand; eknarin.r@psu.ac.th
* Corresponding author: bongkot.w@ku.th

Citation:
Wichachucherd, B., Sagulsawasdipan, K., Rodcharoen, E. Changing of chlorophyll contents in *Caulerpa lentillifera* after five-days harvest. *ASEAN J. Sci. Tech. Report.* **2023**, *26*(4), 47-53. https://doi.org/10.55164/ajstr.v26i4.250150

Article history:
Received: July 6, 2023
Revised: September 21, 2023
Accepted: September 22, 2023
Available online: September 30, 2023

Abstract: *Caulerpa lentillifera* is a marine macroalgae widely consumed in Asia Pacific, including Thailand. Quality and freshness are the main criteria for consumers. Chlorophyll is an important fundamental pigmentation and acts as green in *C. lentillifera.* It can be variable according to light and growth, and then it can indicate the quality of *C. lentillifera* products. This research aimed to observe changing chlorophyll contents in C. lentillifera after harvest during five days from two different months- May and June and two different ponds-ponds 1 and 2 by chlorophyll extraction and measurements of chlorophyll fluorescence. The result showed that the contents of total chlorophyll and chlorophyll A differed between months, but the pattern did not significantly change even in different months and ponds within five days after harvest.

Keywords: *Caulerpa lentillifera*; Chlorophyll; Harvesting

1. Introduction

C. lentillifera is a famous culture species in the Indo-Pacific [1,2]. Because of its grape shape [3], the common name of this species is sea grapes or green caviar. The upright *C. lentillifera* thallus can be up to 10 centimeters long branch. Ramuli has a spherical tip about 1-3 cm in diameter and ramuli are densely clustered on each algae component [4]. *C. lentillifera* grows on rocks or the shallow water sandy ground near the coral reef. It can be found in muddy sand and can be acclimatized to grow well in ponds but cannot tolerate fresh water. It is distributed in tropical and subtropical regions. It is now commonly eaten in Asia-Pacific countries such as Japan, Vietnam, the Philippines, Malaysia, Indonesia, and Thailand [2, 5]. It has become about 1 ton/month in demand in the Thai market. *C. lentillifera* farms are widely along the Gulf of Thailand coast, rich in water nutrients and sunlight. The harvest in those areas is either from natural or ponds [4].

Much research shows that C. lentillifera is one of the functional food causes of rich minerals, essential amino acids, and fiber [1, 6-9]. These may support why this species became in higher demand in the market besides its shape. However, quality and freshness are important considerations for consumers as fresh purchases. Therefore, seaweed pigments can observe one of the quality criteria.

Green seaweed contains an important basic pigment that plays an important role in capturing sunlight for photosynthesis. The basic pigment group is chlorophyll; chlorophyll A is the primary pigmentation. Because it changes with the amount of light intensity, it can also be an indicator of the quality of seaweed [10]. This was the reason for studying the changes in the amount of pigment in *C. lentillifera* after harvesting for sale. The rate of change of chlorophyll content was examined when the algae were harvested for a longer time according to transportation from ponds to the marketplaces. To determine whether seaweed quality after harvest will likely decrease or increase. Therefore, this study aimed to study the chlorophyll change pattern within five days of culture *C. lentillifera* after harvest. The temporal and spatial variation of the chlorophyll change were compared to the environmental condition.

2. Materials and Methods

2.1 Study site and sampling

Samplings were carried out at open-pond cultures (Figure 1) in Ban Laem, where the commercial and original spread out of the fresh Caulerpa around Phetchaburi province and other markets. The test was set to investigate the pattern of chlorophyll quantity change in temporal (May to June) and spatial variation (ponds 1 and 2) during five days of harvest. Five days were settled as more time was spent transporting from pond to sold. The experiment started at the month of growth peak in May and June 2017. *Caulerpa* samples were randomly collected from the pond, placed in a box, and transferred to the laboratory (Figure 2). All specimens were kept in the dark container at room temperature until the day of the test. Specimens were sub-sampled for a series of each-day experiments.

Figure 1. A bottom planting culture pond at Ban Lad in Phetchaburi province.

2.2 Chlorophyll extraction

Specimens (approximately 1 gram) were cleaned from the sediment and then went through the steps of the chlorophyll extraction process. Fresh *Caulerpa* samples were extracted with 80% acetone. The modified chlorophyll extraction protocol was followed by Arnon [11] and Hui et al. [12]. Briefly, specimens were chopped into small pieces and digested in 80% acetone in a cool and dark condition for 5 minutes, then centrifuged at 4,000 *g* for 15 minutes. The supernatant was taken to the cuvette for light absorbance at different wavelengths via spectrophotometer. The total chlorophyll and chlorophyll A were calculated by the equation (1-2) below [12].

$$\text{Total Chlorophyll} = 8.02A_{663} + 20.21A_{664}, \quad (1)$$

$$\text{Chlorophyll A} = 11.85A_{664} - 1.54A_{647} - 0.08A_{630} \quad (2)$$

Figure 2. Fresh *Caulerpa* samples from a culture pond in Phetchaburi province.

2.3 Statistical analysis

Five replications were done throughout all experiments. Two-way ANOVA was employed on the total chlorophyll and chlorophyll A amount on different days, comparing months and ponds. All data were checked for the normal distribution as the criteria. All analyses were carried out with SPSS version 16.0 (SPSS Inc., USA)

3. Results and Discussion

Total chlorophyll and chlorophyll A content were used to determine the change in *Caulerpa* pigmentation. They showed parallel change, as expected, for the main pigment accumulation for green seaweed. The difference in total chlorophyll and chlorophyll A showed a similar trend of wavelength absorbance. Chlorophyll A is the main pigmentation of the green algae [13]. Therefore, changing the main pigmentation would affect the total chlorophyll in cell accumulation [14]. Also, A consistent change in total chlorophyll and chlorophyll A values should give a similar result in similar values when the experiment was done at the same time [15].

3.1. Comparing chlorophyll contents between months of study along five days

By comparing the changes in chlorophyll contents after sampling, it was found that total chlorophyll and chlorophyll A content were changed in similar patterns in both months studied, with fluctuation during the test in May (Figure 3). Chlorophyll contents showed higher in May than in June. In May, the significant difference of both concentrations was found during five days when $p < 0.05$. The high variation was along days 2-4 by a range of 0.68 ± 0.1 mg/l to 0.98 ± 0.2 mg/l for total chlorophyll and a range of 0.34 ± 0.05 mg/l to 0.48 ± 0.1 mg/l for chlorophyll A. It caused a significant difference in chlorophyll content during five days in May.

However, the content between the first day (0.39 ± 0.24 mg/l of total chlorophyll and 0.21 ± 0.12 mg/l of chlorophyll A) and the last day (0.46 ± 0.2 mg/L of total chlorophyll 0.27 ± 0.09 mg/l of chlorophyll A) of the test were not slightly difference. In other words, there was no significant change in June when $p > 0.05$ for both total chlorophyll and chlorophyll A during five days. The range of total chlorophyll was from 0.39 ± 0.1 mg/l to 0.68 ± 0.25 mg/l and 0.18 ± 0.08 mg/l to 0.32 ± 0.09 mg/l for chlorophyll A.

There was a temporal variation in the total chlorophyll and chlorophyll A between different months of sampling and along the day of study. The high fluctuation of those contents occurred in May, which caused the significant difference between months of study when $p < 0.05$. May showed a higher range of both contents

than June, except for the first day of total chlorophyll content. Total chlorophyll and chlorophyll A on the first day were 0.39 ± 0.25 mg/l and 0.21 ± 0.12 mg/l in May and 0.68 ± 0.25 mg/l and 0.32 ± 0.09 mg/l in June, respectively. Otherwise, both contents had no significant differences when $p > 0.05$ on the first day of the study. The significant differences between months showed in days 2 and 3 for total chlorophyll when $p < 0.01$ (Figure 3A) and in days 2, 3, and 4 for chlorophyll A when $p < 0.05$ (Figure 3B).

The chlorophyll concentration was in May rather than June at the start date. This refers to the temporal variation in open culture, which can be affected by the multifactor of environment such as light intensity, temperature, and rainfall. Higher light intensity in May might affect the cell's biological mechanism and raise the chlorophyll content. This evidence could be confirmed by previous research in *Spirulina subsalsa.* The result showed that the decrease of the photosynthetic rate at high light energy was accompanied by increased antioxidant network response, such as carotenoids, total polyphenols, and antioxidant capacity. [16]. The chemical accumulation and function can cause environmental differences that influence seaweed growth [17]. Even though the culture has been manipulated throughout the year in Thailand, *C. lentilifera* grows in the dry season, which starts in February and peaks in May and June, during which this study began. The result of this study referred only to the condition of healthy specimens observed in May and June.

3.2 Comparing chlorophyll contents between ponds of study along five days

Sampling was done in the same months but in different ponds-pond 1 and 2. It indicated the culture spatial variation in total chlorophyll and chlorophyll A of *C. lentilifera.* The total chlorophyll and chlorophyll A changes were not significantly different over five days or between observing ponds. The total chlorophyll varied on the first study day when $p < 0.05$ (Figure 4). The average of total chlorophyll and chlorophyll A for five days were 0.48 ± 0.08 mg/l and 0.53 ± 0.19 mg/l for pond 1 and 0.23 ± 0.08 mg/l and 0.26 ± 0.08 mg/l for pond 2. Typically, the physiological activity of seaweed deteriorates after harvesting. That also causes quantity and quality loss in seaweed. In other words, they arose from changes in both physical and chemical components. Its expression would be found as outward shape, taste, and texture change [18]. These transformations would gradually occur over time after harvest. The constituent pigments, such as chlorophyll, will decompose over time when seaweed has been harvested. However, total chlorophyll and chlorophyll A were not significantly different change during five days after harvest in this study. The result showed that the amounts of chlorophyll A and total chlorophyll were not much different from the five-day study. Chlorophyll may be degraded to some extent, as indicated in the concentration fluctuation. Despite this, it is not so much that it can be a significant difference experiment. Therefore, total chlorophyll and chlorophyll A can remain in the algae tissue within five days without losing all these pigments.

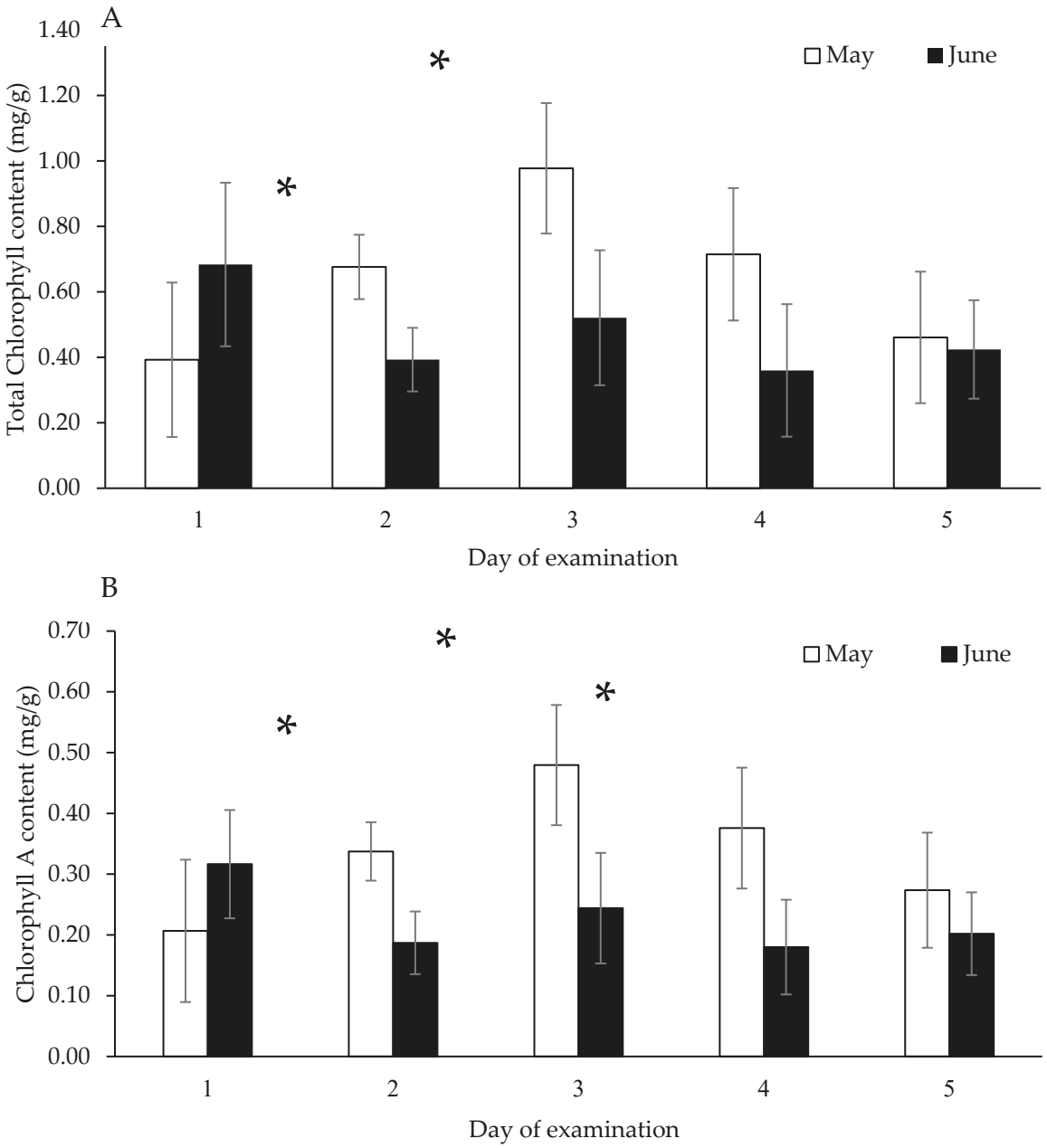

Figure 3. Temporal variation of the total chlorophyll (A) and chlorophyll A (B) contents between May and June during five days. Data represent mean ± SD. Asterisk showed a significant difference between the two months of study.

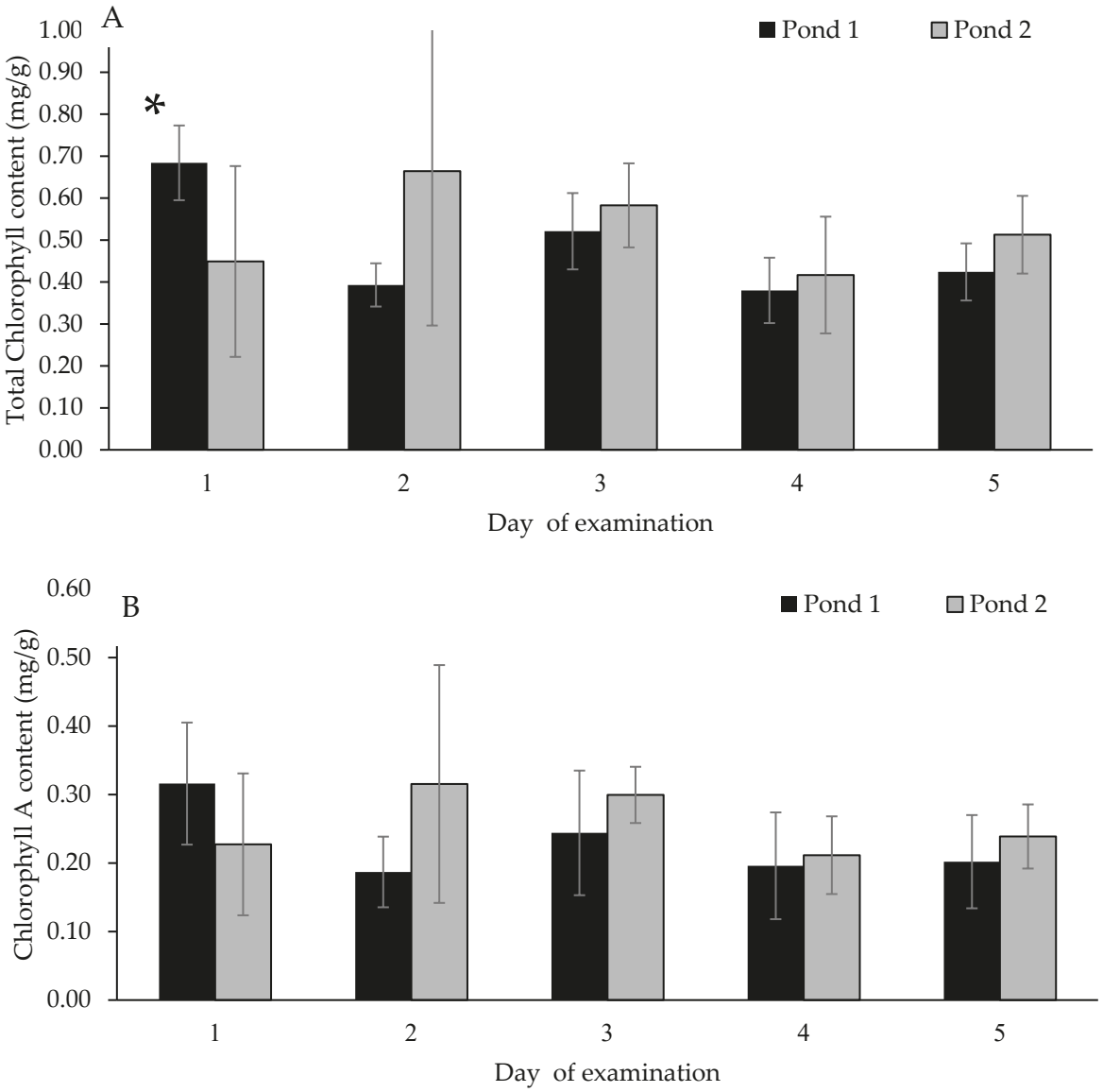

Figure 4. Spatial variation of the total chlorophyll (A) and chlorophyll A (B) contents between Ponds 1 and 2 during five days. Data represent mean ± SD. Asterisk showed a significant difference between the two months of study.

4. Conclusions

In conclusion, the chlorophyll accumulation did not change much in five days after harvest. The fluctuation according to spatial and temporal variation can be observed in *C. lentilifera.*

5. Acknowledgements

This research was funded by Kasetsart University Research and Development Institute KURDI (grant number FF65(KU)15.65).

Author Contributions: Authors all worked and shared contributions as follows: conceptual framework, field sampling through the analysis and shaping up the draft of the manuscript, B. W.; field sampling preparation and methodology, K. S.; laboratory equipment supporting, fieldwork, and investigation, E. R.

Funding: Kasetsart University Research and Development Institute KURDI (grant number FF65(KU)15.65)

Conflicts of Interest: The authors declare no conflict of interest.

References

[1] Paul, N.A.; Neveux, N.; Magnusson, M.; de Nys, R. Comparative production and nutritional value of "sea grapes" — the tropical green seaweeds *Caulerpa lentillifera* and *C. racemosa*. *Journal of Applied Phycology*, 2014; 24, 1833-1844. https://doi.org/10.1007/s10811-013-0227-9

[2] de Gaillande, Payri ,C.; Remoissenet, G.; Zubia, M. *Caulerpa* consumption, nutritional value and farming in the Indo-Pacific region. *Journal of Applied Phycology*, 2016; *29*(5), 2249-2266.

[3] Estrada, J.L.; Dionisio-Sese, M.; Bautista, N.S. Morphological variation of two common sea grapes (*Caulerpa lentillifera* and *Caulerpa racemosa*) from selected regions in the Philippines. *Biodiversitas Journal of Biological Diversity*, 2020; 21, 1823-1832.

[4] Critchley, A.T.; Ohno, M.; Trono, G.C.; Toma, T.; Kawashima, S.; Matsuoka, M.; Oohusa, T.; Largo, D.B.; Fortes, M.D. *Seaweed Cultivation and Marine Ranching,* 1993; 17-23.

[5] Chaiklahan, R.; Srinorasing, T.; Chirasuwan, N.; Tamtin, M.; Bunnag, B. The potential of polysaccharide extracts from *Caulerpa lentillifera* waste. *International Journal of Biological Macromolecules,* 2020; 161,1021-1028.

[6] Ratana-arporn, P.; Chirapart, A. Nutritional Evaluation of Tropical Green Seaweeds *Caulerpa lentillifera* and *Ulva reticulata*. *Kasetsart Journal-Natural science*, 2006; 40, 75-83.

[7] Nguyen, V.T.; Ueng, J.P.; Tsai, G.J. Proximate composition, total phenolic content, and antioxidant activity of seagrape (*Caulerpa lentillifera*). *Journal of Food Sciences*, 2011; *76*(7), 950-958.

[8] du Preez, R.; Majzoub, M.E.; Thomas, T.; Panchal, S.K.; Brown, L. *C. lentillifera* (Sea Grapes) Improves Cardiovascular and Metabolic Health of Rats with Diet-Induced Metabolic Syndrome. *Metabolites*, 2020; *10*(12) https://doi.org/10.3390/metabo10120500

[9] Rushdi, M.I.; Abdel-Rahman, I.A.M.; Attia, E.Z.; Abdelraheem, W.M.; Saber, H.; Madkour, H.A.; Amin, E.; Hassan, H.M.; Abdelmohsen, U.R. A review on the diversity, chemical and pharmacological potential of the green algae genus. *South African Journal of Botany*, 2020; 132, 226-241. https://doi.org/10.1016/j.sajb.2020.04.031

[10] Toivonen, P.M.A. Chlorophyll Fluorescence as a Nondestructive Indicator of Freshness in Harvested Broccoli. *Hortscience*, 1992; *27*(9), 1014-1015.

[11] Arnon, D.I. Copper enzymes in isolated chloroplasts. Polyphenoloxidase in Beta vulgaris. *Plant Physiology*, 1949; 24, 1-15.

[12] Hui, G.; Jianting, Y.; Zhongmin, S.; Delin, D. Effects of salinity and nutrients on the growth and chlorophyll fluorescence of *Caulerpa lentillifera*. *Chinese Journal of Oceanology and Limnology*, 2015; *33*(2), 410-418.

[13] Lee, R.E. *Phycology*. 3, editor. United Kingdom: The Cambridge University Press, 1999; 614.

[14] Irena, P.; Olszówka, K.; Chilczuk, B. Changes in the chlorophyll content in stored Lettuce *Lactuca sativa L.* after pre-harvest foliar application of $CaCl_2$. *Acta Agrobotanica*. 2013; *66*(4), 137-142

[15] Nazeer, A.; Singh, D.B.; Singh, S.R.; Mir, K.A.; Lal, S. Variation in chlorophyll and carotenoid contents in kale (*Brassica oleracea*) as influenced by cultivars and harvesting dates. *Indian Journal of Agricultural Sciences,* 2014; *84*(10), 1178–81

[16] Pistelli, L.; Del Mondo, A.; Smerilli, A.; Corato, F.; Sansone, C.; Brunet, C. Biotechnological response curve of the cyanobacterium *Spirulina subsalsa* to light energy gradient. *Biotechnol Biofuels Bioprod*, 2023, *16*(1), 28. https://doi.org/10.1186/s13068-023-02277-4

[17] Wichachucherd, B.; Pannak, S.; Saengthong, C.; Rodcharoen, E.; Koodkaew, I. Correlation between Growth, Phenolic Content and Antioxidant Activity in the Edible Seaweed, *Caulerpa lentillifera* in Open Pond Culture System. *Journal of Fisheries and Environment*, 2019; *43*(2), 66-75.

[18] Wills, R.B.H.; McGlasson, W.B.; Graham, D.; Joyce, D.C. *Postharvest an introduction to the physiology and handling of fruit, vegetables and ornamentals*. University of New South Wales Press Ltd. Australia. 1998.

ASEAN
Journal of Scientific and Technological Reports
Online ISSN:2773-8752

Research article

Exploring the Efficacy of *Bacillus oceanisediminis* Ba9 from Asian Seabass Cage Sediment in Saline Wastewater Treatment

Sunipa Chankaew[1], and Yutthapong Sangnoi[2]*

[1] Faculty of Natural Resources, Prince of Songkla University, Songkhla, 90110, Thailand; chan.sunipa@gmail.com
[2] Faculty of Natural Resources, Prince of Songkla University, Songkhla, 90110, Thailand; yutthapong.s@psu.ac.th
* Correspondence: yutthapong.s@psu.ac.th

Citation:
Chankaew, S., Sangnoi, Y. Exploring the efficacy of *Bacillus oceanisediminis* Ba9 from Asian seabass cage sediment in saline wastewater treatment. *ASEAN J. Sci. Tech. Report.* **2023**, *26*(4), 54-66. https://doi.org/10.55164/ajstr.v26i4.250805

Article history:
Received: September 4, 2023
Revised: September 26, 2023
Accepted: September 27, 2023
Available online: September 30, 2023

Abstract: Preventing toxicity in aquaculture systems from ammonia and nitrite is important. This study isolated the salt-tolerant Bacillus sp. strain Ba9 from bottom sediment under an Asian Seabass (*Lates calcarifer*) cage cultivating at Koh Yor, Songkhla, Thailand. Morphological characteristics showed that strain Ba9 was rod-shaped, endospore-forming, and Gram-positive. Strain Ba9 grew well at a salinity of 1.5 to 4.0% NaCl. The catalase test of the isolate was positive, while the oxidase test was negative. Based on 16S rRNA gene sequencing data and phylogenetic tree analysis, strain Ba9 was identified as *B. oceanisediminis* with 97% similarity (strain HQB337^T). The result showed that the ammonium removal efficiency of Ba9 in a high ammonium medium was 64.24%. The nitrite and nitrate production were 0.10% and 0.08%, respectively. Consequently, sucrose had been the optimal carbon source for Ba9, which showed ammonium removal was 61.05%. Ammonium sulfate is the most suitable for ammonium oxidation, with 50.53% for the nitrogen source. The optimal C/N ratio of strain Ba9 was 8, with 71.15% ammonia removal. For wastewater improvement, strain Ba9 was inoculated into artificial wastewater for 14 days. The result showed that the ammonium removal efficiency of Ba9 was 96.87%. In addition, the biochemical oxygen demand (BOD) removal efficiency of Ba9 was 90.86%. From this result, the salt-tolerant *B. oceanisediminis* Ba9 has a high potential as a microbial product for water quality management in marine aquaculture.

Keywords: Salt-tolerant *Bacillus* sp.; *B. oceanisediminis*; ammonium removal; BOD; water treatment

1. Introduction

A major element of conventional wastewater treatment processes is nitrogen removal. In an aquaculture pond, genuinely dangerous nitrogen compounds include ammonia (NH_3) and nitrite (NO_2^-). One of the most efficient methods for removing nitrogen from wastewater is a microbiological process (nitrification and denitrification). In principle, aerobic nitrification and anaerobic denitrification are performed to remove nitrogen compounds [1-3]. Most of the microbial population in nitrification are autotrophic nitrifying bacteria. Ammonia-oxidizing bacteria in the members of genera *Nitrosomonas, Nitrosospira, Nitrosococcus, Nitrosolobus*, and *Nitrosovibrio* can transform ammonium into nitrite. Nitrite-oxidizing bacteria, including genera *Nitrobacter, Nitrospira*, and *Nitrococcus*, can convert nitrite to nitrate [4-5]. Then, nitrate is converted to nitrogenous gas because of the denitrification process carried out

by heterotrophic denitrifying microorganisms. Besides, nitrate can be utilized by algae. Moreover, separating aerobic and anaerobic phases, the prolonged life cycle of autotrophic nitrifying bacteria results in a long starting period for nitrogen removal. The specific growth rates of autotrophic nitrifiers are weak, and their biomass is sensitive to toxic substances such as heavy metals and pH [6-7]. Recently, it has been found that nitrification and denitrification can be carried out simultaneously in one system [8], thus overcoming the problems existing in the traditional biological nitrogen removal process.

In addition to autotrophic nitrifying bacteria, a large variety of heterotrophic bacteria can oxidize ammonia, which is important to the natural nitrogen cycle [9]. A previous report showed that the heterotrophic nitrification process outperformed the autotrophic problem regarding ammonia removal [10]. Since heterotrophic nitrifying bacteria have more phylogenetic diversity than their autotrophic counterparts, they can better adapt to their conditions [11]. Several studies have shown that some *Bacillus* can control nitrogenous waste in aquaculture. In a study by Thurlow *et al*. [12], they reported that catfish pond water treated with *Bacillus velezensis* AP193 had reduced levels of nitrate-nitrogen (by 75%) and total nitrogen (by 43%). In a similar finding, Lalloo *et al*. [13] noted decreased nitrate and nitrite in synthetic pond water following *Bacillus* treatment. Regardless of the form, relatively low concentrations of nitrite and nitrate have been recorded. As an illustration, increased nitrate, nitrite, and decreased nitrite-N have been seen following *Bacillus* treatment [13-18]. It has been reported that *Bacillus* can reduce or modulate ammonia toxicity. In particular, aquaculture research has found that *B. subtilis, B. megaterium*, and *B. amyloliquefaciens* reduced ammonia levels in shrimp ponds [16-17,19]. Aquaculture constantly makes use of *Bacillus* spp. They have been developed as a treatment to clean water, enhance growth rates, protect against disease, and increase the immune system. [12,20-23].

In many investigations, Biochemical Oxygen Demand (BOD) and Chemical Oxygen Demand (COD) were lowered when *Bacillus* species were used as water quality modulators in aquaculture. Better feed utilization by fish may be related to this; as a result, less organic material decomposes using Dissolved Oxygen (DO), and potentially, *Bacillus* species require less DO to break down organic material efficiently. For instance, *B. megaterium* effectively lowered the BOD of major carp's pond water [18]. Reduced BOD (above 90%) was again recorded by Reddy *et al*. [24] in *Bacillus* (*B. subtilis, B. mojavensis*, and *B. cereus*) treated ponds. Similarly, a mix of *B. cereus* and *Aeromonas veronii* decreased BOD after effluent treatment [25]. Reduced COD levels were recorded in *B. subtilis, B. megaterium,* and *Bacillus* sp. YB1701 [18, 26] Therefore, elements including organic nutrition, DO, salinity, and application methods influence the efficiency of *Bacillus* in biological treatment.

This study aims to isolate and determine salt-tolerant *Bacillus* sp. based on morphological, biochemical, and 16S rRNA sequence information. Additionally, the purpose is to measure their nitrogen removal efficiency and biochemical oxygen demand in synthetic salinity wastewater.

2. Materials and Methods

2.1 Isolation and screening of *Bacillus* sp.

Salt-tolerant *Bacillus* sp. was isolated from sediment samples collected under a cage of Asian Sea bass (*Lates calcarifer*) culture at Koh Yor, Songkhla province, South Thailand. One gram of the sample was dissolved into 0.7% NaCl and heat shock on a water bath at 80 ^{o}C for 20 min, followed by a cold shock into room temperature water [27]. The suspension of the sample was ten-fold diluted, and then 0.1 ml was pipetted onto nutrient agar (NA) (HiMedia, India) + 0.7% NaCl. Purified strains were obtained after 3-4 times of re-streaking. The single colony was used to determine morphological and biochemical. The Gram staining and cell morphology were examined under a light microscope (Olympus BX50). Catalase activity was tested by bubble formation in 3% H_2O_2 solution. Oxidase activity was tested on a test strip (Merck) to observe the oxidation of *N,N*-dimethyl-1, 4-phenylene diammonium dichloride. Optimal salt requirement of 0-4.0% NaCl (w/v) was examined. One milliliter of bacterial cells was inoculated in tubes containing 9 ml of nutrient broth (NB) (HiMedia, India), with the addition of NaCl in the range of 0, 0.5, 1.0, 1.5, 2.0, 2.5, 3.0, 3.5 and 4.0 g/100 ml.

2.2 Identification of heterotrophic nitrifying bacteria

The Genomic DNA mini kit (Geneaid) was used to extract the genomic DNA of the *Bacillus* species. The 16S rRNA gene universal primers 27F (5'-AGAGTTTGATCATGGCTCAG-3') and 1492R (5′-TACCTTGTTACGACTT) were used to amplify the 16S rRNA genes by PCR [28-30]. The PCR amplification protocol proceeded as follows: initial denaturation (94°C for 3 minutes), 30 cycles of denaturation (94°C for 1 minute), annealing (50°C for 1 minute), extension (72°C for 2 minutes), final extension (72°C for 3 minutes), and storage (4°C for hold). The PCR result was examined using 1% agarose gel electrophoresis after amplification. The PCR products were purified using a GeneFlowTM Gel/PCR Kit (Geneaid Biotech Ltd., Taiwan). The sequencing service provider directly sequenced the purified PCR products on an ABI Prism® 3730XL DNA Sequence (Applied Biosystems, Foster City, California, USA). The 16S rRNA gene sequence was compared with other microorganisms using the Basic Local Alignment Search Tool program (BLAST; http://www.ncbi.nlm.nih.gov/BLAST/Blast.cgi). A phylogenetic tree of partial 16S rRNA gene sequences of the isolates and neighboring species was constructed by the MEGA 11 program [31]. A bootstrap value was performed with 1,000 replicates, and the phylogenetic tree was determined using neighbor-joining, maximum parsimony, and maximum likelihood.

2.3 Ammonium removal efficiency of *Bacillus* sp.

The efficacy of ammonium removal in a high ammonium medium was evaluated on a flask scale. About 1.5 ml (1% v/v) cell suspension of Ba9 cultivated in modified Pep-Beef AOM (peptone 5.0 g, beef extract 3.0 g, $(NH_4)_2SO_4$ 2.0 g, K_2HPO_4 0.75 g, NaH_2PO_4 0.25 g, $MgSO_4$ 0.03 g, $MnSO_4$ 0.01 g and tri-sodium citrate 17.8054 g in seawater (22 ppt) 1,000 mL) was inoculated into 150 ml of high ammonium medium (modified Pep-Beef AOM, which adjusted $(NH_4)_2SO_4$ to 4 g). This was used to examine the ammonium removal efficiency of *Bacillus* sp. and shaken at 170 rpm, 28°C. After 5 days of cultivation, the bacterial cells were removed by centrifugation at 3,500 rpm for 40 minutes [28-30]. After collecting the supernatant, the amounts of ammonium (NH_4^+) and nitrite (NO_2^-) were determined by the colorimetric method, and the concentration of nitrate (NO_3^-) was measured by the cadmium reduction column method [32].

2.6 Optimize carbon and nitrogen sources, C/N ratio, and salt tolerance.

2.6.1 Carbon source

The isolate was cultivated in a high ammonium medium supplemented by different carbon sources: sodium citrate ($C_6H_5Na_3O_7$), sodium acetate (CH_3COONa), glucose ($C_6H_{12}O_6$), sodium succinate ($C_4H_4Na_2O_4$), and sucrose ($C_{12}H_{22}O_{11}$) providing as a single carbon source in high ammonium medium [33]. The amount of $(NH_4)_2SO_4$ (N source) was fixed (the initial concentration of ammonia was set at 790-800 mg-N/L). Then, the medium was autoclaved at 121 °C for 15 min. The 1.5 ml of 10^9 cfu/ml bacterial starter from enrichment culture was inoculated in 250-mL shaker flasks containing 150 mL medium and shaken at 170 rpm, 28°C for 5 days. At the end of cultivation, the suspension was centrifuged at 3,500 rpm for 40 minutes to remove bacterial cells. The supernatant was collected, and then the concentrations of ammonium (NH_4^+), nitrite (NO_2^-), and nitrate (NO_3^-) were measured following the standard method [32]. Then, the highest ammonium removal efficiency was obtained, and the carbon source contained in the selected medium was suggested as the optimal carbon source for further study.

2.6.2 Nitrogen source

The strain was cultivated in a high ammonium medium with different nitrogen sources substituting (the initial concentration of ammonium was fixed at 800-820 mg-N/L) with the appropriate carbon source. Two different nitrogen sources were ammonium sulfate [$(NH_4)_2SO_4$] and ammonium chloride (NH_4Cl). All media were autoclaved at 121 °C for 15 min. The cultural conditions were mentioned above. After incubation for 5 days, the supernatant was obtained through centrifugation and measured. The medium that showed the highest nitrogen removal efficiency was cited as the optimal nitrogen source [34-35]

2.6.3 C/N ratio

Optimal carbon and nitrogen sources were chosen to study the optimal C/N ratio. The C/N ratio was adjusted to 0, 2, 4, 8, and 16 by fixing the amount of $(NH_4)_2SO_4$ (the N source) at 800-830 mg-N/L and adding sucrose as the carbon source. At 121 °C for 15 minutes, all media were autoclaved. The cultural condition was the same as above. Nitrogen removal efficiency in supernatant was analyzed after cultivation and centrifugation, followed by the standard method [32].

2.6.4 Optimization of salt requirement of Bacillus sp.

A single *Bacillus* sp. colony was taken from the plate, inoculated in NB with 0.85% NaCl (w/v), and then incubated at 28°C 180 rpm for 24 hr. NaCl was added at concentrations of 0, 0.5, 1.0, 1.5, 2.0, 2.5, 3.0, 3.5, and 4.0 % (w/v) to the media for the salinity requirement study. Test flasks were incubated at 28°C 180 rpm for 24 hr. After incubation, the supernatant was also used to measure cell density by a spectrophotometer (NanoPhotometer, IMPLEN, Germany) at a wavelength of 600 nm [27].

2.7 The efficient removal of *Bacillus* sp. in the sterilization of synthetic wastewater.

The salinity wastewater was increased by fermenting with an Asian seabass diet (Profeed, Thailand) at 0.5% w/v for 5 days. After 5 days, the salinity wastewater was sterilized by autoclave at 121°C for 15 min. *Bacillus* sp. was tested for the efficiency of BOD and nitrogen removal. Seventy milliliters of bacterial suspension (10^9 cfu/ml) was inoculated into 7 L of prepared wastewater and aeration was given throughout the trial period for 14 days. Every day of cultivation, 200 ml of wastewater was collected and evaluated for the amounts of ammonia, nitrite, and nitrate [32]. The wastewater was collected, and its BOD concentration was measured every 7 days of cultivation [36].

2.8 Statistical methods

The analysis of variance (ANOVA) was applied to the parameters of ammonia, nitrite, nitrate, and BOD. Before analysis, the data was transformed as necessary. The difference between the treatment means was determined using Duncan's new multiple range test (DMRT) method at 95% significance ($P < 0.05$). Data was expressed as Mean ± SE (standard error mean) using a statistical analysis R program.

3. Results and Discussion

3.1 Characterization and its biochemical properties.

Gram-stained morphological analysis of Ba9 demonstrated that the bacterial isolate was Gram-positive, rod-shaped, and endospore-forming (Figure 1). The biochemical characteristics of catalase and oxidase tests were positive and negative, respectively. The information on the Ba9 is shown in Table 1. A blast search result of the partial 16S rRNA gene sequence of Ba9 revealed 97% similarity to *B. oceanisediminis* HQB337^T (KT758497). Also, the identification result of the partial 16S rRNA gene sequence was relevant to the phylogenetic tree analysis (Figure 2). This tree demonstrated the evolutionary branches of strain Ba9 and *B. oceanisediminis* HQB337^T (KT758497) were closely related (Figure 2). However, more identification results of Ba9 should be performed by full-length 16S rRNA gene analysis.

Table 1. Morphology and biochemical test of *Bacillus oceanisediminis* Ba9.

Strain	Colony color	Gram	Shape	Endospore-forming	Catalase tests	Oxidase tests
Ba9	Creamy	Positive	Rod	Positive	Positive	Negative

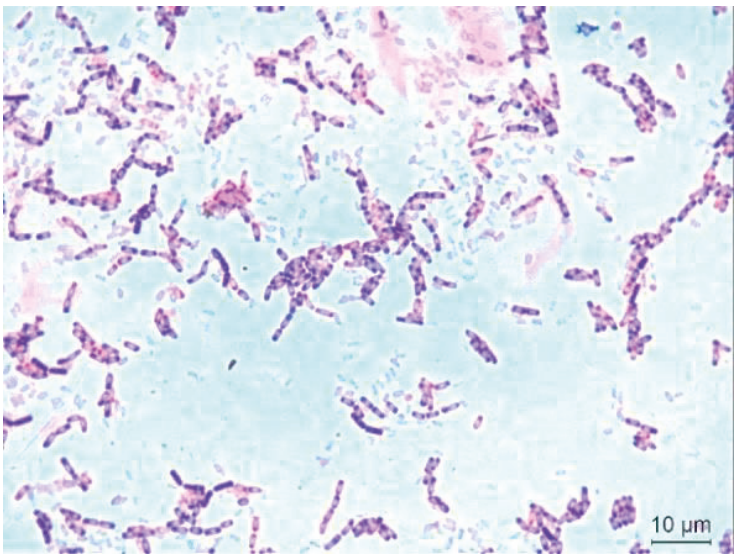

Figure 1. Vegetative cell morphology of *Bacillus* sp. Ba9.

3.2 Efficiency of ammonium removal in a high ammonium medium.

The concentrations of ammonia, nitrite, and nitrate were measured as part of a nitrogen removal efficiency analysis. The results showed that the single culture of the *Bacillus* sp. Ba9 had an ammonium removal efficiency of 64.24%. Nitrite and nitrate were produced by Ba9 from 0.00 mg-N/L to 0.01 and 0.08 mg-N/L, respectively (Figure 3). According to previous studies, the result suggested that *B. subtilis* A1 provided an excellent ability for ammonium removal. Lu and co-workers [35] reported a maximum ammonium removal of another heterotrophic bacterium, *Alcaligenes faecalis* WT14, for 95% in high ammonium concentration treatment (about 400 mg-N/L). However, the ammonium removal efficiency of *A. faecalis* WT14 decreased to 60% when an ammonium concentration increased to 700-1,600 mg-N/L. Also, the report of Xiao *et al*. [37] that demonstrated the efficacy of *Bacillus subtillis* AYC for nitrogen removal proceeded that had initial ammonium 10 mg-N/L, after 10 min the concentration of ammonium dramatically decreased, after 30 min, the ammonium concentration was low and remained to steadiness. The lowest ammonium removal efficiency was 43% when the high ammonium concentration was 2,000 mg-N/L. Other reports indicated that *Alcaligenes faecalis* no.4 had a high efficiency of ammonium removal at high ammonium levels (1,050 mg-N/L in 68 hrs.) [38]. Moreover, the immobilized cells of *Alcaligenes* sp.TD-94 and *Paracoccus* sp. TD-10 for treating high-ammonia-nitrogen wastewater was reported. Their contributions of biodegradation and adsorption to ammonium nitrogen removal were 90.27% and 9.73%, respectively. Bacterial immobilized cells were used to treat genuine high-ammonia-nitrogen wastewater, and the removal rates of ammonium reached 75.21 mg/L per day and removal efficiency of 99.27% after 48 hours of reaction. [23].

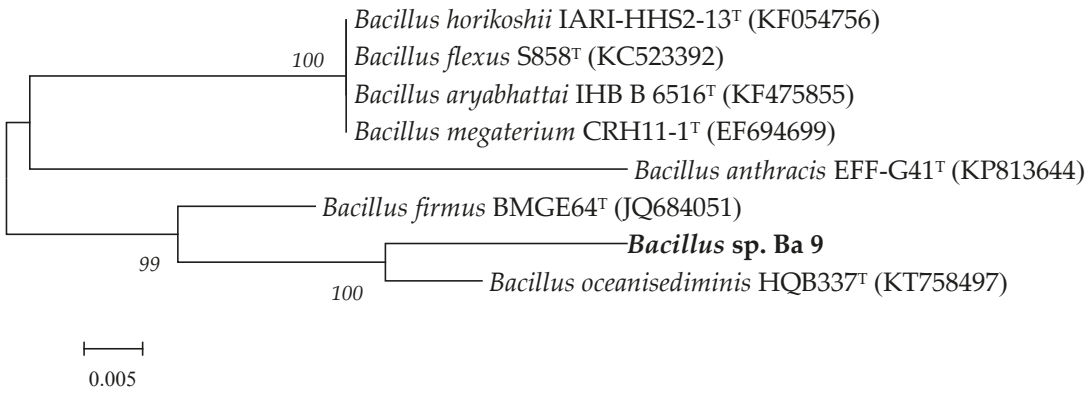

Figure 2. Phylogenetic tree of partial 16S rRNA gene sequences of *Bacillus* sp. Ba9 and related species (Bar = 0.005).

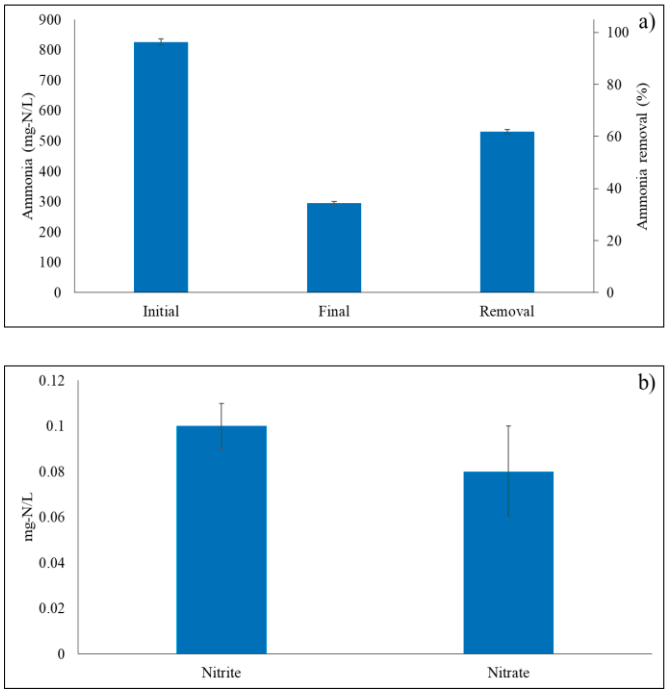

Figure 3. Nitrogen removal efficiency, a) ammonium removal efficiency, and b) nitrite and nitrate concentration (mg-N/L).

3.3 Optimize carbon and nitrogen sources, C/N ratio, and salt tolerance.

3.3.1 Carbon and Nitrogen Sources

Bacillus sp. Ba9 was employed during the research to determine the most effective carbon sources for ammonium removal (initial ammonia of 789-893 mg-N/L). Strain Ba9 using sucrose as a carbon source had ammonium removal of 61.05% (Figure 4a) and a nitrite content of 0.02 mg-N/L (Figure 4b). In comparison, other carbon sources such as glucose, sodium acetate, sodium succinate, and sodium citrate had given ammonium removal of 46.14, 39.76, 50.83 and 56.56%, respectively. The study differed from Zeng and co-workers [39], which illuminated that growth and ammonium removal were optimum for glucose, followed by citrate, sucrose, acetate, and starch. A publication suggested sodium citrate was an excellent carbon source for *A. faecalis* WT14 with a maximum of 98% ammonium removal [35]. Yang *et al*. [34] reported the four different carbon sources (acetate, glucose, citrate, and succinate); the result showed that all the tested carbon sources supported *B. subtillis* A1 had a percentage of ammonium removal up to 50.

As the nitrogen source requirement, *Bacillus* sp. Ba9 was studied based on sucrose as a carbon source. In contrast, ammonium sulfate and chloride were used as different nitrogen sources. The result showed that ammonium sulfate was the most effective nitrogen source for *Bacillus* sp Ba9. In this condition, strain Ba9 could decrease ammonia by 50.53% (Figure 5a), whereas nitrate production of these two nitrogen sources was non-significant (Figure 5b). This study result was consistent with the experiment by Lu *et al*. [35], which reported the ammonium reduction efficiency of *Alcaligenes* sp. W14 using different nitrogen sources. In agreement with the results, ammonium sulfate decreased total ammonium, having the highest effectiveness. Thus, it may be said that sodium citrate and ammonium sulfate were the optimum carbon and nitrogen sources for the heterotrophic nitrifying bacterium *Alcaligenes* sp. W1. The report was agreeable with this study, which *Bacillus* sp. Ba9 had sucrose and ammonium sulfate as appropriate carbon and nitrogen sources. In contrast, Yang *et al*. [34] mentioned that when four different carbon sources (acetate, glucose, sodium acetate, and succinate) and ammonium sulfate were used for investigation, *Bacillus subtilis* A1 was capable of removing ammonia but did not show significant differences (P>0.05).

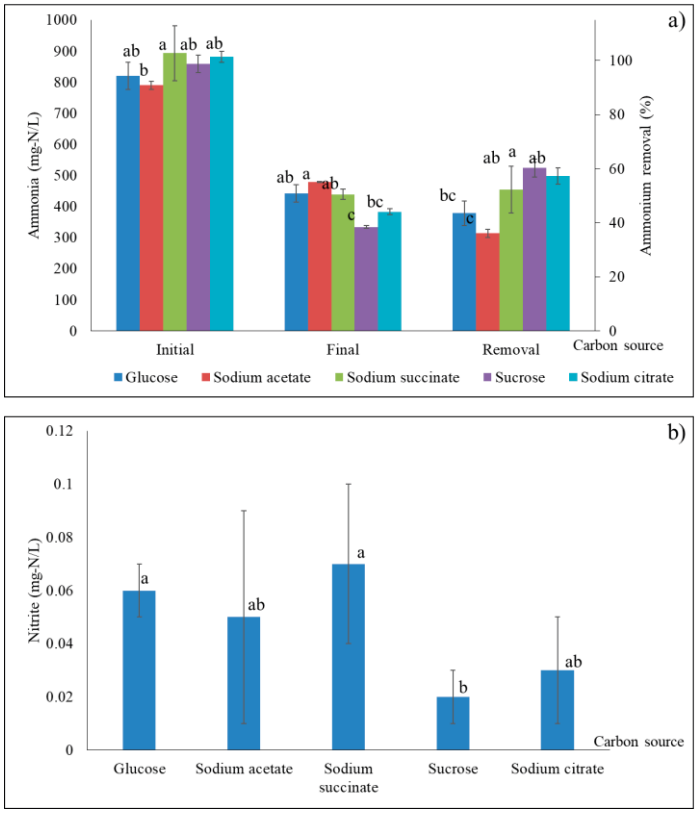

Figure 4. The optimization of the carbon source of *Bacillus* sp. Ba9, a) ammonium removal efficiency, b) nitrite production.

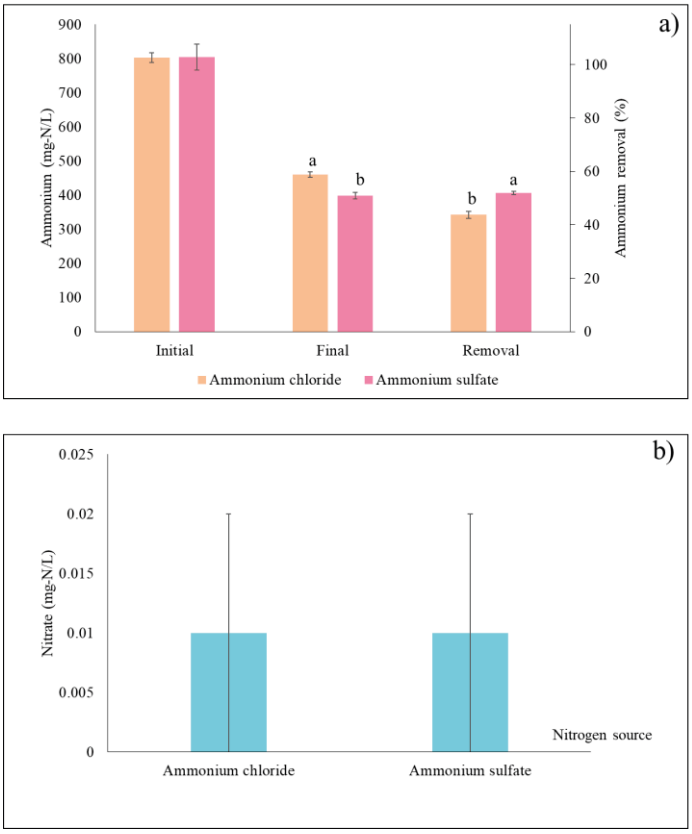

Figure 5. The optimization of the nitrogen source of *Bacillus* sp. Ba9, a) ammonium removal, b) nitrate production.

3.3.2 C/N ratio

Based on the above result, sucrose and ammonium sulfate were used as carbon and nitrogen sources, respectively. The optimum C/N ratio of Ba9 was 4, which can eliminate ammonia by 42.55%. This is followed by C/N ratios 12, 8, 2, and 0, which can remove ammonia for 37.84, 37.78, 32.53, and 19.94, respectively (Figure 6a). The result showed that the ammonium removal efficiency was low when the C/N ratios were lower or higher than 4. In the case of nitrite production, C/N ratio 2 showed the highest amount rather than ratio 4 (Figure 6b). This suggested that ratio 2 may be suitable for converting ammonia to nitrite. The C/N ratio result in this study was related to the optimization of C/N of *A. faecalis* strain NR, which had the ammonium removal of 19.2 mg/L at C/N ratio 5 in 48 hrs. [3]. The optimum C/N ratio of bacteria may depend on species or strains. While *A. faecalis* strain no. 4 showed high-efficiency ammonium removal at C/N ratio 10 [35]. A high C/N ratio can have a significant effect because it improves the volume of organic matter provided to the heterotrophic nitrifying bacteria. However, the optimal C/N ratio shows that the heterotrophic nitrifying bacterial capacity to remove nitrogen cannot be continuously improved by increasing the C/N ratio [33,38]. In addition, it has been reported that the most suitable was 10, which has the high percentage of ammonium removal by *B. subtillis* AYC showed at C/N ratios 10, 20, and 30 were 93.55%, 94.19%, and 96.77%, respectively [37]. Additionally, it became apparent that with a C/N ratio higher than 10, the heterotrophic nitrifying bacteria required carbon sources for growing like a biofloc formation.

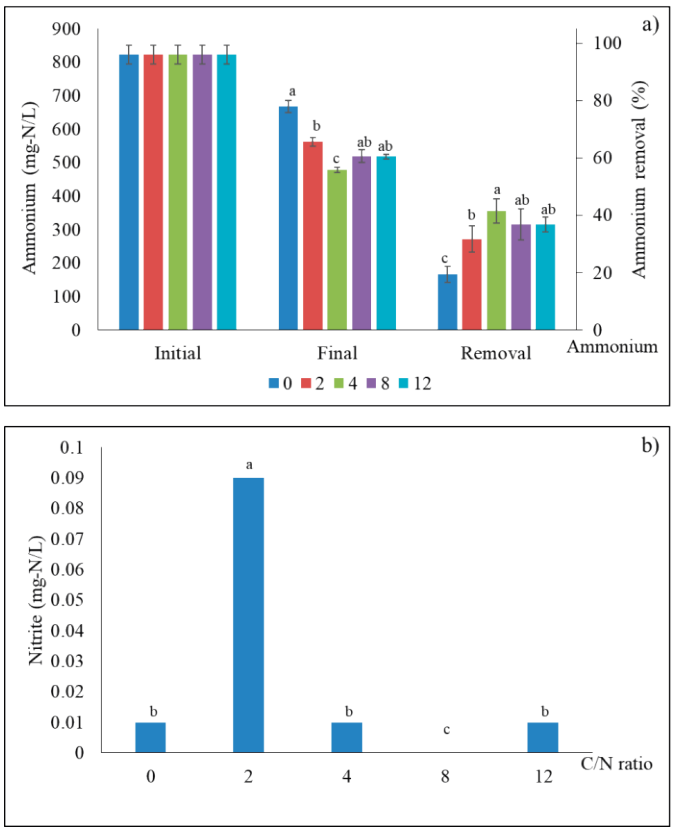

Figure 6. The optimization of C/N of *Bacillus* sp. Ba9, a) ammonium removal efficiency, b) nitrite production.

3.3.3 Optimization of salt tolerance of Bacillus sp. Ba9

The optimal salinity requirement for *Bacillus* sp. Ba9 was tested at 9 levels of salinities: 0, 0.5, 1.0, 1.5, 2.0, 2.5, 3.0, 3.5 and 4.0% NaCl (w/v). The result found that Ba9 could grow well at a salinity range of 1.5 to 4.0% NaCl (w/v) (Figure 7). Purivirojkul *et al*. [27] described that *B. pumilius, B. sphaericus*, and *B. subtilis* may grow in environments with salinities ranging from 0% to 10% NaCl (w/v). Bacterium *B. oceanisediminis* was isolated from South China Sea sediments by Zhang *et al*. [40] and can grow at salt concentrations within 0 and 13% NaCl

(w/v), with the optimum 0.5% NaCl (w/v). Moreover, *B. aerius* NY6 could grow at up to 6% NaCl (w/v) (optimum 2% NaCl (w/v)), and *B. maritimus* may survive in conditions as high as 7% NaCl (w/v) (optimum 5% NaCl) [41-42].

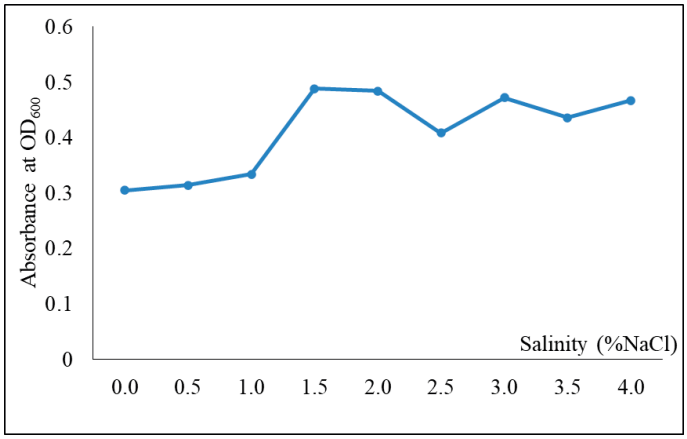

Figure 7. The growth rate of *Bacillus* sp. Ba9 at different salinity levels.

3.4 The efficiency of *Bacillus* sp. Ba9 to improve synthetic wastewater.

The ammonium removal efficiency in sterilized synthetic wastewater showed that *Bacillus* sp. Ba9 can remove ammonia from 191.38 ± 0.02 mg-N/L to 5.99 ± 1.12 mg-N/L (96.87%) on day 14 (Figure 8a-b). There is a report of tilapia wastewater treatment belonging to *Pseudomonas* sp. HBf01 and *Acinetobacter baumannii* HHf01 have an ammonium removal efficiency after 48 h for 67.9% [43]. The efficiency of nitrite production showed that all the treatments were decreased on day 7, and nitrite concentration increased on day 14. *Bacillus* sp. Ba9 had the highest nitrite production from 0.02 to 0.14 mg-N/L (Figure 8c-d). Another publication described that ammonia was reduced by 41.02% by *B. methytotrophicus* L7 of the nitrification effectiveness for 9 days, with ammonia levels beginning at 146.71 mg-N/L and ending at 38.29 mg-N/L [44]. The results showed that after 14 days of the experiment, all trials showed an increase in nitrate concentration. By day 14, *Bacillus* sp. Ba9 had a nitrate concentration of 0.23 ± 0.01 mg-N/L (Figure 8e-f). The result of nitrogen removal can prove that *B. oceanisediminis* Ba9, a member of the heterotrophic nitrifying bacteria group, had a higher ammonium removal efficiency at high ammonium levels than autotrophic nitrifying bacteria [45]. The mix of two strains, *B. cereus* PK5 and *B. subtilis* PK8, had ammonium removal efficiency at 72.0% (initial 50.0 ± 1.5 mg-N/L) [46]. It has been reported to be used *Bacillus* sp. in shrimp aquaculture (*Litopenaeus vannamei*) by *Bacillus* sp. N31 effectively reduced ammonium, nitrite, and nitrate for 86.3%, 89.3%, and 89.4%, respectively (nitrogen concentration starts at 250 mg-N/L) [47]. In the case of BOD, the efficiency of BOD removal on days 0, 7, and 14 was determined (the initial was 2636.86 ± 0.00 mg/L). The result showed a tendency to decrease in all trials except the control experiment. At the end of the experiment (14 days), *Bacillus* sp. Ba9 can remove BOD for 90.86%, while the control trial had removed BOD for about 15.77% (Figure 9). In several studies, the BOD was lower when *Bacillus* species were applied as water quality stimulators in aquaculture compared to controls. As a result, less organic matter dissolves using DO, and probably less DO is needed for *Bacillus* species to dissolve organic matter efficiently. This is possibly related to fish that consume their diet more successfully. For instance, *B. megaterium* effectively lowered the BOD of significant carp in pond water relative to the control [18]. Reduced BOD (above 90 %) was again recorded by Reddy *et al*. [24] in *Bacillus (B. subtilis, B. mojavensis*, and *B. cereus*) treated ponds. Similarly, a mix of *B. cereus* and *Aeromonas veronii* decreased BOD after effluent treatment [25]. These results provided strong evidence that *Bacillus* spp. is effective for BOD removal.

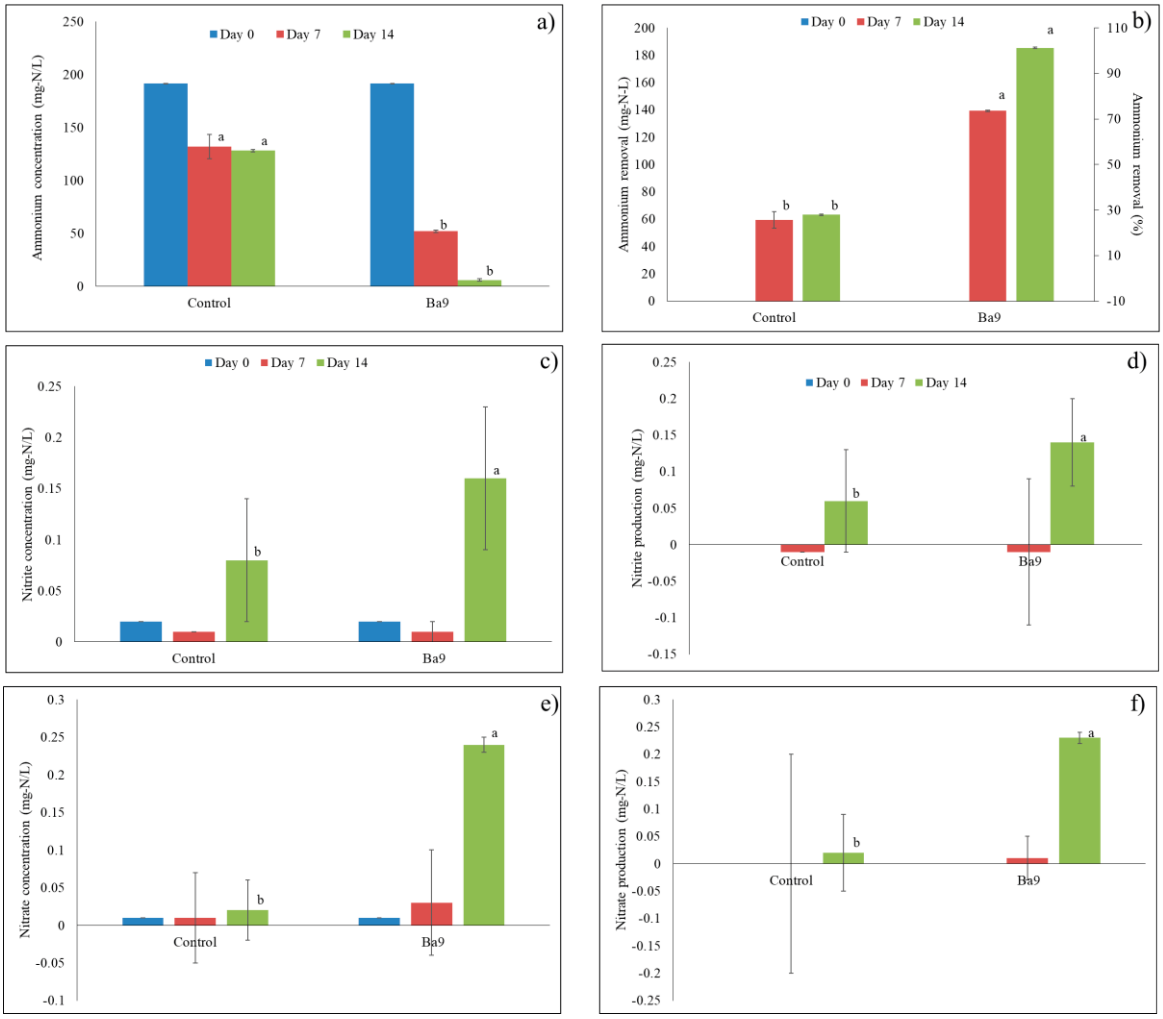

Figure 8. The efficiency of *Bacillus* sp. Ba9 for improving synthetic wastewater.

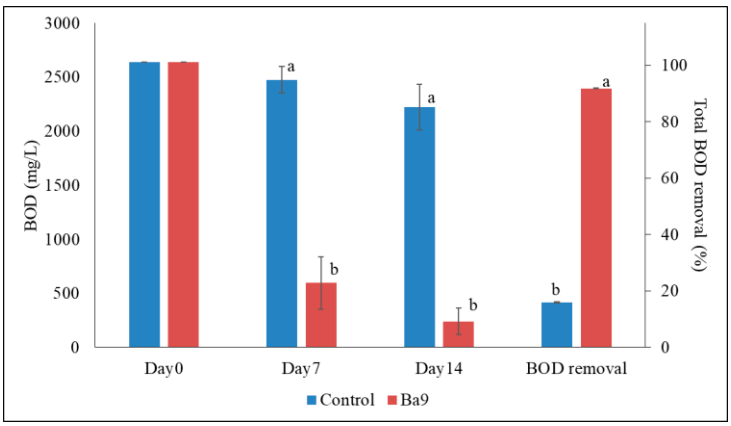

Figure 9. Biochemical oxygen demand (BOD) removal efficiency in synthetic wastewater of *Bacillus* sp. Ba9

4. Conclusions

Following these studies, *Bacillus* sp. strain Ba9 was unusually salt-tolerant heterotrophic nitrifying bacteria. According to the measurements of nitrogen removal efficiency. *Bacillus* sp. Ba9 was effective for oxidizing ammonium and reducing BOD. Therefore, it might be a significant opportunity for improvement in sectors including marine aquatic animals and saline wastewater treatment.

5. Acknowledgements

We would like to thank Anutsara Thongsang and Thunyarate Konkaew who collected and isolated the bacterial strain.

Author Contributions: Conceptualization, S.C., and Y.S; methodology, S.C., and Y.S.; software, S.C.; validation, Y.S.; formal analysis, S.C., and Y.S.; investigation, S.C., and Y.S.; writing—original draft preparation, S.C., and Y.S.; writing—review and editing, S.C., and Y.S.

Funding: This research was funded by Agricultural Research Development Agency (ARDA), grant number CRP6105020740.

Conflicts of Interest: The authors declare no conflict of interest.

References

[1] Gupta, A. B.; Gupta, S. K. Simultaneous carbon and nitrogen removal from high strength domestic wastewater in an aerobic RBC biofilm. *Water Res*. 2001; *35*, 1714–1722.

[2] Herrero, M.; Stuckey, D. C. Bioaugmentation and its application in wastewater treatment: A review. *Chemosphere* 2015; *140*, 119–128.

[3] Zhao, B.; Tian, M.; An, Q.; Ye, J.; Guo, J. S. Characteristics of a heterotrophic nitrogen removal bacterium and its potential application on treatment of ammonium-rich wastewater. *Bioresour. Technol.* 2017; *226*, 46–54.

[4] Kim, T. S.; Kim, H. S.; Kwon, S.; Park, H. D. Nitrifying bacterial community structure of a full-scale integrated fixed-film activated sludge process as investigated by pyrosequencing. *Microb*. *Biotechnol.* 2011; *21*, 293–298.

[5] Zhao, B.; An, Q.; He, Y. L.; Guo, J. S. N_2O and N_2 production during heterotrophic nitrification by *Alcaligenes faecalis* strain NR. *Bioresour. Technol.* 2012; *116*, 379–385.

[6] Kim, Y. M.; Park, D.; Lee, D. S.; Park, J. M. Inhibitory effects of toxic compounds on nitrification process for cokes wastewater treatment. *J. Hazard. Mater.* 2008; *152*, 915–921.

[7] Zheng, H. Y.; Liu, Y.; Gao, X. Y.; Ai, G. M.; Miao, L. L.; Liu, Z. P. Characterization of a marine origin aerobic nitrifying-denitrifying bacterium. *J. Biosci. Bioeng.* 2012, *114*, 33–37.

[8] Zhao, B.; Cheng, D. Y.; Tan, P.; An, Q.; Guo, J. S. Characterization of an aerobic denitrifier *Pseudomonas stutzeri* strain XL-2 to achieve efficient nitrate removal. *Bioresour. Technol.* 2018; *250*, 564–573.

[9] Li, Y.; Chapman, S. J.; Nicol, G. W.; Yao, H. Nitrification and nitrifiers in acidic soils. *Soil Biol. Biochem.* 2018; *116*, 290–301.

[10] Pan, Z.; Zhou, J.; Lin, Z.; Wang, Y.; Zhao, P.; Zhou, J.; Liu, S.; He, X. Effects of COD/TN ratio on nitrogen removal efficiency, microbial community for high saline wastewater treatment based on heterotrophic nitrification-aerobic denitrification process. *Bioresour. Technol*. 2020; *301*, 122726.

[11] Duan, S.; Zhang, Y.; Zheng, S. Heterotrophic nitrifying bacteria in wastewater biological nitrogen removal systems: A review. *Crit. Rev. Env. Sci. Tec.* 2021; *52*, 1–37.

[12] Thurlow, C. M.; Williams, M. A.; Carrias, A.; Ran, C.; Newman, M.; Tweedie, J.; Allison, E.; Jescovitch, L. N.; Wilson, A. E.; Terhune, J. S.; Liles, M. R. *Bacillus velezensis* AP193 exerts probiotic effects in channel catfish (*Ictalurus punctatus*) and reduces aquaculture pond eutrophication. *Aquaculture* 2019; *503*, 347–356.

[13] Lalloo, R.; Ramchuran, S.; Ramduth, D.; Görgens, J.; Gardiner, N. Isolation and selection of *Bacillus* spp. As potential biological agents for enhancement of water quality in culture of ornamental fish. *J. Appl. Microbiol.* 2007; *103*, 1471–1479.

[14] Song, Z. F.; An, J.; Fu, G. H.; Yang, X. L. Isolation and characterization of an aerobic denitrifying *Bacillus* sp. YX-6 from shrimp culture ponds. *Aquaculture* 2011; *319*, 188–193.

[15] Nimrat, S.; Suksawat, S.; Boonthai, T.; Vuthiphandchai, V. Potential *Bacillus* probiotics enhance bacterial numbers, water quality and growth during early development of white shrimp (*Litopenaeus vannamei*). *Vet. Microbiol.* 2012; *159*, 443–450.

[16] Xie, F.; Zhu, T.; Zhang, F.; Zhou, K.; Zhao, Y.; Li, Z. Using *Bacillus amyloliquefaciens* for remediation of aquaculture water. SpringerPlus 2013; *2*, 119.

[17] Zokaeifar, H.; Babaei, N.; Saad, C. R.; Kamarudin, M. S.; Sijam, K.; Balcazar, J. L. Administration of *Bacillus subtilis* strains in the rearing water enhances the water quality, growth performance, immune response, and resistance against *Vibrio harveyi* infection in juvenile white shrimp, *Litopenaeus vannamei*. *Fish Shellfish Immun.* 2014; *36*, 68–74.

[18] Hura, M. U. D.; Zafar, T.; Borana, K.; Prasad, J. R.; Iqbal, J. Effect of commercial probiotic *Bacillus megaterium* on water quality in composite culture of major carps. *Int. J. Curr. Agric. Sci.* 2018; *8*, 268–273.

[19] Cha, J. H.; Rahimnejad, S.; Yang, S. Y.; Kim, K. W.; Lee, K. J. Evaluations of *Bacillus* spp. as dietary additives on growth performance, innate immunity and disease resistance of olive flounder (*Paralichthys olivaceus*) against *Streptococcus iniae* and as water additives. *Aquaculture* 2013; *402–403*, 50–57.

[20] Das, A.; Nakhro, K.; Chowdhury, S.; Kamilya, D. Effects of potential probiotic *Bacillus amyloliquifaciens* FPTB16 on systemic and cutaneous mucosal immune responses and disease resistance of catla (*Catla catla*). *Fish Shellfish Immun.* 2013; *35*, 1547–1553.

[21] Saputra, F.; Shiu, Y. L.; Chen, Y. C.; Puspitasari, A. W.; Danata, R. H.; Liu, C. H.; Hu, S. Y. Dietary supplementation with xylanase-expressing *B. amyloliquefaciens* R8 improves growth performance and enhances immunity against *Aeromonas hydrophila* in Nile tilapia (*Oreochromis niloticus*). *Fish Shellfish Immun.* 2016; *58*, 397–405.

[22] Fei, H.; Lin, G. D.; Zheng, C. C.; Huang, M. M.; Qian, S. C.; Wu, Z. J.; Sun, C.; Shi, Z. G.; Li, J. Y.; Han, B. N. Effects of *Bacillus amyloliquefaciens* and *Yarrowia lipolytica* lipase 2 on immunology and growth performance of hybrid sturgeon. *Fish Shellfish Immun.*, 2018; *82*, 250–257.

[23] Zhang, F.; Xie, F.; Zhou, K.; Zhang, Y.; Zhao, Q.; Song, Z.; Cui, H. Nitrogen removal performance of novel isolated *Bacillus* sp. capable of simultaneous heterotrophic nitrification and aerobic denitrification. *Appl. Biochem. Biotech.* 2022; *194*, 3196–3211.

[24] Reddy, K. V.; Reddy, A. V. K.; Babu, B. S.; Lakshmi, T. V. Applications of *Bacillus* sp. in aquaculture wastewater treatment. *Int. J. S. Res. Sci. Tech.* 2018; *4*, 1806–1812.

[25] Divya, M. Isolation, Characterization and biodegradation potential of bacterial strains of seafood processing plant effluent for bioremediation. *Int. J. Appl. Res.* 2015; *1*, 530–537.

[26] Zhou, S.; Xia, Y.; Zhu, C.; Chu, W. Isolation of marine *Bacillus* sp. with antagonistic and organic-substances-degrading activities and its potential application as a fish probiotic. Mar. Drugs 2018; *16*, 196.

[27] Purivirojkul, W.; Maketon, M.; Areechon, N. Probiotic properties of *Bacillus pumilus*, *Bacillus sphaericus* and *Bacillus subtilis* in Black tiger shrimp (*Penaeus monodon* Fabricius) culture. *Kasetsart Journal Natural Science* 2005; *39*, 262–273.

[28] Chankaew, S.; O-Thong, S.; Sangnoi, Y. *Halomonas* sp. SKNB4, a proficient ammonium oxidizing bacterium. Proceedings of the 3rd National Meeting on Biodiversity Management in Thailand, June 15-17, 2016; Publisher Nan province, Thailand. 2016; 187–192.

[29] Chankaew, S.; O-Thong, S.; Sangnoi, Y. Nitrogen removal efficiency of salt-tolerant heterotrophic nitrifying bacteria. *Chiang Mai. J. Sci.* 2018; *45*, 11–20.

[30] Sangnoi, Y.; Chankaew, S.; O-Thong, S. Indigenous *Halomonas* spp., the potential nitrifying bacteria for saline ammonium wastewater treatment. *Pak. J. Biol. Sci.* 2017; *20(1),* 52–58.

[31] Tamura, K.; Stecher, G.; Kumar, S. MEGA11: Molecular evolutionary genetics analysis version 11. *Mol. Biol. Evol.* 2021; *38*, 3022–3027.

[32] Strickland, J. D. H.; Parsons, T. R. *A Practical Handbook of Seawater Analysis*, 2nd ed.; The Alger Press Ltd.: Fishery Research Board, Canada, 1972; 49–131.

[33] Chen, J.; Xu, J.; Zhang, S.; Liu, F.; Peng, J.; Peng, Y.; Wu, J. Nitrogen removal characteristics of a novel heterotrophic nitrification and aerobic denitrification bacteria, *Alcaligenes faecalis* strain WT14. *J. Environ. Manage.* 2021; *282*, 111961.

[34] Yang, X. P.; Wang, S. M.; Zhang, D. W.; Zhou, L. X. Isolation and nitrogen removal characteristics of an aerobic heterotrophic nitrifying–denitrifying bacterium, *Bacillus subtilis* A1. *Bioresour. Technol.* 2011; *102*, 854–862.

[35] Lu, Y.; Wang, X.; Liu, B.; Liu, Y.; Yang, X. Isolation and characterization of heterotrophic nitrifying strain W1. *Chinese. J. Chem. Eng.* 2012; *20*, 995–1002.
[36] APHA. *Standard Methods for the Examination of Water and Wastewater, Part 3, Determination of Metals*, 17th ed, American Public Health Association Inc.: Washington DC, 1989.
[37] Xiao, J.; Zhu, C.; Sun, D.; Guo, P.; Tian, Y. Removal of ammonium-N from ammonium-rich sewage using an immobilized *Bacillus subtilis* AYC bioreactor system. *J. Environ. Sci.* 2011; *23*, 1279–1285.
[38] Joo, H. S.; Hirai, M.; Shoda, M. Piggery wastewater treatment using *Alcaligenes faecalis* strain No. 4 with heterotrophic nitrification and aerobic denitrification. *Water Res.* 2006; *40*, 3029–3036.
[39] Zeng, J.; Liao, S.; Qiu, M.; Chen, M.; Ye, J.; Zeng, J.; Wang, A. Effects of carbon sources on the removal of ammonium, nitrite and nitrate nitrogen by the red yeast *Sporidiobolus pararoseus* Y1. *Bioresour. Technol.* 2020; *312*, 123593.
[40] Zhang, J.; Wang, J.; Fang, C.; Song, F.; Xin, Y.; Qu, L.; Ding, K. *Bacillus oceanisediminis* sp. nov., isolated from marine sediment. *Int. J. Syst. Evol. Micr*. 2010; *60*, 2924–2929.
[41] Zhang, X.; Gao, J.; Zhao, F.; Zhao, Y.; Li, Z. Characterization of a salt-tolerant bacterium *Bacillus* sp. from a membrane bioreactor for saline wastewater treatment. *J. Environ. Sci.* 2014; *26*, 1369–1374.
[42] Pal, D.; Kumar, R. M.; Kaur, N.; Kumar, N.; Kaur, G.; Singh, N. K.; Krishnamurthi, S.; Mayilraj, S. *Bacillus maritimus* sp. nov., a novel member of the genus *Bacillus* isolated from marine sediment. *Int. J. Syst. Evol. Micr*. 2017; *67*, 60–66.
[43] Fan, L.; Chen, J.; Liu, Q.; Wu, W.; Meng, S.; Song, C.; Qu, J.; Xu, P. Exploration of three heterotrophic nitrifying strains from a tilapia pond for their characteristics of inorganic nitrogen use and application in aquaculture water. *J. Biosci. Bioeng.* 2015; *119*, 303–309.
[44] Zhang, Q. L.; Liu, Y.; Ai, G. M.; Miao, L. L.; Zheng, H. Y.; Liu, Z. P. The characteristics of a novel heterotrophic nitrification–aerobic denitrification bacterium, *Bacillus methylotrophicus* strain L7. *Bioresour. Technol.* 2012; *108*, 35–44.
[45] Khin. T.; Annachhatre, A. P. Nitrogen removal in a fluidized bed bioreactor by using mixed culture under oxygen limited conditions. *Water Sci. Technol.* 2004; *50*, 313–320.
[46] Kim, J. K.; Park, K. J.; Cho, K. S.; Nam, S. W.; Park, T. J.; Bajpai, R. Aerobic nitrification–denitrification by heterotrophic *Bacillus* strains. *Bioresour. Technol*. 2005; *96*, 1897–1906.
[47] Huang, F.; Pan, L.; Lv, N.; Tang, X. Characterization of novel *Bacillus strain* N31 from mariculture water capable of halophilic heterotrophic nitrification–aerobic denitrification. *J. Biosci. Bioeng.* 2017; *124*, 564–571.

ASEAN
Journal of Scientific and Technological Reports
Online ISSN:2773-8752

Research article

Effects of Ultrasonic Stimulation and Light Intensity on the Growth Rate and Biomass Productivity of *Chlorella ellipsoidea* in a Closed-Batch Cultivation System

Sudarat Theerapisit[1], Somrak Rodjaroen[2], and Siriluk Sintupachee[3*]

[1] Faculty of Science and Technology, Nakhon Si Thammarat Rajabhat University, Nakhon Si Thammarat, 80280, Thailand; sudarat_the@nstru.ac.th
[2] Faculty of Science and Technology, Nakhon Si Thammarat Rajabhat University, Nakhon Si Thammarat, 80280, Thailand; somrak_rod@nstru.ac.th
[3] Faculty of Science and Technology, Nakhon Si Thammarat Rajabhat University, Nakhon Si Thammarat, 80280, Thailand; siriluk_sint@nstru.ac.th
* Correspondence: siriluk_sint@nstru.ac.th

Citation:
Theerapisit, S., Rodjaroen, S., Sintupachee, S. Effects of ultrasonic stimulation and light intensity on the growth rate and biomass productivity of *Chlorella ellipsoidea* in a closed-batch cultivation system. *ASEAN J. Sci. Tech. Report.* **2023**, *26*(4), 67-74. https://doi.org/10.55164./ajstr.v26i4.249960

Article history:
Received: June 21, 2023
Revised: September 28, 2023
Accepted: September 29, 2023
Available online: September 30, 2023

Abstract: Microalgae exhibit high nutritional value as animal feed in aquatic animal nurseries. Therefore, approaches to enhance biomass productivity are of great economic significance. This study aimed to evaluate the effect of ultrasonic wave stimulation on the specific growth rate and biomass yield of *Chlorella ellipsoidea* strain TISTR 8260. *C. ellipsoidea* stimulated by ultrasonic waves at 50 Hz for 1, 5, and 10 min were cultivated in a closed-batch cultivation system with varying light intensities. Data revealed that stimulation for 1 min and rearing at 71.43 μmol m^{-2} s^{-1} resulted in the highest biomass productivity and specific growth rates, with averages of 0.89±0.008 g/L/day and 0.59±0.009 per day, respectively. The findings of this study emphasize the usefulness of ultrasonic waves in enhancing the biomass productivity of microalgae.

Keywords: Biomass; *Chlorella ellipsoidea*; Growth rate; Microalgae; Ultrasonic stimulation

1. Introduction

Ultrasonic sound waves, operating within the high-frequency range of 20 to 20,000 hertz, pose risks to small animals but are safe for humans. "acoustic cavitation" refers to the formation and subsequent collapse of bubbles within a liquid when exposed to an ultrasonic field [1-2]. This phenomenon gives rise to various physical effects, including shock waves, microjets, and turbulence, as these cavitation bubbles oscillate and implode [3-4]. Consequently, cavitation finds applications in diverse areas, such as cleaning, extraction, and emulsification. Ultrasonic sound waves can also generate nanoscale zinc oxide, enhancing green light emission. In medicine, ultrasonic sound waves are employed to create a device for parental gender diagnosis, producing embryo images with frequencies ranging from 1 to 20 KHz during echocardiogram procedures for fetuses [5-6]. Similarly, ultrasonic waves between 1 and 3 MHz can detect bone fractures. Furthermore, ultrasonic sound waves, particularly at 20 KHz, can disrupt microalgae cell walls and extract fats, a process referred to as lipoproteinization [7-8]. Additionally, ultrasonic waves have effectively preserved the color of unripe

mangoes by inhibiting chemical oxidation and the accumulation of phenol and malondialdehyde. Utilizing ultrasonic waves in irrigation water for pest management is environmentally friendly, as they leave no chemical residues. Moreover, ultrasonic waves enhance the extraction of fats from green microalgae [9]. These waves induce chemical and physical changes through the cavitation phenomenon, encompassing compression (molecule clumping) and wave expansion. Sound can separate molecules by generating rhythmic changes that mimic vigorous agitation, facilitating molecular diffusion. Consequently, the extraction rate increases due to the heightened contact area between the solvent and the sample and reduced extraction time [10-11]. Ultrasonic therapy has emerged as a potential alternative to enhancing microbial growth and chemical production. In the case of small, detectable algae, it has the potential to augment either endogenous chemical synthesis or cell development. The efficacy of this technique depends on the specific microorganisms involved and the operational conditions employed. Employing ultrasound to combat detrimental algal blooms carries significant ecological implications and threatens drinking water sources. The study examined the mortality of *Microcystis aeruginosa* cells and the release of intracellular organic substances by utilizing ultrasonic frequencies at 20 kHz, 740 kHz, and 1120 kHz during the cultivation of the small green algae *M. aeruginosa* in freshwater in Wuhan, China [12]. Light is another crucial factor that significantly influences the algae growth rate, serving as the primary energy source for autotrophic organisms like microalgae. Natural light, when direct, exhibits significant variation in intensity based on seasonal and geographical factors. As the algae population expands, light penetration becomes limited due to cell growth, especially for bottom-dwelling algae, impacting their access to adequate light. Consequently, this limitation affects cellular photosynthesis efficiency. To address this, a Light-emitting diode (LED) offers the flexibility to adjust wavelength, light intensity, and illumination duration, providing tailored lighting conditions for the algae [13]. Light intensity and spectral characteristics shape cell growth and biomass composition. Light intensities of 100, 250, and 500 μmol m^{-2} s^{-1}, along with three different light sources such as fluorescent lamps, RGB LEDs, and white LEDs, affect three green algae species: *Chlamydomonas reinhardtii*, *Desmodesmus quadricauda*, and *Parachlorella kessleri* both the growth rate and biomass productivity [14]. Moreover, light intensity plays a pivotal role in synthesizing various crucial compounds within algae, offering advantages in both their growth and utilization [15].

The increased biomass production of single-celled algae holds particular importance, given their pivotal role as a primary component of animal feed in aquatic animal breeding facilities [16-17]. The economic significance of these tiny green algae in the fish farming industry is underscored by their remarkable nutritional content, especially their rich protein content, which is crucial for fish growth. *Chlorella* sp. is a green microalgae renowned for its nutrient-rich profile, featuring high protein and fiber content, boasting an impressive protein level of 60%. Moreover, *Chlorella* sp. contains alpha-linolenic acid, which is associated with reducing cholesterol levels in blood vessels. It is also abundant in essential elements such as vitamin B12, A, beta-carotene, and nucleic acid. In Thailand, using algae in aquaculture farms as a beneficial dietary supplement has been instrumental in safeguarding economically significant aquatic species like fish and shrimp from diseases. These advantages, including rapid production and enhanced biomass productivity, have the potential to impact the local economy [18-19] significantly. This study aimed to investigate the impact of ultrasonic waves on the specific growth rate and biomass productivity of *Chlorella ellipsoidea* strain TISTR 8260, a microalga. To conduct this research, we utilized a closed-batch culture system capable of regulating various light intensities, including 14.29, 42.86, and 71.43 μmol m^{-2} s^{-1}, in addition to fluorescent light (114.29 μmol m^{-2} s^{-1}).

2. Materials and Methods

2.1 Experimental design

A completely randomized design (CRD) was employed to study the specific growth rate and biomass productivity of the green microalga *C. ellipsoidea* strain TISTR 8260. The growth parameters of *C. ellipsoidea* stimulated by ultrasonic waves at 50 Hz for 1, 5, and 10 min were compared to the untreated control group. The treatments were cultured in the BG-11 medium with light intensities of 14.29, 42.86, and 71.43 μmol m^{-2} s^{-1}, as well as fluorescent light (114.29 μmol m^{-2} s^{-1}). Each experimental set included three replicates.

2.2 Test strain and composition of the culture medium

The *C. ellipsoidea* strain TISTR 8260 was obtained from the Biotechnology Department, Thailand Institute of Scientific and Technological Research (TISTR). The microalga was grown in the BG-11 culture medium at a nutrient-to-alga ratio of 9:1. One-liter volumes of the BG-11 medium (HiMedia, India) were prepared in 2L-flasks and sterilized by autoclaving at 121 °C for 15 min. The nutrient formula of BG-11 was as follows: $NaNO_3$ (15.0 g/L), K_2PHO_4 (0.4 g/L), $MgSO_4.7H_2O$ (0.75 g/L), $CaCl_2$ $2H_2O$ (0.36 g/L), citric acid (0.06 g/L), C_6H_5+4yFexNyO_7 (0.06 g/L), EDTA disodium magnesium salt (0.01 g/L), Na_2CO_3 (0.02 g/L), and 1.0 mL trace metal mix A5 (consisting of H_3BO_4 28.6 g/L, $MnCl_2{\cdot}4H_2O$ 18.1 g/L, $ZnSO_4{\cdot}7H_2O$ 2.22 g/L, $NaMoO_4{\cdot}2H_2O$ 3.9 g/L, $CuSO_4{\cdot}5H_2O$ 0.079 g/L, and $Co(NO_3)2{\cdot}6H_2O$ 0.494 g/L) and the pH was adjusted to 7.0 [20]. The starter culture of the microalga was cultivated for 14 days with shaking at 150 rpm in a closed, intelligently controlled cabinet exposed to a light intensity of 42.86 μmol m^{-2} s^{-1} for 12 h per day. The starter culture was used at an optical density at 600 nm (OD_{600} nm) of 0.244.

2.3 The rearing experiment

The starter culture of *C. ellipsoidea* TISTR 8260 was used for the rearing experiment. Different light intensities were applied, and the specific growth rates and biomass productivities were measured. The rearing experiment was conducted in a closed-shift intelligent control cabinet at a temperature of 28 ± 1 °C and light intensities of 14.29, 42.86, and 71.43 μmol m^{-2} s^{-1} form the light emitting diode (LED) (9 watts, B1, Thailand), as well as fluorescent lamp (36 watts, Silver, Thailand) at 114.29 μmol m^{-2} s^{-1} for 12 h per day over 14 days.

2.4 Determination of specific growth rates and biomass productivity

To assess the microalga growth, the OD_{600} nm of different treatments was measured using a spectrophotometer (Brand Peak, model C-7100, USA). Aliquots of 1 mL of the cultures were collected and measured daily to generate a linear regression model. The specific growth rates were calculated using Equation 1, and the biomass productivity using Equation 2 [21]. The daily algal biomass measurement is calculated by employing a linear regression equation that compares the OD_{600} of the current sample to that of the initial cultivation.

$$P = \frac{X_1 - X_0}{t_1 - t_0} \quad (1)$$

$$\mu = \frac{\mathrm{In}(X_1 - X_0)}{t_1 - t_0} \quad (2)$$

where P is the mass productivity (biomass productivity; g/L/day),
μ is the specific growth rate (per day), and
X_1 and X_0 are the alga mass (g/L) at day T_1 and T_0, respectively

2.5 Statistical analysis

Each experiment was repeated three times for each sample (n = 3), and the standard deviations (SD) were calculated. The differences between groups were determined using the R program's one-way analysis of variance (ANOVA), followed by Tukey's multiple comparison analysis. At 95% confidence, a *p*-value of 0.05 was considered statistically significant.

3. Results and Discussion

3.1 The effect of ultrasonic waves on biomass productivity

To evaluate how high-frequency sound waves at 50 Hz affect the growth of *C. ellipsoidea* strain TISTR 8260, we exposed the microalgae to different durations of ultrasonic treatment while keeping the light intensity at various levels. These experimental conditions were implemented following ultrasonic treatment intervals of 1, 5, and 10 minutes, as opposed to the control group, which did not undergo ultrasonic stimulation. The results revealed that at 14.29 μmol m^{-2} s^{-1}., the mean biomasses were 0.64 ± 0.028, 0.77 ± 0.007, and 0.72 ± 0.012 g/L/day at 1, 5,

and 10 min, respectively. Among the three time points, the biomass at 1 min was significantly less, with a *p*-value of 0.0001 (DF = 3, F(3, 52) = 133.5), while the control group had an average biomass of 0.70 ± 0.009 g/L/day (Figure. 1a).

At 42.86 μmol m^{-2} s^{-1}, the 10-min ultrasonic stimulation yielded the highest average biomass productivity (0.79 ± 0.015 g/L/day). This value was significantly (*p*-value = 0.0001; DF = 3, F(3, 52) = 12.58) higher than the 1-min and 5-min ultrasonic stimulation and the control group, with average biomass productivity of 0.75 ± 0.020, 0.75 ±0.023, and 0.76 ± 0.011 g/L/day, respectively (Figure. 1b). In addition, the ultrasonic stimulation for 1 min and 5 min at 71.43 μmol m^{-2} s^{-1} produced higher biomass productivity than the 10 min stimulation and the control groups with a *p*-value of 0.0001 (DF = 3, F(3, 52) = 322.5). The *p*-value was 0.0020 when comparing the mean values at 1 and 5 min. The average biomass productivity values of *C. ellipsoidea* stimulated by ultrasonic waves were 0.89 ±0.008, 0.87 ± 0.008, and 0.80 ± 0.012 g/L/day at 1, 5, and 10 min, respectively, while the biomass of the control group was 0.82 ± 0.006 g/L/day. At the fluorescent light intensity, the average biomass productivity of *C. ellipsoidea* strain TISTR 8260 resulting from ultrasonic stimulation at the different time points was higher than that of the non-stimulated control group. The biomass values were 0.66 ± 0.023, 0.69 ± 0.020, 0.67 ± 0.025, and 0.53 ± 0.003 g/L/day at 1, 5, and 10 min of stimulation and the control, respectively. The *p*-value was 0.0001 (DF = 3, F(3, 52) = 185.1) compared to the control group. When comparing the 1 min and 5 min biomass, the *p*-value was 0.0015, while it was 0.0151 when comparing the 5 min and 10 min values.

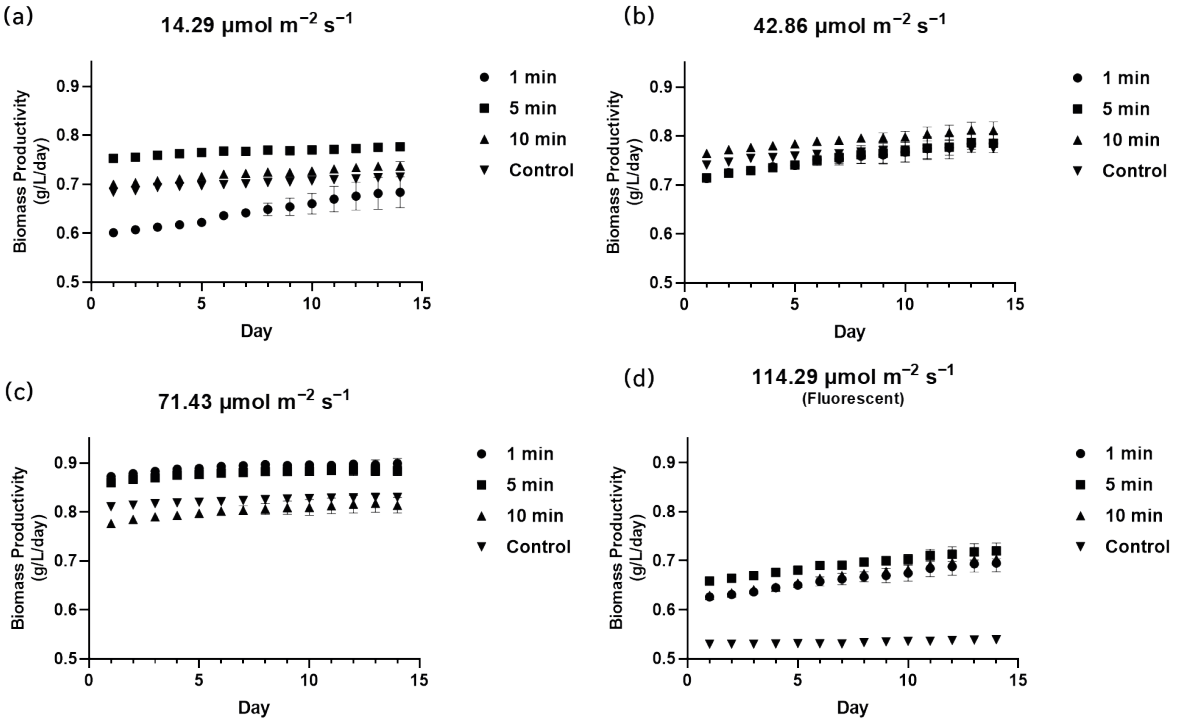

Figure 1. The biomass productivity according to the light intensity culture (a): 14.29 μmol m^{-2} s^{-1}, (2): 42.86 μmol m^{-2} s^{-1}, (3): 71.43 μmol m^{-2} s^{-1} and (4): Fluorescent after ultrasonic stimulation at 1, 5, and 10 min and control.

3.2 The impact of ultrasonic stimulation on the specific growth rates

The specific growth rate is an important parameter to evaluate the quality of the cultivation process. We further assessed the effect of ultrasonic stimulation on *C. ellipsoidea* growth by determining the specific growth rates of strain TISTR 8260 when stimulated by ultrasonic waves for 1, 5, and 10 min, compared to the control group. The mean specific growth rates at 14.29 μmol m^{-2} s^{-1} were 0.26 ± 0.044, 0.44 ± 0.009, 0.37 ± 0.017, and 0.35 ± 0.014 per day for the 1-, 5-, and 10-min stimulation groups and the control group, respectively (Figure. 2a). The highest specific growth rate value was recorded for the 5-min stimulation group with a *p*-

value of 0.0001 (DF = 3, F(3, 52) = 120.8). The *p*-value was 0.0246 when comparing the mean specific growth rates of the 10-min ultrasonic wave exposure with the control group. At a light intensity of 42.86 μmol m^{-2} s^{-1}, the exposure to ultrasonic waves for 10 min resulted in the highest specific growth rate (0.47 ± 0.018), with a *p*-value of 0.0001 (DF = *3*, F(3, 52) = 12.28) compared to the other treatment groups and the control. Exposure to sound waves for 1 and 5 min led to specific growth rates similar to the control group, with values of 0.42 ± 0.030, 0.42 ± 0.031, and 0.44 ± 0.014 per day, respectively (Figure. 2b). The results also revealed that at 71.43 μmol m^{-2} s^{-1}, higher specific growth rate values were recorded for the 1- and 5-min stimulation groups compared to the 10-min and control groups, with a *p*-value of 0.0001 (DF = *3*, F(3, 52). = 318). The mean specific growth rates were 0.59 ± 0.009, 0.57 ± 0.009, 0.48 ± 0.016, and 0.56 ± 0.007 per day for the stimulation groups of 1, 5, and 10 min. The control group, respectively (Figure. 2c). In addition, at the fluorescent light intensity, the three ultrasonic exposure times resulted in mean specific growth rates significantly higher than the control group, with a *p*-value of 0.0001 (DF = 3, F(3, 52) = 226.4). The 1-min and 10-min stimulation groups had similar growth rates. The mean specific growth rate values were 0.29 ±0.035, 0.34 ±0.029, 0.30 ± 0.037, and 0.07 ± 0.006 per day for the 1-, 5-, and 10-min stimulation groups and the control, respectively (Figure. 2d).

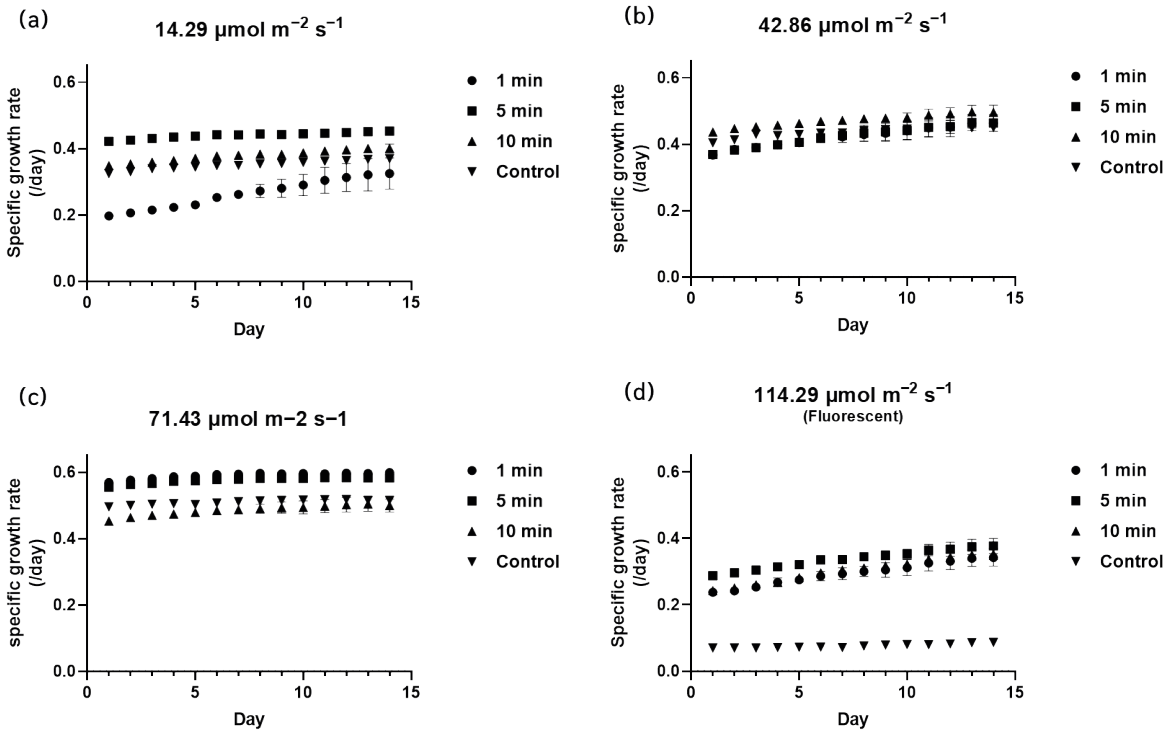

Figure 2. The specific growth rate according to the light intensity culture (a): 14.29 μmol m^{-2} s^{-1}, (2): 42.86 μmol m^{-2} s^{-1}, (3): 71.43 μmol m^{-2} s^{-1} and (4): Fluorescent after ultrasonic stimulation at 1, 5, and 10 min and control.

In this study, the biomass productivity resulting from the stimulation of ultrasonic growth at 50 Hz for 5 and 10 min ranged from 0.65 to 0.89 g/L/day. Previous research on the semi-continuous cultivation of *C. vulgaris* for lipid production tested four ultrasonic wave frequencies and recorded the highest biomass yield at 20 Hz [22]. Other studies have reported varying optimal frequencies for different algae strains: *C. sorokiniana* SDEC-18 achieved its highest biomass (0.63 g/L/day) with 15 Hz stimulation, increasing lipid production from 50.53% to 64.38%. *Scendesmus* sp., when stimulated at a frequency of 20 Hz for 2 minutes, yielded a maximum biomass of 0.68 g/L/day [23]. In this investigation, the highest average biomass (0.89 g/L/day) of *C. ellipsoidea* strain TISTR 8260 was attained when the algae were cultivated at 71.43 μmol m^{-2} s^{-1} with ultrasonic wave stimulation at 50 Hz for 1 min [24]. Notably, this study employed a frequency twice as high as previous research, which might account for the shorter time needed to enhance the desired growth rate. Furthermore,

the biomass productivity in this study surpasses last year by approximately 23%. The exposure to high-frequency ultrasonic waves may have activated the cell walls of algae, potentially leading to accelerated cell division [12].

Ultrasonic stimulation with varying light intensity levels significantly influences growth rate and biomass productivity. The peak yield is achieved at a light intensity of 71.43 μmol m^{-2} s^{-1}, whereas the lowest product is observed at 114.29 μmol m^{-2} s^{-1} in the culture. This phenomenon resembles findings in the batch cultivation of *Squama quadricauda*, where the highest biomass yield of 0.68 g/L/day was recorded at a light intensity of 42.86 μmol m^{-2} s^{-1} for 5 min. Similarly, *Scenedesmus obliquus* (FACHB12) displayed a biomass production of 0.69 g/L/day when cultured at 14.29 μmol m^{-2} s^{-1} after 3 min of sound wave stimulation at 23 Hz [25]. Based on the results, lower light intensity is optimal for accelerating the growth rate and biomass production of algae in this study. Offering excess light intensity may lead to cell overexposure rather than promoting accelerated algae proliferation. Employing an ultrasonic pulse enhances membrane permeability and induces changes in enzyme structure, facilitating improved aeration and the release of cell clusters during cultivation. These alterations also extend to cellular and genetic components, as illustrated in Figure 2, showcasing the impact of this application on microalgae growth. These transformative effects arise from cavitation events. Ultrasonic sound waves induce metabolic changes, increasing transmembrane permeability and enzyme structural modifications. This process introduces air and releases cellular clusters, consequently affecting cell count and producing elevated chemicals [26].

In contrast to our findings, the cultivation of *B. braunii*, stimulated by sound waves at a frequency of 40 Hz every four days, resulted in a maximum specific growth rate of 0.089 per day and a biomass output of 0.043 g/L/day [27]. In our study, we employed ultrasonic sound waves at 50 Hz and allowed the algae to grow for 14 days, with specific growth rates and biomass under these conditions. The highest specific growth rate recorded was 0.59 per day when *C. ellipsoidea* was exposed to ultrasound waves for 1 min and cultivated under a light intensity of 71.43 μmol m^{-2} s^{-1}. In comparison, *Nannochloris* sp., stimulated at 20 Hz for 2 min and cultured in the Bold medium, exhibited the highest specific growth rate of 0.42 per day and a biomass yield of 0.78 g/L. Interestingly, the exposure of *C. vulgaris* to sound waves at the same frequency as in our study did not result in an enhanced growth rate; instead, it achieved a specific growth rate of 0.65 per day and a biomass output of 0.772 g/L/day [28]. This entails initiating ultrasonic stimulation at the onset of the growth phase, thereby sustaining a continuous increase in biomass productivity through repeated algae stimulation.

4. Conclusions

In this study, we evaluated the effect of ultrasonic stimulation on the growth of *C. ellipsoidea* strain TISTR 8260 using a batch-cultivation system. *C. ellipsoidea* was exposed to ultrasonic waves at 50 Hz for 1, 5, and 10 min and cultivated at different light intensities. They stimulated *C. ellipsoidea* with ultrasonic waves for 1 min and rearing at a light intensity of 71.43 μmol m^{-2} s^{-1} improved biomass productivity and specific growth rates. Beyond creating the optimal conditions to stimulate growth and enhance algae biomass production in our experiment, these methods could be extended to other commercially significant algae strains. Leveraging ultrasonic sound waves to accelerate the cultivation of economically valuable green microalgae, thereby reducing their growth cycle and increasing biomass output, presents considerable promise. This strategy may yield economic advantages for entrepreneurs within the marketing ecosystem.

5. Acknowledgements

We thank Mr. Supachai Phromchan for supervising and controlling the microalgae culture tank system and collecting samples for measuring the OD values. We are also grateful to Mr. Boonyarid Boonmart for ensuring constant access to the equipment used for the microalga cultivation and OD measurements.

Author Contributions: A short paragraph specifying their contributions must be provided for research articles with several authors. The following statements should be used "Conceptualization, S.T. and S.S..; methodology, S.T..; software, S.S..; validation, S.T., S.R.., and S.S..; formal analysis, X.X.; investigation, S.R..;

resources, S.T..; data curation, S.T..; writing-original draft preparation, S.T..; writing-review and editing, S.S..; visualization, S.R..; supervision, S.S..; project administration, S.R. and S.S.. All authors have read and agreed to the published version of the manuscript." Please turn to the CRediT taxonomy for the term explanation. Authorship must be limited to those who have contributed substantially to the work reported.

Funding: This research received no external funding

Conflicts of Interest: The authors declare no conflict of interest.

References

[1] Zhang, H.; Qing-Kai, F.; Fan, C. et al. Effect of pulsed powder ultrasound on plasma morphology and its changing mechanism. *Int J Adv Manuf Technol*, 2021; 116, 1225–1232. https://doi.org/10.1007/s00170-021-07540-2.

[2] Valero, D.; Zhang, G.; Bung, D.B.; Chanson H. On the estimation of free-surface turbulence using ultrasonic sensors. *Flow Measurement and Instrumentation*, 2018; 60, 171-184. https://doi.org/10.1016/j.flowmeasinst.2018.02.009.

[3] Qifa, Z.; Sienting, L.; Dawei, W.; Kirk S. Piezoelectric films for high frequency ultrasonic transducers in biomedical applications. *Progress in Materials Science*, 2011; *56*(2), 139-174. https://doi.org/10.1016/j.pmatsci.2010.09.001.

[4] Bulliard-Sauret, O.; Berindei, J.; Ferrouillat, S.; Vignal, L.; Memponteil, A.; Poncet, C.; Leveque, J.M.; Gondrexon N. Heat transfer intensification by low or high frequency ultrasound: Thermal and hydrodynamic phenomenological analysis. *Experimental Thermal and Fluid Science*, 2019; 104, 258-271, https://doi.org/10.1016/j.expthermflusci.2019.03.003

[5] Xiong, J.; Wang, Y.; Ma, G-M.; Zhang, Q.; Zheng S-S. Field Applications of Ultra High Frequency, Techniques for Defect Detection in GIS. *Sensors*, 2018; *18*(8), 2425 pp.https://doi.org/10.3390/s18082425.

[6] Deffieux, T.; Konofagou, E. E. Numerical study of a simple transcranial focused ultrasound system applied to blood-brain barrier opening. *in IEEE Transactions on Ultrasonics, Ferroelectrics, and Frequency Control*, 2010; *57*(12), 2637-2653. https://doi: 10.1109/TUFFC.2010.1738.

[7] Shahram, N.; Seyed, H.H.; Meysam, M.R. CFD simulation of acoustic cavitation in a crude oil upgrading sonoreactor and prediction of collapse temperature and pressure of a cavitation bubble. *Chemical Engineering Research and Design*, 2014; *92*(1), 166-173. https://doi.org/10.1016/j.cherd.2013.07.002

[8] Muthupandian, A. The characterization of acoustic cavitation bubbles – An overview. *Ultrasonics Sonochemistry*, 2011; *18*(4), 864-872, https://doi.org/10.1016/j.ultsonch.2010.11.016.

[9] Khalesi, B.; Sohani, B.; Ghavami, N.; Ghavami, M.; Dudley, S.; Tiberi G. A Phantom Investigation to Quantify Huygens Principle Based Microwave Imaging for Bone Lesion Detection. *Electronics*, 2019; *8*(12), 1505. https://doi.org/10.3390/electronics8121505.

[10] Glacio, S.; Araujo, L.; Matos, J.B.L.; Jader, O.; Fernandes, S.; Cartaxo J.M.; Luciana, R.B.; Gonçalves, F.; Fernandes, A.N.; Wladimir, R.L. Extraction of lipids from microalgae by ultrasound application: Prospection of the optimal extraction method, *Ultrasonics Sonochemistry*, 2013; *20*(1), 95-98. https://doi.org/10.1016/j.ultsonch.2012.07.027.

[11] Mubarak, M.; Shaija, A.; Suchithra, T.V. A review on the extraction of lipid from microalgae for biodiesel production. *Algal Research*, 2015; 7, 117-123. https://doi.org/10.1016/j.algal.2014.10.008.

[12] Peng, Y.; Zhang, Z.; Kong, Y., Li, Y.; Zhou, Y.; Shi, X.; Shi, X. Effects of ultrasound on Microcystis aeruginosa cell destruction and release of intracellular organic matter, *Ultrasonics Sonochemistry*, 2020; *63*, 1350-4177, https://doi.org/10.1016/j.ultsonch.2019.104909.

[13] Xiaoying, L.; Shirong, G.; Taotao, C.; Zhigang, X.; Tezuka, T. Regulation of the growth and photosynthesis of cherry tomato seedlings by different light irradiations of light emitting diodes (LED). African journal of biotechnology, 2012; *11* (Suppl. 22), 6169-6177)

[14] Bialevich, V.; Zachleder, V.; Bišová, K. The Effect of Variable Light Source and Light Intensity on the Growth of Three Algal Species. *Cells* 2022; *11*, 1293. https://doi.org/10.3390/cells11081293.

[15] Tran-Nguyen, Q. A.; Tran, T. T. V.; Trinh-Dang, M. Effects of Light on the Growth and β-carotene Accumulation in the Green Algae Dunaliella salina. *Asian Journal of Biology*, 2023; *18*(1), 1–10. https://doi.org/10.9734/ajob/2023/v18i1332

[16] Parniakov, O.; Apicella, E.; Koubaa, M.; Barba, F.J.; Grimi, N., Lebovka, N.; Pataro, G.; Ferrari, G.; Vorobiev E. Ultrasound-assisted green solvent extraction of high-added value compounds from microalgae *Nannochloropsis* spp. *Bioresource Technology*, 2015; 198, 262-267. https://doi.org/10.1016/j.biortech.2015.09.020.

[17] Ulker, D.; Keris-Sen, U.; Sen, G.; Soydemir, M.; Gurol, D. An investigation of ultrasound effect on microalgal cell integrity and lipid extraction efficiency. *Bioresource Technology*, 2014; 152, 407-413, https://doi.org/10.1016/j.biortech.2013.11.018.

[18] Seyfabadi, J.; Ramezanpour, Z.; Amini Khoeyi, Z. Protein, fatty acid, and pigment content of Chlorella vulgaris under different light regimes. *Journal of Applied Phycology*, 2011; *23*: 721–726. https://doi.org/10.1007/s10811-010-9569-8.

[19] Dawczynski, C.; Schubert, R.; Jahreis, G. Amino acids, fatty acids, and dietary fibre in edible seaweed products. *Food Chemistry*, 2007; *103*(3): 891-899. https://doi.org/10.1016/j.

[20] Carvalho, D.V.; Pereira, E.M.; Cardoso, J.S. Machine learning interpretability: a survey on methods and metrics. *Electronics*, 2019; 8, 832. https://doi.org/10.3390/electronics8080832.

[21] Tang, D.; Han, W.; Li, P.; Miao, X.; Zhong, J. CO_2 biofixation and fatty acid composition of Scenedesmus obliquus and *Chlorella Pyrenoidosa* in response to different CO_2 levels. *Bioresource Technol*, 2011; 102, 3071-3076.

[22] Xiaotong, Z.; Kaiwei, X.; Wenjuan, C.; Yanhui, Q.; Yanpeng, L. 2021. Rapid extraction of lipid from wet microalgae biomass by a novel buoyant beads and ultrasound assisted solvent extractionmethod. *Algal Research*, 2021; 58, https://doi.org/10.1016/j.algal.2021.102431

[23] Ramachandran, S.; Aran I. Low power ultrasound treatment for the enhanced production of microalgae biomass and lipid content. *Biocatalysis and Agricultural Biotechnology*, 2019; 20. https://doi.org/10.1016/j.bcab.2019.101230.

[24] Zhen, X.; Haiyan, P.; Lijie, Z.; Zhigang, Y.; Changliang, N.; Qingjie, H.; Ze Y. Accelerating lipid production in freshwater alga *Chlorella sorokiniana* SDEC-18 by seawater and ultrasound during the stationary phase. *Renewable Energy*, 2020; 161, 448-456. https://doi.org/10.1016/j.renene. 2020.07.038.

[25] Qun, W.; Jinjie, Y.; Ruge, C.; Shangru, Y.; Yonghe, T.; Xiangmeng, M. Low-frequency ultrasound and nitrogen limitation induced enhancement in biomass production and lipid accumulation of *Tetradesmus obliquus* FACHB-12. *Bioresource Technology*, 2022; 358. https://doi.org/10.1016/j.biortech.2022.127387.

[26] Pereira, R.N.; Jaeschke, D.P.; Mercali, G. et al. Impact of ultrasound and electric fields on microalgae growth: a comprehensive review. *Braz. J. Chem. Eng*. 2023; *40*, 607–622. https://doi.org/10.1007/s43153-022-00281-z

[27] Xu, L.; Wang, SK.; Wang, F. et al. Improved Biomass and Hydrocarbon Productivity of *Botryococcus braunii* by Periodic Ultrasound Stimulation. *Bioenerg Res*, 2019; 7, 986–992. https://doi.org/10.1007/s12155-014-9441-9.

[28] Dianursanti, S.A.R.; Maeda, Y.; Yoshino, T.; Tanaka, T. The Effects of Solvents and Solid-to-Solvent Ratios on Ultrasound-Assisted Extraction of Carotenoids from *Chlorella vulgaris. International Journal of Technology*, 2020; *11*(5), 941-950. https://doi.org/10.14716/ijtech.v11i5.4331.

Lists of Reviewers Manuscripts of research articles and academic articles of ASEAN Journal of Scientific and Technological Reports (AJSTR). ISSN 2773-8752 (Online), Volume 26, No. 1-4. (January – December 2023) were reviewed by the reviewers as follows:

1.	Prof. Dr. Paisarn Naphon	Faculty of Engineering, Srinakharinwirot University
2.	Prof. Dr. Pattamarat Rattanachuay	Faculty of Science, Prince of Songkla University
3.	Prof. Dr. Suchila Techawongstien	Faculty of Agriculture, Khon Kaen University
4.	Prof. Dr. Weeraya Khummueng	Faculty of Science and Technology, Prince of Songkla University
5.	Assoc. Prof. Boonrucksar Soonthornthum	National Astronomical Research Institute of Thailand (NARIT)
6.	Assoc. Prof. Dr. Boonchoo Sritularak	Faculty of Pharmaceutical Sciences, Chulalongkorn University
7.	Assoc. Prof. Dr. Chanagun Chitmanat	Faculty of Fisheries Technology and Aquatic Resources, Maejo University
8.	Assoc. Prof. Dr. Chatchai Sirisumpunwong	Faculty of Science, Naresuan University
9.	Assoc. Prof. Dr. Farung Surina Bunthit	Faculty of Science and Technology, Chiang Rai Rajabhat University
10.	Assoc. Prof. Dr. Intiraporn Mulasastra	Faculty of Engineering, Kasetsart University
11.	Assoc. Prof. Dr. Jantana Praiboon	Faculty of Fisheries, Kasetsart University
12.	Assoc. Prof. Dr. Jaray Jaratjaroonphong	Faculty of Science, Burapha University
13.	Assoc. Prof. Dr. Jompob Waewsak	Faculty of Science, Thaksin University
14.	Assoc. Prof. Dr. Kitti Nilpueng	College of Industrial Technology, King Mongkut's University of Technology North Bangkok
15.	Assoc. Prof. Dr. Korbtham Sathirakul	Faculty of Pharmacy, Mahidol University
16.	Assoc. Prof. Dr. Malinee Sriariyanun	Faculty of Engineering, King Mongkut's University of Technology North Bangkok
17.	Assoc. Prof. Dr. Nopparat Buddhakala	Faculty of Science and Technology, Rajamangala University of Technology Thanyaburi
18.	Assoc. Prof. Dr. Onanong Pringsulaka	Faculty of Science, Srinakharinwirot University
19.	Assoc. Prof. Dr. Panupon Hongpakdee	Faculty of Agriculture, Khon Kaen University
20.	Assoc. Prof. Dr. Piyarat Boonsawang	Faculty of Agro-Industry, Prince of Songkla University
21.	Assoc. Prof. Dr. Pornsiri Jongkol	Institute of Engineering, Suranaree University of Technology
22.	Assoc. Prof. Dr. Pornthap Thanonkeo	Faculty of Technology, Khon Kaen University
23.	Assoc. Prof. Dr. Puangpaka Umpunjun	Faculty of Science, Mahidol University
24.	Assoc. Prof. Dr. Rattana Jariyaboon	Faculty of Science and Technology, Prince of Songkla University
25.	Assoc. Prof. Dr. Ruangyote Pilajun	Faculty of Agriculture; Ubon Ratchathani University
26.	Assoc. Prof. Dr. Sakda Jongkaewwattana	Faculty of Agriculture. Chiang Mai University
27.	Assoc. Prof. Dr. Saowapa Chotisuwan	Faculty of Science and Technology, Prince of Songkla University
28.	Assoc. Prof. Dr. Savitri Vatanyoopaisarn	Faculty of Applied Science, King Mongkut's University of Technology North

29.	Assoc. Prof. Dr. Sira Saisorn	Department of Engineering, King Mongkut's Institute of Technology Ladkrabang Chumphon Campus
30.	Assoc. Prof. Dr. Sorapong Benchasri	Faculty of Technology and Community Development, Thaksin University
31.	Assoc. Prof. Dr. Suneerat Fukuda	Faculty of Engineering, King Mongkut's University of Technology Thonburi
32.	Assoc. Prof. Dr. Suratsavadee Koonlaboon Korkua	School of Engineering and Technology, Walailak University
33.	Assoc. Prof. Dr. Thawathcai Wongchang	Faculty of Engineering and Technology, King Mongkut's University of Technology North Bangkok
34.	Assoc. Prof. Dr. Warangkana Jutidamrongphan	Faculty of Environmental Management, Prince of Songkla University
35.	Assoc. Prof. Dr. Watchariya Purivirojku	Faculty of Science, Kasetsart University
36.	Assoc. Prof. Dr. Wirat Vanichsriratana	Faculty of Agro-Industry, Kasetsart University
37.	Assoc. Prof. Dr. Yaowapha Jirakiattikul	Faculty of Science and Technology, Thammasat University
38.	Assoc. Prof. Dr. Yutthana Tirawanichakul	Faculty of Science, Prince of Songkla University
39.	Assoc. Prof. Dr.Vidhaya Trelo-Ges	Faculty of Agriculture, Khon Kaen University
40.	Assoc. Prof. Nuchsara Kriengkorakot	Faculty of Engineering, Ubon Ratchathani University
41.	Assoc. Prof. Panitas Sureeyatanapas	Faculty of Engineering, Khon Kaen University
42.	Asst. Prof. Dr. Parawee Rattanakit	School of Science, Walailak University
43.	Asst. Prof. Dr. Arak Tira-umphon	Institute of Agricultural, Suranaree University of Technology
44.	Asst. Prof. Dr. Boonthida Kositsup	Faculty of Science, Chulalongkorn University
45.	Asst. Prof. Dr. Chokchai Mueanmas	Faculty of Engineering, Thaksin University
46.	Asst. Prof. Dr. Jaturong Sukontachat	Faculty of Science, Srinakharinwirot University
47.	Asst. Prof. Dr. Kraiyot Saelim	Faculty of Agricultural Technology, Burapha University
48.	Asst. Prof. Dr. Mayuree Krajayklang	Faculty of Agriculture, Naresuan University
49.	Asst. Prof. Dr. Naraid Suanyuk	Faculty of Natural Resourses, Prince of Songkla University
50.	Asst. Prof. Dr. Nattapong Chanchula	Thailand Institute of Scientific and Technological Research
51.	Asst. Prof. Dr. Oraporn Bualuang	Faculty of Science and Technology, Surat Thani Rajabhat University
52.	Asst. Prof. Dr. Patlada Suthamwong	Faculty of Agriculture, Ubon Ratchanthani University
53.	Asst. Prof. Dr. Paweena Dikit	Faculty of Science and Technology, Songkhal Rajabhat University
54.	Asst. Prof. Dr. Peeranart Kiddee	Faculty of Science, Thaksin University
55.	Asst. Prof. Dr. Pensri Plangklang	Faculty of Technology, Khon Kaen University
56.	Asst. Prof. Dr. Pichittra Kaewsorn	Faculty of Agriculture, Kasetsart University
57.	Asst. Prof. Dr. Pimsiree Suwanna	Faculty of Science, Kasetsart University
58.	Asst. Prof. Dr. Pongsak Noparat	Faculty of Science and Technology, Suratthani Ratjabhat University

59.	Asst. Prof. Dr. Prapansak Srisapoome	Faculty of Fisheries, Kasetsart University
60.	Asst. Prof. Dr. Punyisa Trakoonyingcharoen	Faculty of Agriculture at Kamphaeng Saen, Kasetsart University
61.	Asst. Prof. Dr. Saichai Kaew-on	Faculty of Agro-industry, Rajamangala University of Technology Srivijaya
62.	Asst. Prof. Dr. Sakunkan Simla	Faculty of Technology, Mahasarakham University
63.	Asst. Prof. Dr. Saowakon Hemwong	Faculty of Agriculture and Technology, Nakhon Phanom University
64.	Asst. Prof. Dr. Saowapa Chotisuwan	Faculty of Science and Technology, Prince of Songkla University
65.	Asst. Prof. Dr. Sasitorn Nakthong	Faculty of Agriculture, Kasetsart University
66.	Asst. Prof. Dr. Suban Foiklang	Faculty of Animal Science and Technology, Maejo University
67.	Asst. Prof. Dr. Suphada Kiriratnikom	Faculty of Science, Thaksin University
68.	Asst. Prof. Dr. Tanate Chaichana	School of Renewable Energy, Maejo University
69.	Asst. Prof. Dr. Tanyarath Utaipan	Faculty of Science and Technology, Prince of Songkla University
70.	Asst. Prof. Dr. Thanawadee Promchan	Faculty of Animal Sciences and Agricultural Technology, Silpakorn University
71.	Asst. Prof. Dr. Usarat Ratanakamnua	Faculty of Science, Maejo University
72.	Asst. Prof. Dr. Visit Boonchom	Faculty of Science, Thaksin University
73.	Asst. Prof. Dr. Wichamanee Yuenyongputtakal	Faculty of Science, Burapha University
74.	Asst. Prof. Dr. Yutthapong Sangnol	Faculty of Natural Resources, Prince of Songkla University
75.	Asst. Prof. Ronnakrit Rattanamala	Faculty of Science and Technology, Nakhon Ratchasima Rajabhat University
76.	Dr. Adisak Intana	Faculty of Technology and Environment, Prince of Songkla University
77.	Dr. Kitiyanee Asanok	National Astronomical Research Institute of Thailand (Public Organization)
78.	Dr. Nareemas Chehlaeh	Faculty of Science and Technology, Prince of Songkla University
79.	Dr. Siriporn Lunprom	Faculty of Technology, Khon Kaen University
80.	Dr. Uraiwan Phetkul	Faculty of Science and Technology, Rajamangala University of Technology Srivijaya
81.	Mr. Adulsman Sukkaew	Faculty of Science Technology and Agriculture, Yala Rajabhat University

ASEAN
Journal of Scientific and Technological Reports
Online ISSN: 2773-8752

Article type

Type of the Paper (Article, Review, Communication, etc.) *about 8,000 words maximum*

Title (Palatino Linotype 18 pt, bold)

Firstname Lastname[1], Firstname Lastname[2] and Firstname Lastname[2*]

[1] Affiliation 1; e-mail@e-mail.com
[2] Affiliation 2; e-mail@e-mail.com
* Correspondence: e-mail@e-mail.com; (one corresponding authors, add author initials)

Citation:
Lastname, F.; Lastname, F.; Lastname, F. Title. *ASEAN J. Sci. Tech. Report.* **2023**, *26*(X), xx-xx. https://doi.org/10.55164/ajstr.vxxix.xxxxxx

Article history:
Received: date
Revised: date
Accepted: date
Available online: date

Abstract: A single paragraph of about 400 words maximum. Self-contained and concisely describe the reason for the work, methodology, results, and conclusions. Uncommon abbreviations should be spelled out at first use. We strongly encourage authors to use the following style of structured abstracts, but without headings: (1) Background: Place the question addressed in a broad context and highlight the purpose of the study; (2) Methods: briefly describe the main methods or treatments applied; (3) Results: summarize the article's main findings; (4) Conclusions: indicate the main conclusions or interpretations.

Keywords: keyword 1; keyword 2; keyword 3 (List three to ten pertinent keywords specific to the article yet reasonably common within the subject discipline.)

1. Introduction

The introduction should briefly place the study in a broad context and highlight why it is crucial. It should define the purpose of the work and its significance. The current state of the research field should be carefully reviewed and critical publications cited. Please highlight controversial and diverging hypotheses when necessary. Finally, briefly mention the main aim of the work. References should be numbered in order of appearance and indicated by a numeral or numerals in square brackets—e.g., [1] or [2, 3], or [4–6]. See the end of the document for further details on references.

2. Materials and Methods

The materials and methods should be described with sufficient details to allow others to replicate and build on the published results. Please note that your manuscript's publication implicates that you must make all materials, data, computer code, and protocols associated with the publication available to readers. Please disclose at the submission stage any restrictions on the availability of materials or information. New methods and protocols should be described in detail, while well-established methods can be briefly described and appropriately cited.

Interventional studies involving animals or humans, and other studies that require ethical approval, must list the authority that provided approval and the corresponding ethical approval code.

2.1 Subsection

2.1.1. Subsubsection

3. Results and Discussion

This section may be divided by subheadings. It should provide a concise and precise description of the experimental results, their interpretation, as well as the experimental conclusions that can be drawn.Authors should discuss the results and how they can be interpreted from previous studies and the working hypotheses. The findings and their implications should be discussed in the broadest context possible. Future research directions may also be highlighted.

3.1. Subsection

3.1.1. Subsubsection

3.2. Figures, Tables, and Schemes

All figures and tables should be cited in the main text as Figure 1, Table 1, etc.

Figure 1. This is a figure. Schemes follow the same formatting.

Table 1. This is a table. Tables should be placed in the main text near the first time they are cited.

Title 1	Title 2	Title 3
entry 1	data	data
entry 2	data	data [1]

[1] Table may have a footer.

3.3. Formatting of Mathematical Components

This is example 1 of an equation:

$$a = 1, \tag{1}$$

The text following an equation need not be a new paragraph. Please punctuate equations as regular text. This is example 2 of an equation:

$$a = b + c + d + e + f + g + h + i + j + k + l + m + n + o + p + q + r + s + t + u \tag{2}$$

The text following an equation need not be a new paragraph. Please punctuate equations as regular text. The text continues here.

4. Conclusions

Concisely restate the hypothesis and most important findings. Summarize the significant findings, contributions to existing knowledge, and limitations. What are the future directions? Conclusions MUST be well stated, linked to original research question & limited to supporting results.

5. Acknowledgements

Should not be used to acknowledge funders – funding will be entered as a separate. As a matter of courtesy, we suggest you inform anyone whom you acknowledge.

Author Contributions: For research articles with several authors, a short paragraph specifying their individual contributions must be provided. The following statements should be used "Conceptualization, X.X. and Y.Y.; methodology, X.X.; software, X.X.; validation, X.X., Y.Y. and Z.Z.; formal analysis, X.X.; investigation, X.X.; resources, X.X.; data curation, X.X.; writing—original draft preparation, X.X.; writing—review and editing, X.X.; visualization, X.X.; supervision, X.X.; project administration, X.X.; funding acquisition, Y.Y. All authors have read and agreed to the published version of the manuscript." Please turn to the CRediT taxonomy for the term explanation. Authorship must be limited to those who have contributed substantially to the work reported.

Funding: Please add: "This research received no external funding" or "This research was funded by NAME OF FUNDER, grant number XXX" and "The APC was funded by XXX". Check carefully that the details given are accurate and use the standard spelling of funding agency names at https://search.crossref.org/funding. Any errors may affect your future funding.

Conflicts of Interest: Declare conflicts of interest or state "The authors declare no conflict of interest." Authors must identify and declare any personal circumstances or interest that may be perceived as inappropriately influencing the representation or interpretation of reported research results. Any role of the funders in the design of the study; in the collection, analyses or interpretation of data; in the writing of the manuscript, or in the decision to publish the results must be declared in this section. If there is no role, please state "The funders had no role in the design of the study; in the collection, analyses, or interpretation of data; in the writing of the manuscript, or in the decision to publish the results".

References

References must be numbered in order of appearance in the text (including citations in tables and legends) and listed individually at the end of the manuscript. We recommend preparing the references with a bibliography software package, such as EndNote, ReferenceManager to avoid typing mistakes and duplicated references. Include the digital object identifier (DOI) for all references where available.

Citations and references in the Supplementary Materials are permitted provided that they also appear in the reference list here.

In the text, reference numbers should be placed in square brackets [ ] and placed before the punctuation; for example [1], [1–3] or [1, 3]. For embedded citations in the text with pagination, use both parentheses and brackets to indicate the reference number and page numbers; for example [5] (p. 100), or [6] (pp. 101–105).

[1] Author 1, A.B.; Author 2, C.D. Title of the article. *Abbreviated Journal Name* Year, *Volume*, page range.

[2] Author 1, A.; Author 2, B. Title of the chapter. In *Book Title*, 2nd ed.; Editor 1, A., Editor 2, B., Eds.; Publisher: Publisher Location, Country, 2007; Volume 3, pp. 154–196.

[3] Author 1, A.; Author 2, B. *Book Title*, 3rd ed.; Publisher: Publisher Location, Country, 2008; pp. 154–196.

[4] Author 1, A.B.; Author 2, C. Title of Unpublished Work. *Abbreviated Journal Name* stage of publication (under review; accepted; in press).
[5] Author 1, A.B. (University, City, State, Country); Author 2, C. (Institute, City, State, Country). Personal communication, 2012.
[6] Author 1, A.B.; Author 2, C.D.; Author 3, E.F. Title of Presentation. In Title of the Collected Work (if available), Proceedings of the Name of the Conference, Location of Conference, Country, Date of Conference; Editor 1, Editor 2, Eds. (if available); Publisher: City, Country, Year (if available); Abstract Number (optional), Pagination (optional).
[7] Author 1, A.B. Title of Thesis. Level of Thesis, Degree-Granting University, Location of University, Date of Completion.
[8] Title of Site. Available online: URL (accessed on Day Month Year).

Reviewers sugestion

1. Name, Address, e-mail
2. Name, Address, e-mail
3. Name, Address, e-mail
4. Name, Address, e-mail

URL link:

Notes for Authors >>
https://drive.google.com/file/d/1r0zegnIVeQqe4iLQyT1xDEIinNggINPD/view?usp=sharing
https://drive.google.com/file/d/1r0zegnIVeQqe4iLQyT1xDEIinNggINPD/view?usp=sharing

Online Submissions >> https://ph02.tci-thaijo.org/index.php/tsujournal/user/register

Current Issue >> https://ph02.tci-thaijo.org/index.php/tsujournal/issue/view/16516

AJSTR Publication Ethics and Malpractice >> https://ph02.tci-thaijo.org/index.php/tsujournal/ethics

Journal Title Abbreviations >> http://library.caltech.edu/reference/abbreviations

ASEAN
Journal of Scientific and Technological Reports
Online ISSN:2773-8752

ASEAN Journal of Scientific and Technological Reports (AJSTR)
Research and Innovation Institute, Thaksin University, Phatthalung Campus
222 Moo. 2, Baan Prao Sub-District, Papayom District, Phatthalung, 93210, Thailand
Tel. +668 1540 7304